1997

Separation of ions in acidic solution by capillary electrophoresis

Michelle Jo Thornton
Iowa State University

INFORMATION TO USERS

This manuscript has been reproduced from the microfilm master. UMI films the text directly from the original or copy submitted. Thus, some thesis and dissertation copies are in typewriter face, while others may be from any type of computer printer.

The quality of this reproduction is dependent upon the quality of the copy submitted. Broken or indistinct print, colored or poor quality illustrations and photographs, print bleedthrough, substandard margins, and improper alignment can adversely affect reproduction.

In the unlikely event that the author did not send UMI a complete manuscript and there are missing pages, these will be noted. Also, if unauthorized copyright material had to be removed, a note will indicate the deletion.

Oversize materials (e.g., maps, drawings, charts) are reproduced by sectioning the original, beginning at the upper left-hand corner and continuing from left to right in equal sections with small overlaps. Each original is also photographed in one exposure and is included in reduced form at the back of the book.

Photographs included in the original manuscript have been reproduced xerographically in this copy. Higher quality 6" x 9" black and white photographic prints are available for any photographs or illustrations appearing in this copy for an additional charge. Contact UMI directly to order.

UMI

A Bell & Howell Information Company
300 North Zeeb Road, Ann Arbor MI 48106-1346 USA
313/761-4700 800/521-0600

Separation of ions in acidic solution by capillary electrophoresis

by

Michelle Jo Thornton

A dissertation submitted to the graduate faculty

in partial fulfillment of the requirements for the degree of

DOCTOR OF PHILOSOPHY

Major: Analytical Chemistry

Major Professor: James S. Fritz

Iowa State University

Ames, Iowa

1997

Graduate College
Iowa State University

This is to certify that the Doctoral dissertation of

Michelle Jo Thornton

has met the dissertation requirements of Iowa State University

Signature was redacted for privacy.

Major Professor

Signature was redacted for privacy.

For the Major Program

Signature was redacted for privacy.

For the Graduate College

TABLE OF CONTENTS

ABSTRACT

Capillary electrophoresis (CE) is an effective method for separating ionic species according to differences in their electrophoretic mobilities. Separations of anions are usually achieved by adding a quaternary ammonium salt to the electrolyte solution to reverse the electroosmotic flow (EOF). It is now shown that excellent separations of inorganic anions such as the anionic chloro complexes of the platinum group elements (PGEs) and anionic metal oxides are obtained using an acidic electrolyte carrier. The EOF is minimized at an acidic pH which eliminates the need to reverse it. The acidic solution also helps to stabilize some analytes such as metal ions.

CE separations of amino acids by direct detection are difficult due to their similar electrophoretic mobilities and low absorbances. However, native amino acids can be separated by CE as cations at a low pH by adding an alkanesulfonic acid to the electrolyte carrier which imparts selectivity to the system. Derivatization is unnecessary when direct UV detection is used at 185 nm.

Capillary electrophoresis can be used under more acidic conditions than previously used for the detection of metal cations. CE can be used to detect UV absorbing metal cations directly in an aqueous electrolyte carrier near pH 2 with a detection wavelength of 185 nm or 214 nm. Simultaneous speciation of metal cations such as vanadium (IV) and vanadium (V) can easily be performed without complexation prior to analysis. An indirect UV detection scheme for acidic conditions was also developed using guanidine as the background carrier electrolyte (BCE) for the indirect detection of metal cations.

CHAPTER 1. GENERAL INTRODUCTION

Dissertation Organization

This dissertation begins with a general introduction containing a review of pertinent literature. This is followed by a research paper that has been published in a scientific journal and two other research papers which will soon be submitted for publication. Permission from the publisher extending reproduction and distribution rights has been obtained. Each paper is similar to the published version, although additional figures and tables have been added. Figures and tables are contained in the text of the paper at the appropriate location. References cited within each paper are listed after the conclusions of each paper. A general conclusion section follows the three papers.

Literature Review

Principles of capillary electrophoresis

Experimental setup

The capillary electrophoresis (CE) system is comprised of a high voltage power supply connected to electrodes that are placed in two separate vials filled with an electrolyte solution. The power supply is capable of delivering up to 30 kV. The electric circuit is completed by a fused silica capillary filled with the electrolyte solution. One end of the capillary is placed in the sample vial, and the other end is placed in the collection vial. For the determination of inorganic ions, the capillary has a 50 or 75 μm

i.d. and is 50 to 75 cm in length. The capillary passes through a fixed detector. Only a spectrophotometric detector is available on many commercial CE instruments. Figure 1 shows a diagram of a CE system with a high voltage power supply.

Prior to an analysis, a small volume of the sample is introduced into the left end of the capillary. There are two common modes that are used. In hydrostatic injection, the sample is introduced into the capillary by applying a pressure across the capillary while the capillary end is dipped into the sample solution at a given depth for a certain amount of time (e.g. 5 to 50 s). With electrokinetic injection, a voltage is applied across the capillary while the capillary end is dipped in the sample solution.

Theory

After a sample is injected into the capillary, a voltage potential is applied across the capillary which creates an electric field. Charged analytes respond to the electric field by migrating along the capillary. CE separates ions or charged analytes on the basis of their different velocities in the electrolyte filled capillary under the influence of the electric field. The differential migration of the charged analytes moves toward the cathode and passes through the detector before reaching the collection end of the capillary.

The velocity of an analyte is described by the following equation:

$$v = \mu E \text{ (cm/s)} \qquad (1)$$

where

v = velocity of the analyte (cm/s)

μ = mobility of the analyte ($cm^2/V \cdot s$)

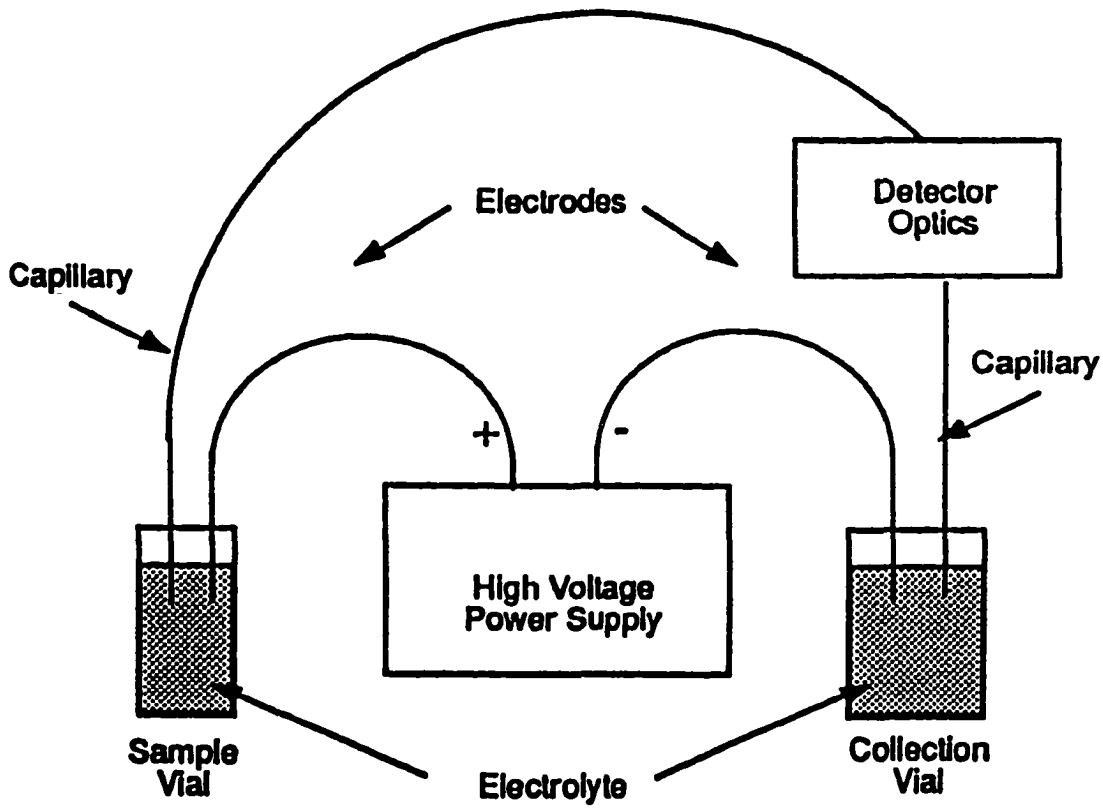

Figure 1. CE apparatus with a positive power supply.

E = strength of the electric field (V/cm)

The field strength, E, is described by the equation:

$$E = V/L \text{ (V/cm)} \quad (2)$$

where

V = applied voltage (V)

L = length of the capillary (cm)

The velocity of an analyte can also be determined by observing its migration time to the detector. The velocity for an analyte can be calculated from the following equation:

$$v = L_d/t_d \text{ (cm/s)} \quad (3)$$

where

v = velocity of analyte (cm/s)

L_d = length of the capillary to the detector (cm)

t_d = observed migration time to the detector (s)

Types of flow

Since the applied voltage and capillary length are the same for all analytes during a separation, the factor that determines the separation is the mobility of a particular analyte. The analyte's total mobility (μ) has two components:

$$\mu = \mu_{ep} + \mu_{eo} \text{ (cm}^2\text{/V·s)} \quad (4)$$

where

μ_{ep} = electrophoretic mobility ($cm^2/V \cdot s$)

μ_{eo} = electroosmotic mobility ($cm^2/V \cdot s$)

The overall mobility of any analyte (μ) is the sum of the electrophoretic mobility (μ_{ep}) and the electroosmotic mobility (μ_{eo}).

The analyte's total mobility can also be determined using the observed migration time. The equation for the mobility of an analyte is:

$$\mu = L_d L_t / t_d V \ (cm^2/V \cdot s) \qquad (5)$$

where

μ = total mobility of analyte ($cm^2/V \cdot s$)

V = applied voltage (V)

The electrophoretic mobility (μ_{ep}) is the component that causes the separation of analytes. Negatively charged analytes migrate toward the anode (+), and the positively charged analytes migrate toward the cathode (-). An analyte's electrophoretic mobility is a function of its charge and its size. Analytes with a higher charge have a higher mobility than the analytes with a lower charge. Large analytes move at a slower rate than small analytes.

Theoretical selectivity of ion separations in CE can be predicted on the basis of the equivalent ionic conductivities [1] of the ions, λ_i. The equivalent ionic conductivities are directly related to the electrophoretic mobilities [2], μ_{ep}, of the ions:

$$\mu_{ep} = \lambda_i / F \ (cm^2/V \cdot s) \qquad (6)$$

where F is the Faraday constant. The closer the equivalent ionic conductivities are for each ion, the more difficult the separation. The differences in the equivalent ionic conductivities for anions are sometimes large enough that selective separations are possible [3]. The opposite is true for most cations. Their equivalent ionic conductivities, and thus their mobilities, are usually too similar to expect selective separations.

The second component of analyte mobility is the migration resulting from electroosmosis (μ_{eo}). For most ions, the electroosmotic vector is larger than the electrophoretic vector. This causes the analytes, both cations and anions, to migrate towards the cathode. The cations migrate faster than the electroosmotic flow, and the anions migrate slower than the electroosmotic flow. Separation occurs through differences in the electrophoretic velocities of the ions. Figure 2 shows a vector diagram of analyte migration in a fused silica capillary.

The velocity of the electroosmotic flow (EOF) is dependent on the charge of the capillary wall or the zeta potential. The polarity of the charge on the wall determines the direction of the flow, while the amount of the charge, or zeta potential, determines the magnitude of the flow. The zeta potential is affected by the pH of the solution. Since the silanol groups on the capillary wall are weakly acidic (pK_a = 7-8) [4], the degree of their ionization is dependent on the pH of the electrolyte. The number of dissociated silanol groups increases as the pH increases, and the EOF increases also. The EOF is low up to pH 4.5, rises rapidly between pH 4.5 to 8, and levels off at still higher pH values [5,6]. At about pH 2, the dissociation of the surface silanol groups is completely suppressed, and the value of the zeta potential approaches zero [7]. At this low pH, the EOF should be minimal or approaching zero.

Peak shape

Mikkers et al. [8] studied peak shapes in CE. They found that the peak shape is symmetrical only when the mobility of the carrier electrolyte ion closely matches the mobility of the analyte ion and they have the same charge. Peak tailing occurred when

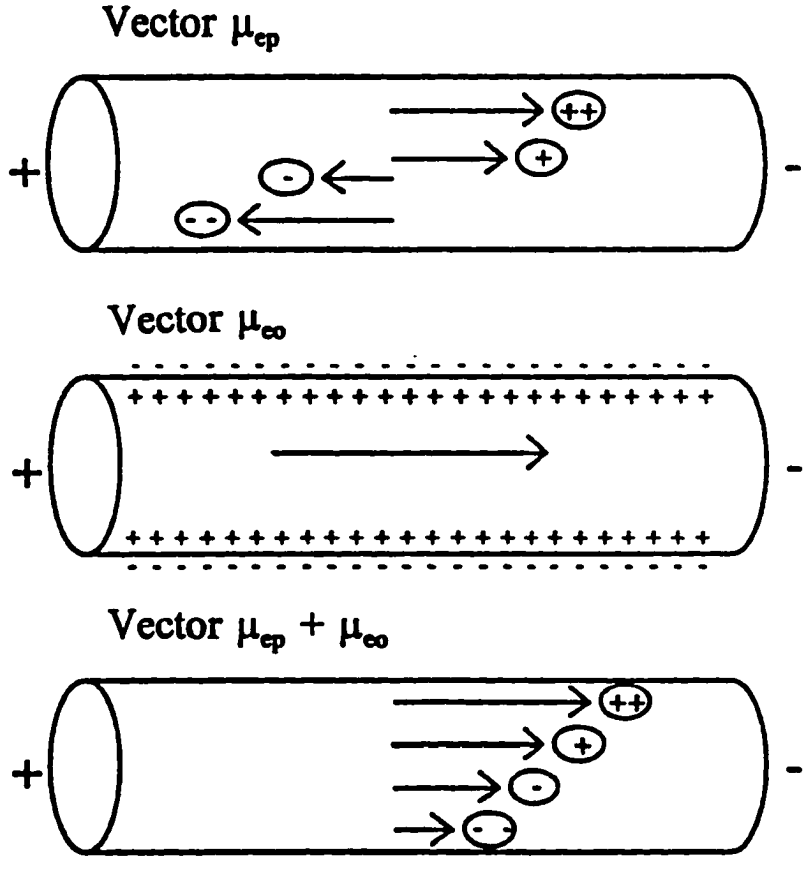

Figure 2. Vector diagram of analyte migration in a fused silica capillary under typical CE conditions.

the mobility of the analyte ion was slower than that of the carrier electrolyte ion. They found that peaks will front when the mobility of the analyte ion is faster than that of the carrier electrolyte ion. They reasoned that the analyte ions must alter the electrical field strength in order for the tailing and fronting to occur. They found that the ratio of buffer to sample concentration affected the degree to which tailing and fronting occurred. They concluded that the buffer concentration needed to be at least 100 times greater than the analyte ion concentration, or else there was a decline in the peak efficiency.

Hjérten [9] discussed peak asymmetry in regards to a conductivity difference observed at the boundary between the migrating analyte zone and the carrier electrolyte. The conductivity difference (Δk) is described by the following equation:

$$\Delta k = c_B[(\mu_A - \mu_B)(\mu_R - \mu_B)]/\mu_B \qquad (7)$$

where

c_B = analyte ion concentration

μ_B = mobility of the analyte ion

μ_A = mobility of the electrolyte co-ion

μ_R = mobility of the electrolyte counterion

According to Equation 7, peak shape in CE can be optimized not only by matching the mobilities of the analyte and co-ion, but also by selecting the correct counter-ion for the carrier electrolyte. The equation also indicates that peak asymmetry increases with an increasing concentration of the analyte ion in the migrating zone.

Electrostacking

Electrostacking, also known as sample stacking, [10-13] is a technique that causes a concentration of the analyte zone into a sharp band. It occurs when a voltage is applied along the capillary tube containing a sample plug with a higher electric resistivity, and thus a lower ionic strength, than that of the surrounding carrier electrolyte. An example of electrostacking is when the sample is dissolved in a low-conductivity solution like water.

The lower ionic strength of the sample zone creates a higher resistance which produces a higher field strength compared to that of the electrolyte. The increased field strength of the sample zone forces the analyte ions to migrate rapidly toward the boundary between the plug and the carrier electrolyte. Once the ions pass the concentration boundary between the sample plug and the carrier electrolyte, they immediately experience a lower electric field and slow down. The net effect of the difference in migration rates is the accumulation of the sample ions inside a very narrow zone at the sample-carrier electrolyte boundary. This leads to an increase in the number of theoretical plates (N):

$$N = L/H \tag{8}$$

where

L = length of the capillary (cm)

H = plate height (cm)

due to the decrease of the height of the analyte zone.

The difference in the concentrations inside the capillary also generates an electroosmotic pressure at the concentration boundary. A laminar flow results from the

electroosmotic pressure and causes extra peak broadening [14]. Sample stacking and the laminar broadening work against each other, so the best matrix for the preparation of the analyte is somewhere between pure water and the normal concentration of the carrier electrolyte used for the separation [13].

Separation of inorganic anions by capillary electrophoresis

Introduction

Capillary electrophoresis (CE) has been used mainly for applications involving the separation of non-metal analytes. In comparison, there have been very few publications dealing with inorganic separations. The majority of these papers involve the separation of inorganic anions. The methods developed for the separations of anions by CE are highly sensitive and efficient with limits of detection in the nanogram range and theoretical plate numbers between 20,000 to 1,000,000 [11,15-17]. These methods very often require the use of an alkaline pH. Direct or indirect spectrophotometric detection has been used, although conductivity [18], and other techniques have also been employed for detection.

Very few papers have investigated the separation of inorganic anions at an acidic pH [10,19,20]. The majority of publications have concentrated on using chromate in the electrolyte carrier at an alkaline pH for indirect detection of inorganic anions [21-24]. In Chapter 2, a method is developed to separate and detect inorganic anions directly using an acidic pH with excellent results.

Direct detection

The complete complexation of metals with ligands to form anions has been investigated [2,25,26]. Aguilar et al. [27] and Buchberger et al. [28] have separated metal-cyanide complexes in CE followed by direct UV detection. Aguilar et al. [27] separated hexacyanoferrate (II) and (III) ions using an electrolyte solution of a 20 mM mixture of NaH_2PO_4 and Na_2HPO_4 at pH 7. The authors stated that the ionic mobilities of the highly negatively charged metal cyanides are so large that they will migrate towards the anode and against the EOF. Buchberger et al. [28] separated 12 metal-cyanide complexes using a 20 mM phosphate buffer containing 1-2 mM sodium cyanide as the electrolyte solution.

A variation of this approach is to add the complexing ligand to the carrier electrolyte [2,29]. This establishes an equilibrium between the free and complexed metal ions. Swaile and Sepaniak [30] reported the separation of Ca (II), Mg (II), and Zn (II) with the chelating agent, 8-hydroxyquinoline-5-sulfonic acid (HQSH). In aqueous solution, the anion, HQS^-, is formed and binds with metal ions to form fluorescent complexes. The electrolyte solution contained 2.5 mM HQS^-, 10 mM Na_2HPO_4, and 6 mM $Na_2B_4O_7$ and was adjusted to pH 8. HQS^- was added to the carrier electrolyte, so that the metal-HQS complexes were formed within the capillary, and detected on-column by laser-based fluorescence.

Indirect detection

Anions are usually analyzed by indirect detection. A background absorbance is achieved by adding a low concentration of an anion that absorbs strongly in the visible

or UV region to the electrolyte solution. The visualization reagent passes through the detector at a fixed rate and establishes the background absorbance. In the sample zone, the concentration of the visualization reagent is reduced by an amount proportional to the sample ion concentration in order to maintain a constant ionic current in the capillary. This results in a negative detection peak due to the decrease in the concentration of the visualization reagent within the sample zone.

The most commonly used anion for indirect detection is chromate [21-24]. The use of chromate for indirect detection was introduced by Jones and Jandik [17] in 1990. A concentration of 5 mM is used usually, and the indirect detection is done at a wavelength of 254 nm. The chromate solution is buffered at pH 8, so it is completely in its ionized form.

In the vast majority of publications, separations of anions are carried out at an alkaline pH to ensure that the analytes and the chemical used for indirect detection will be in the anionic rather than the neutral form. Romano et al. [21] optimized conditions involving the use of chromate to separate inorganic anions, organic acids, or alkylsulfonates. Jandik and Jones [22] separated 30 anions in 3 minutes using a carrier electrolyte adjusted to pH 8.0 and containing 5 mM chromate and an EOF modifier. Wildman et al. [24] used chromate in their carrier electrolyte at pH 8.0 for indirect detection of the weak acid anions, oxalate and citrate, and the inorganic anions, chloride, sulfate, nitrate, phosphate and carbonate, in diluted urine. They were also able to detect the oxyanions of arsenic, arsenite and arsenate, in a matrix of diluted urine that had been spiked.

Electroosmotic flow modifiers

When analyzing for anions, injection is made at the cathode so the anions migrate toward the anode (+) and the detector. The electroosmotic flow (EOF) is in the opposite direction towards the cathode (-). If the electrophoretic mobility of the anions is less than the EOF, a flow modifier is required to reverse the EOF towards the anode so the anions can be detected.

Quaternary ammonium salts (Q^+) are used to modify the EOF. The positive charge of the Q^+ is attracted to the negatively charged silanol groups. The long hydrocarbon chains of the quaternary ammonium salts stick out from the wall and attract additional Q^+ molecules. They are attracted hydrophobically to the hydrocarbon tails, so the charge of the N^+ sticks out and away from the wall. This mechanism provides a net positive charge on the capillary surface which reverses the direction of the EOF. The most common Q^+ reagents are cetyltetraammonium bromide (CTAB) and tetradecyltetraammonium bromide (TTAB).

Timerbaev et al. [25] studied the use of 8-hydroxyquinoline-5-sulphonic acid (HQS^-) for the precolumn formation of negatively charged chelates. By adding HQS^- to the borate buffer at pH 9.2, they were able to separate a mixture of six transition metals in about ten minutes followed by direct UV detection at 254 nm. The fused-silica capillary column needed to be pretreated with a tetraalkylammonium salt to modify the electroosmotic flow. The salt reversed the direction of the electroosmotic flow (EOF) so that the complexes migrated in the same direction as the EOF. Otherwise, the electrophoretic mobility (EPM) could not overcome the magnitude of the EOF.

Zhang et al. [10] were able to separate and detect palladium (II) ($PdCl_4^{2-}$) within

three minutes in the presence of rhodium (III), ruthenium (III), osmium (III), and iridium (III) chloro complexes with an applied voltage of -17 kV and direct detection at 214 nm. They used a carrier electrolyte containing 50 mM HCl-KCl and 0.2 mM CTAB at pH 3.0.

Water-miscible organic solvents are used also to modify the EOF [31-33]. Methanol and acetonitrile are common solvents. Organic solvents increase the viscosity of the solution initially and decrease the dielectric constant [34] and the zeta potential [35]. These factors contribute to the reduction of the EOF.

Benz and Fritz [36] used butanol in conjunction with Q^+ to reverse the EOF. Under typical experimental conditions, a concentration of greater than 0.25 mM Q^+ is required in the carrier electrolyte to reverse the direction of the EOF. They found that by adding a low concentration of 1-butanol, less Q^+ was needed to reverse the EOF. A combination of 4-5% 1-butanol and 0.03 mM Q^+ gave optimum separations of complex mixtures of anions.

Chloro complexes of metals

The initial goal of the research presented in Chapter 2 was to study the separation of the chloro complexes of gold (III) and the platinum group elements (PGEs) ruthenium, rhodium, palladium, osmium, iridium, and platinum. An acidic electrolyte solution containing chloride was needed to form stable chloro complexes and avoid extensive hydrolysis. By operating at a very acidic pH, the silanol groups of a fused silica capillary are less ionized. They become completely protonated at pH 2 [7]. Due to a large number of the silanol groups of the capillary not being ionized, the EOF

would be minimal by working at an acidic pH. This would eliminate the need to use a flow modifier which is used commonly when anions are separated at an alkaline pH with a negative power supply. The flow modifier could also cause precipitation of the metals.

The difficulty is that if a high chloride concentration is present, the electrolyte carrier will have a high ionic strength which results in high conductivity, a large current, and large Joule heating. As the research was being completed, the publications by Baraj et al. [19,20] were noted. They separated $AuCl_4^-$, $PdCl_4^{2-}$, and $PtCl_6^{2-}$ within 18 minutes using an electrolyte solution containing 0.1 M HCl and 0.4 M NaCl. The high concentration of chloride appeared to decrease hydrolysis, but only a low applied voltage of -7 kV and a longer capillary column of 80 cm could be used due to the high conductivity of the carrier solution caused by its acidity and high ionic strength.

Separation of amino acids by capillary electrophoresis

Introduction

The research presented in Chapter 3 of this dissertation involved the separation of the twenty common amino acids as cations and detecting them directly without derivatization. A major challenge in analytical biochemistry is the separation of the amino acids commonly found in protein hydrolysates and physiological fluids. Only a few amino acids like tryptophan, tyrosine, phenylalanine, and cysteine absorb strongly in the range of 230 to 300 nm. Other amino acids only absorb at wavelengths below 220 nm, so many derivatizing reagents have been developed.

Derivatized amino acids

The most widely used detection method for amino acids uses pre- or post-column derivatization of the analytes with fluorescent probes and detection by measuring fluorescence or laser-induced fluorescence (LIF). The most popular derivatization reagents have been those that have already been used with HPLC like o-phthalaldehyde (OPA), fluorescamine, dansyl chloride (DNS), and phenylthiohydantoin (PTH) [37]. Naphthalenedialdehyde (NDA), fluorescein isothiocyanate (FITC), and fluorescamine have also been used. These reagents react with the ionic amino group, so the amino acids need to be separated by micellar electrokinetic chromatography (MEKC).

Liu et al. [38] designed a new fluorogenic reagent called 3-(4-carboxybenzoyl)-2-quinolinecarboxaldehyde (CBQCA) that had optimal migration behavior in CE, reactivity with a variety of peptides, adequate stability of the reaction products, and a matching excitation spectrum of the reaction products with the 442-nm output of the helium/cadmium laser. It formed highly fluorescent derivatives with amino acids and peptides, but required a reaction time of at least one hour prior to sample injection. They were able to separate 17 of the primary amino acids that are commonly found in proteins within 30 minutes using an electrolyte carrier containing 50 mM 2-[N-[tris(hydroxymethyl)methyl]amino]- ethanesulfonic acid (TES) and 50 mM sodium dodecyl sulfate (SDS) at pH 7. They were able to detect quantities in the low attomole (10^{-18} mol) range.

Cheng and Dovichi [39] reported detection limits of less than 6000 molecules by derivatizing the amino acids with fluorescein-5-isothiocyanate and using LIF detection. Albin et. al [40] evaluated the derivatizing reagents fluorescein isothiocyanate (FITC),

fluorescamine, 9-fluorenylmethyl chloroformate (FMOC), and o-phthaldialdehyde (OPA) using both pre- and postcapillary derivatizations with fluorescence detection in CE for the separation of six amino acids. The optimum conditions for precapillary derivatization were with FMOC, 25 mM SDS, and 20 mM sodium tetraborate at pH 9.5. The concentration limit of detection with FMOC was 10 ng/mL. The optimum conditions for postcapillary derivatization were 3.7 mM OPA, 0.5% β-mercaptoethanol (β-ME), and 2% methanol at 40°C. The concentration limit of detection with OPA was 60 ng/mL.

Cladrowa-Runge and Rizzi [41] derivatized amino acids with 6-aminoquinolyl-N-hydroxysuccinimidyl carbamate (AQC). They investigated the use of native and five modified β-cyclodextrins (β-CD) as buffer additives for enantioseparation of the AQC-derivatized amino acids. The electrolyte carrier contained 5 mM of the β-CD and 10 mM 1,3-bis-[tris(hydroxymethyl)methylamino]propane (BTP) at pH 7.0.

Derivatization with PTH has been popular [42-44] because PTH amino acids absorb strongly around 254 nm, and most commercial CE systems are equipped with UV detection. Otsuka et al. [42] separated 22 PTH amino acids using an electrolyte carrier containing 50 mM SDS. Terabe et al. [43] added 4 M urea to the electrolyte carrier to increase the migration window. Little and Foley [44] added Brij 35 which is a neutral surfactant to the anionic surfactant, SDS, which increased the separation efficiency but decreased the migration window.

Underivatized amino acids

The derivatization process requires considerable additional work which may be time consuming. Derivatization also changes the native electrophoretic mobility of the analytes. The detection of underivatized amino acids can be accomplished by indirect fluorescence [45-48], indirect amperometric [49], refractive index gradient [50], and indirect absorbance [51-54] detection methods.

Olefirowicz and Ewing [49] separated three amino acids using 0.1 mM dihydroxybenzylamine (DHBA), 25 mM 2-morpholinoethanesulfonic acid (MES), 10% ethanol at pH 5.5 with indirect amperometric detection. They achieved detection limits in the range of 500-attomoles. Pawliszyn [50] used a refractive index gradient to detect three amino acids using a 10 mM phosphate buffer at pH 7.

Ma et al. [53] used quinine sulfate for the indirect UV detection of amino acids at 236 nm. The electrolyte carrier contained 8 mM quinine sulfate and 20% ethanol at pH 5.9. Bruin et al. [52] used salicylate for the indirect UV detection of seven amino acids at pH 11.

Lee and Lin [51] separated 17 amino acids within 25 minutes using 10 mM 4-(N,N-dimethyl)aminobenzoic acid (DMAB) at pH 11 with indirect absorbance detection. They separated 19 amino acids using 10 mM p-aminosalicylic acid (PAS) and 0.05 mM Mg^{2+} at pH 10.3 within 50 minutes. Lee and Lin [54] improved their separations by adding cyclodextrins (CD) to the electrolyte carrier. They could separate 20 amino acids except leucine and isoleucine within 35 minutes using 10 mM PAS and 20 mM α-CD at pH 11. They obtained better resolution by replacing PAS with DMAB; however, a 55 minute analysis time was required. Complete CE separation of leucine and isoleucine

could only be achieved by replacing the α-CD with 15 mM β-CD, but it resulted in worse separations for some of the other amino acids.

Little has been published on the analysis of underivatized amino acids using direct absorbance detection. Bergman [55] separated six amino acids using a 50 mM phosphate buffer at pH 2.5 with an applied voltage of 25 kV and direct absorbance detection at 214 nm.

Separation of inorganic cations by capillary electrophoresis

Introduction

The research presented in Chapter 4 of this dissertation involved the detection of metal ions under acidic conditions using direct or indirect UV absorbance. Capillary electrophoresis (CE) has been used for many applications involving the separation of organic analytes. There are a few papers dealing with inorganic separations, but they mainly deal with anions. There are a few reasons for the lack of research involving the use of CE in the separation of metal cations. Other sensitive techniques are available for the detection of metal ions like ion chromatography [21,56-59], suppressed conductivity [60], atomic spectroscopies, and electrochemical methods [61-63]. The lack of a detection scheme was also a problem until Foret et al. [29] solved it by using indirect UV detection.

The first publication involving inorganic cations was in 1967 by Hjérten where he described the separation of bismuth and copper [64]. There were very few publications in the 1970's and 1980's [18,65,66]. The 1990's have shown some activity in this area

with an increase in the number of publications.

Experimental parameters

Research has been done in various areas concerning metals separation using CE. Factors that affect the separation like pH, ionic strength, viscosity, and composition of background carrier electrolyte (BCE) have been investigated. Many papers have dealt with enhancing the separations of metal cations with similar electrophoretic mobilities through complexing agents.

Beck and Engelhardt [67] studied several background carrier electrolytes (BCE) or UV-visualizing reagents for indirect UV detection. They found imidazole to be suitable for the separation of metal ions. Beck and Engelhardt [68] have also reported the use of p-aminopyridine and 2-hydroxybutyric acid for the separation of a few metal ions. Beck and Engelhardt [67] and Weston et al. [69] determined that the mobilities of analyte ions must match that of the BCE in order to achieve good separations.

Weak complexing agents

The addition of weak complexing agents in CE was introduced in the early 1990's by Foret et al. [29]. They used α-hydroxyisobutyric acid (HIBA) as the complexing reagent to separate 14 lanthanide cations within five minutes using creatinine for indirect UV detection. The weak complexing agents work by partially complexing the metal cations so there is an equilibrium between free and complexed metal ions. This increases the differences in the effective mobilities of the metal cations.

Weston et al. [70] used 4.0 mM α-hydroxyisobutyric acid (HIBA) at pH 4.4 to

separate 19 alkali, alkaline earth metals, and lanthanides in less than two minutes using 10 mM Waters UVCat-1 as the UV background-providing component of the electrolyte at 214 nm. They also studied the use of ammonia and citric acid as weak complexers.

Shi and Fritz [71] studied systems containing phthalic acid, tartrate, lactate, HIBA, malonic acid, and succinic acid. They separated 27 metal ions, including the 13 lanthanides, in six minutes using 15 mM lactic acid as the weak complexer at pH 4.25 and 8 mM 4-methylbenzylamine as the UV-visualization agent at 214 nm.

Shi and Fritz [72] reported being able to separate K^+ and NH_4^+ by adding 18-crown-6 ether to the lactate buffer. They also investigated the effect of methanol on the separation. They found that the electroosmotic mobility decreased linearly as the percentage of methanol in the buffer was increased.

Lin et al. [73] studied acetic, glycolic, lactic, hydroxyisobutyric, oxalic, malonic, malic, tartaric, succinic, and citric acids as weak complexing agents for separating a mixture of six alkali and alkaline earth metals using imidazole for indirect UV detection at 215 nm. They all worked, but lactic, succinic, hydroxyisobutyric, and malonic acid gave the best overall performances.

Lee and Lin [74] reported methods of separating cations using glycolic acid, α-hydroxyisobutyric acid, or succinic acid as the complexing agent and imidazole, benzylamine, ephedrine, or pyridine as the carrier buffer and the UV-visualizing agent. Silver (I) and aluminum (III) could not be separated from a mixture of 17 other cations using 10 mM pyridine as the background carrier electrolyte (BCE) and 12 mM glycolic acid at pH 4.0. The same result could also be achieved using 10 mM benzylamine and 16 mM glycolic acid at pH 4.0. Al^{3+} and Ag^+ could only be separated from the 17 ions

using 5 mM pyridine with the pH adjusted to 3.2 by sulfuric acid which also acts as a complexing agent.

pH

Lin et al. [73] looked at the role of the buffer pH. They found that the optimum pH for separating ions in the presence of a complexing agent is around the pK_1 of the acid. They found that operating above the pK_2 of di- and triprotic acids resulted in a decrease in the mobility of the divalent ions and a decrease in the number of theoretical plates due to complex formation.

Weston et al. [69,70] also investigated the role of pH. They found that lowering the pH increased the migration times due to the decreasing electroosmotic flow. This results from a change in the number of dissociated, negatively charged silanol groups on the inside of the capillary wall.

Strong complexing agents

Complete complexation or chelation has also been investigated [25,26,75]. The mobility of the metal cations can be selectively moderated due to the formation of metal complexes which have different stabilities within the capillary. Aguilar et al. [27] and Buchberger et al. [28] have separated metal-cyanide complexes in CE followed by direct UV detection. Motomizu et al. [76] used the UV-absorbing chelate, ethylenediaminetetraacetic acid (EDTA), to form complexes with alkaline earth metals at pH 9.2.

Timerbaev et al. [25] studied the use of 8-hydroxyquinoline-5-sulphonic acid (HQS)

for the precolumn formation of negatively charged chelates. By adding HQS to the borate buffer at pH 9.2, they were able to separate a mixture of six transition metals in about ten minutes followed by direct UV detection at 254 nm. The fused silica capillary column needed to be pretreated with a tetraalkylammonium salt to reverse the electroosmotic flow.

Cationic chelate complexes have also been used to separate metal ions. Timerbaev et al. [77] used 2,6-diacetylpyridine bis(N-methylenepyridiniohydrazone) (H_2dapmp) in a 10 mM sodium borate buffer at pH 9.0 to separate 14 metal ions within 12 minutes followed by direct UV detection at 254 nm. A micellar buffer system was used by adding tetradecyltrimethylammonium bromide to the running buffer to improve the resolution. The ion-pairing counterion was sodium n-octanesulfonate.

Noncomplexing agent

Shi and Fritz [72] reported a method where a complexing agent was not used, and the buffer was also used as UV-visualizing co-ion for indirect detection. They used a 8.0 mM nicotinamide-formate buffer at pH 3.2. They were able to detect Al^{3+} and VO^{2+} indirectly.

Other detection methods

Indirect fluorescence detection has been used in CE. Gross and Yeung [48] used indirect fluorescence detection to look at several metal cations. Bachmann et al. [78] used Ce (III) as a fluorescent carrier electrolyte and was able to detect ammonium, alkali, and alkaline earth metal ions. Swaile and Sepaniak [30] reported the separation

of three divalent cations with the chelating and fluorescent reagent, 8-hydroxyquinoline-5-sulphonic acid (HQS).

Mass spectrometry has also been tried as a detection scheme for CE [79,80]. Corr and Anacleto [79] have used mass spectrometry with an ion spray source to detect metal cations after separation by CE. They evaluated several separation buffers like creatinine, ammonium acetate and tris[hydroxymethyl]aminomethane.

References

1. P. R. Haddad and P. E. Jackson, *Ion Chromatography, (Journal of Chromatography Library, Vol. 46)*, Elsevier, Amsterdam, New York, 1990.
2. A. Weston, P. R. Brown, P. Jandik, W. R. Jones and A. L. Heckenberg, *J. Chromatogr.*, 593 (1992) 289.
3. W. R. Jones, P. Jandik, and A. Weston, *J. Chromatogr.*, 546 (1991) 445.
4. M. L. Hair and W. Herte, *J. Phys. Chem.*, 74 (1970) 91.
5. K. D. Lucas and J. W. Jorgenson, *J. High Resolut. Chromatogr.*, 8 (1985) 407.
6. R. M. McCormick, *Anal. Chem.*, 60 (1988) 2322.
7. P. Jandik and G. Bonn, *Capillary Electrophoresis of Small Molecules and Ions*, VCH Publishers, New York, 1993.
8. F. E. P. Mikkers, F. M. Everaerts and Th. P. E. M. Verheggen, *J. Chromatogr.*, 169, (1979) 1.
9. S. Hjérten, *Electrophoresis*, 11 (1990) 665.
10. H. W. Zhang, L. Jia and Z. D. Hu, *J. Chromatogr. A*, 704 (1995) 242.
11. F. E. P. Mikkkers, F. M. Everaerts and Th. P. E. M. Verheggen, *J. Chromatogr.*, 169, (1979) 11.
12. R. L. Chien and D. S. Burgi, *J. Chromatogr.*, 559, (1991) 141.

13. R. L. Chien and D. S. Burgi, *Anal. Chem.*, 63, (1991) 2042.

14. R. L. Chien and J. C. Helmer, *Anal. Chem.*, 63, (1991) 1354.

15. F. Foret, M. Deml, V. Kahle and P. Boček, *Electrophoresis*, 7 (1986) 430.

16. L. Gross and E. S. Yeung, *J. Chromatogr.*, 60 (1989) 169.

17. W. R. Jones and P. Jandik, *Am. Lab.*, 22 (1990) 51.

18. X. Huang, T. J. Pang, M. J. Gordon and R. N. Zare, *Anal. Chem.*, 59 (1987) 2747.

19. B. Baraj, A. Sastre, A. Merkoci and M. Martínez, *J. Chromatogr. A*, 718 (1995) 227.

20. B. Baraj, A. Sastre, M. Martínez and K. Spahiu, *Anal. Chim. Acta*, 319 (1996) 191.

21. J. Romano, P. Jandik, W. R. Jones and P. E. Jackson, *J. Chromatagr.*, 546 (1991) 411.

22. P. Jandik and W. R. Jones, *J. Chromatagr.*, 546 (1991) 431.

23. W. R. Jones and P. Jandik, *J. Chromatagr.*, 546 (1991) 445.

24. B. J. Wildman, P. E. Jackson, W. R. Jones and P. G. Alden, *J. Chromatagr.*, 546 (1991) 459.

25. A. R. Timerbaev, W. Buchberger, O. P. Semenova and G. K. Bonn, *J. Chromatogr.*, 630 (1993) 379.

26. M. Iki, H. Hoshino and T. Yotsuyanagi, *Chem. Lett.*, (1993) 701.

27. M. Aguilar, X. Huang and R. N. Zare, *J. Chromatogr.*, 480 (1989) 427.

28. W. Buchberger, O. P. Semenova and A. R. Timerbaev, *J. High Resolut. Chromatogr.*, 16 (1993) 153.

29. F. Foret, S. Fanali, A. Nardi and P. Boček, *Electrophoresis*, 11 (1990) 780.

30. D. F. Swaile and M. J. Sepaniak, *Anal. Chem.*, 63 (1991) 179.

31. K. Salomon, D. Burgi and J. Helmer, *J. Chromatogr.*, 559 (1991) 69.

32. S. Fugiwara and S. Honda, *Anal. Chem.*, 59 (1987) 487.

33. J. Gorse, A. T. Balchunas, D. F. Swaile and M. J. Sepaniak, *J. High Resolut. Chromatogr. Chromatogr. Commun.*, 11 (1988) 554.

34. G. M. Janini, K. C. Chan, J. A. Barnes, G. M. Muschik and H. J. Issaq, *Chromatographia*, 35 (1993) 497.

35. A. D. Tran, S. Park, P. J. Lisi, O. T. Huynh, R. R. Ryall and P. A. Lane, *J. Chromatogr.*, 542 (1991) 459.

36. N. J. Benz and J. S. Fritz, *J. Chromatogr.*, 671 (1994) 437.

37. W. G. Kuhr and D. Perrett, in P. Camilleri (Editor), *Capillary Electrophoresis: Theory and Practice*, CRC Press, Boca Raton, FL, 1993.

38. J. Liu, Y.-Z. Hsieh, D. Wiesler and M. Novotny, *Anal. Chem.*, 63 (1991) 408.

39. Y. F. Cheng and N. J. Dovichi, *Science*, 242 (1988) 562.

40. M. Albin, R. Weinberger, E. Sapp and S. Moring, *Anal. Chem.*, 63 (1991) 417.

41. S. Cladrowa-Runge and A. Rizzi, *J. Chromatogr. A*, 759 (1997) 157.

42. K. Otsuka, S. Terabe and T. Ando, *J. Chromatogr.*, 332 (1985) 219.

43. S. Terabe, Y. Ishihama, H. Nishi, T. Fukuyama and K. Otsuka, *J. Chromatogr.*, 545 (1991) 359.

44. E. L. Little and J. P. Foley, *J. Microcol. Sep.*, 4 (1992) 145.

45. E. S. Yeung and W. G. Kuhr, *Anal. Chem.*, 63 (1991) 275A.

46. W. G. Kuhr and E. S. Yeung, *Anal. Chem.*, 60 (1988) 1832.

47. T. W. Garner and E. S. Yeung, *J. Chromatogr.*, 515 (1990) 639.

48. L. Gross and E. S. Yeung, *Anal. Chem.*, 62 (1990) 427.

49. T. M. Olefirowicz and A. G. Ewing, *J. Chromatogr.*, 499 (1990) 713.

50. J. Pawliszyn, *Anal. Chem.*, 60 (1988) 2796.

51. Y.-H. Lee and T.-I. Lin, *J. Chromatogr. A*, 680 (1994) 287.

52. G. J. M. Bruin, A. C. van Asten, X. Xu and H. Poppe, *J. Chromatogr.*, 608 (1992) 97.

53. Y. Ma, R. Zhang and C. L. Cooper, *J. Chromatogr.*, 608 (1992) 93.

54. Y.-H. Lee and T.-I. Lin, *J. Chromatogr. A*, 716 (1995) 335.

55. T. Bergman, B. Agerberth and H. Jörnvall, *FEBS Letters*, 283 (1991) 100.

56. D. T. Gjerde and J. S. Fritz, *Ion Chromatography*, Hüthig, New York, 1987.

57. R. E. Smith, *Ion Chromatography Applications*, CRC Press, Boca Raton, FL, 1988.

58. W. R. Jones, P. Jandik and R. Pfeifer, *Am. Lab.*, May (1991) 40.

59. S. C. Grocott, L. P. Jefferies, T. Bowser, J. Carnevale and P. E. Jackson, *J. Chromatogr.*, 602 (1992) 249.

60. N. Avdalovic, C. A. Pohl, R. D. Rocklin and J. D. Stillian, *Anal. Chem.*, 65 (1993) 1470.

61. W. Lu, R. M. Cassidy and A. S. Baranski, *J. Chromatogr.*, 640 (1993) 433.

62. D. A. Skoog and J. J. Leary, *Principles of Instrumental Analysis*, Saunders, New York, 4th ed., 1992.

63. Z. Yi, G. Zhuang and P. R. Brown, *J. Liq. Chromatogr.*, 16 (1993) 3133.

64. S. Hjerten, *Chromatogr. Rev.*, 9 (1967) 122.

65. T. Tsuda, K. Nomura and G. Nakagawa, *J. Chromatogr.*, 264 (1983) 385.

66. J. L. Beckers, Th. P. E. M. Verheggen and F. M. Everaerts, *J. Chromatogr.*, 452 (1988) 591.

67. W. Beck and H. Engelhardt, *Chromatographia*, 33 (1992) 313.

68. W. Beck and H. Engelhardt, *Fresenius' J. Anal. Chem.*, 346 (1993) 618.

69. A. Weston, P. R. Brown, P. Jandik, A. L. Heckenberg and W. R. Jones, *J. Chromatogr.*, 602 (1992) 249.

70. A. Weston, P. R. Brown, P. Jandik, W. R. Jones and A. L. Heckenberg, *J. Chromatogr.*, 593 (1992) 289.

71. Y. Shi and J. S. Fritz, *J. Chromatogr.*, 640 (1993) 473.

72. Y. Shi and J. S. Fritz, *J. Chromatogr. A*, 671 (1994) 429.

73. T.-I. Lin, Y.-H. Lee and Y.-C. Chen, *J. Chromatogr. A*, 654 (1993) 167.

74. Y.-H. Lee and T.-I. Lin, *J. Chromatogr. A*, 675 (1994) 227.

75. S. Motomizu, S. Nishimura, Y. Obata and H. Tanaka, *Anal. Sci.*, 7 (1991) 253.

76. S. Motomizu, M. Oshima, S. Matsuda, Y. Obata and H. Tanaka, *Anal. Sci.*, 8 (1992) 619.

77. A. R. Timerbaev, O. P. Semenova, G. K. Bonn and J. S. Fritz, *Anal. Chim. Acta*, 296 (1994) 119.

78. K. Bachmann, J. Boden and I. Haumann, *J. Chromatogr.*, 626 (1992) 259.

79. J. J. Corr and J. F. Anacleto, *Anal. Chem.*, 68 (1996) 2155.

80. Y. Lui, V. Lopez-Avila and J. J. Zhu, *Anal. Chem.*, 67 (1995) 2020.

CHAPTER 2. SEPARATION OF INORGANIC ANIONS IN ACIDIC SOLUTION BY CAPILLARY ELECTROPHORESIS

A paper published in the Journal of Chromatography A[1]

Michelle J. Thornton[2,3] and James S. Fritz[2,4]

Abstract

Inorganic anions are almost always determined by CE at an alkaline pH, so the analytes will be fully ionized. However, a long-chain quaternary ammonium salt usually must be added as a flow modifier to the carrier electrolyte to reverse the direction of the electroosmotic flow. By working at a sufficiently acidic pH, the electroosmotic flow in fused-silica capillaries is virtually eliminated, and anions can be separated simply by differences in their electrophoretic mobilities. Excellent separations were obtained for $AuCl_4^-$ and the chloro complexes of platinum group elements in HCl solution at pH 2.0 to 2.4. No additional buffer or flow modifier was needed. This CE technique is an excellent way to follow slow hydrolytic reactions in which one or more of the chloride ligands is replaced by water. Sharp peaks and good separations were also obtained for MnO_4^-, VO_3^-, chromate, molybdate, ferrocyanide, ferricyanide and stable complex ions such as chromium oxalate ($CrOx_3^{3-}$).

---

[1]Reprinted with permission of *J. Chromatogr. A*, 770 (1997) 301.

[2]Graduate student and Professor, respectively, Department of Chemistry and Ames Laboratory, Iowa State University, Ames, IA 50011, USA.

[3]Primary researcher and author

[4]Author for correspondence

1. Introduction

Inorganic anions separated by capillary electrophoresis (CE) are usually analyzed by indirect photometric detection. The introduction of chromate in 1990 for indirect detection of anions was a major advance [1]. Many excellent separations have been reported using chromate [2-6], including the separation of 30 anions in only 3 min [5]. For these separations, it was necessary to add a long-chain quaternary ammonium salt (Q^+) as a flow modifier to coat the capillary surface and reverse the direction of the electroosmotic flow vector.

Direct photometric detection has also been used in the CE separation of anions having sufficient absorbance in the UV- or visible spectral region. Aguilar et al. [7] separated hexacyanoferrate(II) and (III) ions at pH 7. The ionic mobilities of these highly charged ions are so large that they migrated toward the anode and against the electroosmotic flow. Buchberger et al. [8] separated 12 metal-cyanide complexes in an electrolyte containing a 20 mM phosphate buffer and 1-2 mM sodium cyanide.

In the vast majority of publications, CE separations of inorganic anions are carried out at an alkaline pH to ensure that the analytes will be in the ionic rather than the neutral form. In our research, a very acidic pH is used for the CE separation of inorganic anions. Special attention was paid to the anionic chloro complexes of gold(III) and the platinum group elements (PGEs), which are more resistant to hydrolysis in more acidic solutions. By working at lower pH values, the capillary's silanol groups are hardly ionized, and consequently, the electroosmotic flow is minimal. No flow modifier is therefore needed.

2. Experimental

2.1. Apparatus

CE was performed with a Waters Quanta 4000 capillary electrophoresis system (Millipore Waters, Milford, MA, USA). The polyimide-coated, fused-silica capillaries used (Polymicro Technology, Phoenix, AZ, USA) were 60 cm in length with an I.D. of 75 μm. The distance from the point of injection to the window of on-column detection was 52.25 or 52.75 cm. Direct UV detection was employed at 214 and 254 nm. A voltage of -10 kV was applied for the separations. The time of hydrodynamic injection was 30 seconds. Electropherograms were collected and plotted by the data acquisition system Chrom Perfect Direct (Justice Innovations, Mountain View, CA, USA).

2.2. Procedure

New capillaries were conditioned by rinsing with 0.1 M NaOH for one h followed by a 1-h rinse with deionized water. At the start of each day, the capillary was rinsed with 0.1 M NaOH for 10 min, deionized water for 10 min, 0.1 M HCl for 10 min, deionized water for 10 min, and the electrolyte solution for 30 min. The capillary was also purged with the electrolyte solution for five min before each run.

2.3. Reagents

All standards and electrolytes were prepared with analytical-reagent grade chemicals and 18 MΩ deionized waters obtained from a Barnstead Nanopure II system (Sybron Barnstead, Boston, MA, USA). For the electrolyte solution, a dilute solution of reagent grade sodium hydroxide was added to 50 mL of 0.1 M HCl to adjust the pH to 2.4.

The electrolyte solution contained 4 mM H^+ (pH 2.4) and 25 mM Cl^- (Fisher Scientific, Fairlawn, NJ, USA). The potassium salts of the chloro complexes of the platinum group metals and gold and the mercury (II) chloride were obtained from Aldrich (Milwaukee, WI, USA). The stock solutions were prepared at a concentration of 4 g/L in 40% HCl. The potassium permanganate, potassium perrhenate (VII), ammonium metavanadate, sodium chromate, sodium molybdate (VI) dihydrate, potassium chromium (III) oxalate trihydrate, potassium ferricyanide (III), and potassium ferrocyanide (II) trihydrate were also obtained from Aldrich (Milwaukee, WI, USA). The stock solutions were prepared at a concentration of 4 g/L in deionized water.

3. Results and discussion

3.1. Chloro complexes of gold (III) and PGEs

In establishing conditions for CE separations, the capillary electrolyte contained chloride ions at an acidic pH to provide an environment where the chloro complex anions would be stable.

Preliminary experiments were carried out by diluting stock solutions of $AuCl_4^-$, $PtCl_6^{2-}$, and $RhCl_6^{3-}$ with water just before analysis by CE. Spectral measurements indicated that direct detection at 254 nm or 214 nm would be feasible. At first, buffers prepared by adding hydrochloric acid to ß-alanine or glycine were used at pH values ranging from about pH 3.5 to 2.5. No peak for $AuCl_4^-$ was observed with the ß-alanine buffer. Peaks were obtained for the sample ions in the glycine buffer, but they were broad and the baseline was noisy. Much better results were obtained when only

hydrochloric acid was added to the aqueous electrolyte solution. The best results were obtained at a pH of 2.4, although the sample anion peaks were almost as sharp at pH 2.0. The electropherograms were very poor when higher HCl concentrations were used and the pH was below 1.8.

The relatively high concentration of HCl in the electrolyte solution results in a high current (> 200 μA in some cases) and a noisy baseline, probably due to Joule heating. Reduction of the applied voltage from -20 kV to -10 kV greatly improved the separations. An applied voltage of -10 kV was found to be the optimum. The electropherogram in Fig. 1 shows a very sharp, reproducible peak for gold (III) and a flat, smooth baseline.

Chloro complexes of PGE also gave sharp peaks under the same conditions used for gold (III). A sharp single peak was obtained for $OsCl_6^{2-}$ (7.41 min) (Fig. 1A), $PdCl_4^{2-}$ (9.30 min) (Fig. 1B) and $PtCl_4^{2-}$ (6.19 min) (Fig. 1C). Palladium (IV) gave a single peak at the same time as palladium (II), indicating that the palladium (IV) had been reduced in the solution used (Fig. 1D).

Several PGE anions gave more than one peak. Platinum (IV) had a major peak at 7.5 min, a much smaller peak at 15.0 min and a contaminant peak at 6.6 min (Fig. 1E). The contaminant peak is not seen when the sample is analyzed at a wavelength of 254 nm (Fig. 1F). Iridium (III) gave a peak at 6.5 min and a somewhat smaller peak at 8.7 min (Fig. 1G). Iridium (IV) and Ru (III) are shown in Figs. 1H and 1I, respectively. It is suspected that the stock solution of Ir (IV) has traces of Ir (III) present and these represent peaks 1 and 3. The second peak in these cases is probably the result of hydrolysis in which one of the chloride atoms is replaced by water. Such

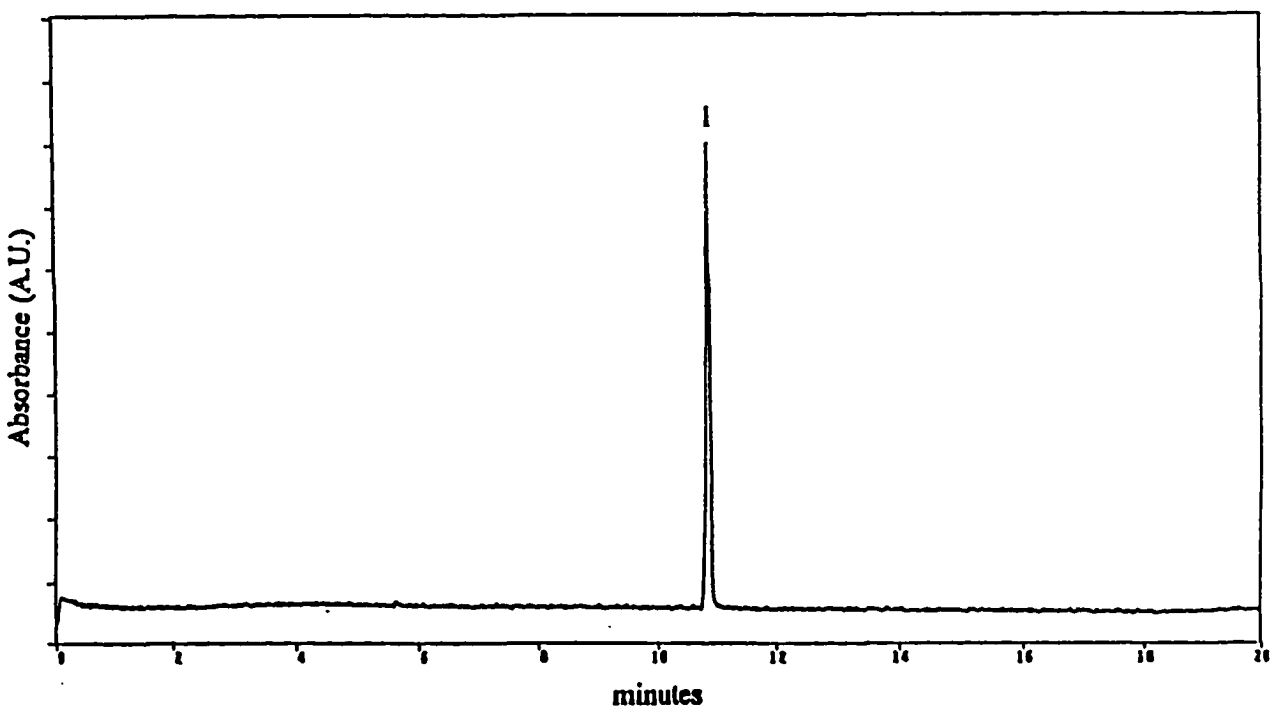

Figure 1. Electropherogram of 10 μg ml^{-1} of gold (III) ($AuCl_4^-$). Conditions: fused-silica capillary, 60 cm x 75 μm I.D. (52.75 cm to detector); carrier solution, 4 mM H^+ - 25 mM Cl^-; applied voltage, -10 kV; UV detection at 214 nm; sampling time, 30 s. Peak: (1) $AuCl_4^-$.

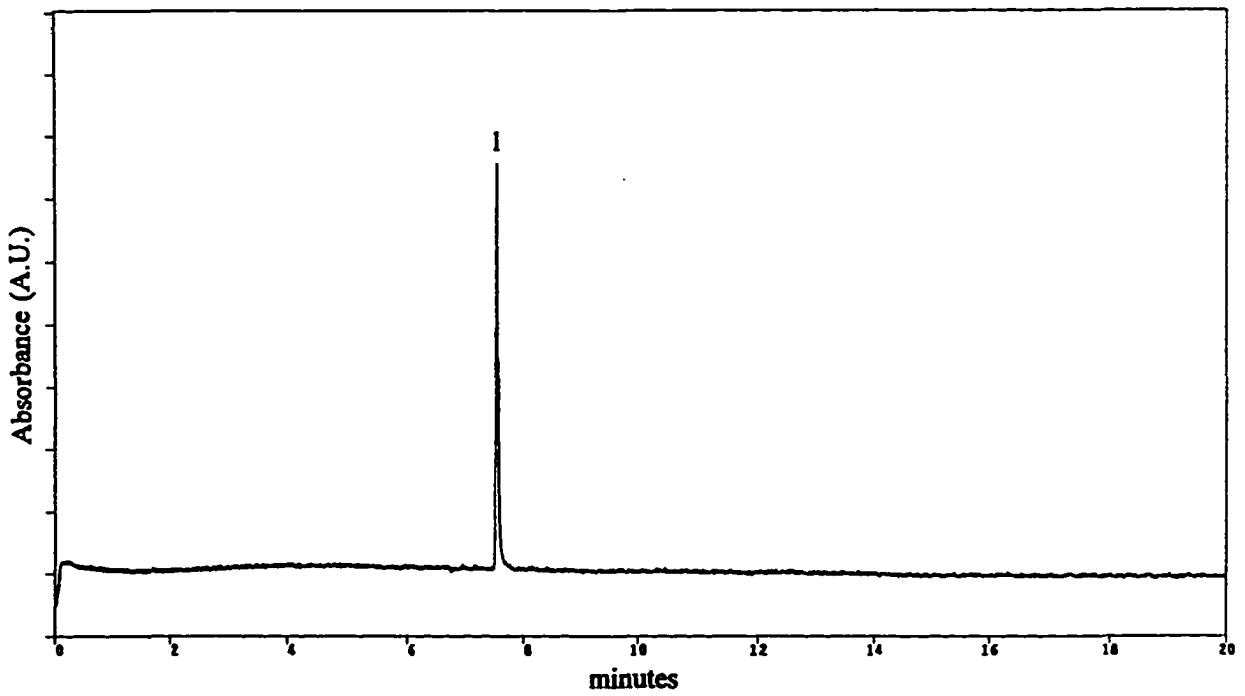

Figure 1A. Electropherogram of 10 μg ml^{-1} of osmium (IV) ($OsCl_6^{2-}$). Conditions: fused-silica capillary, 60 cm x 75 μm I.D. (52.25 cm to detector); carrier solution, 4 mM H^+ - 25 mM Cl^-; applied voltage, -10 kV; UV detection at 214 nm; sampling time, 30 s. Peak: (1) $OsCl_6^{2-}$.

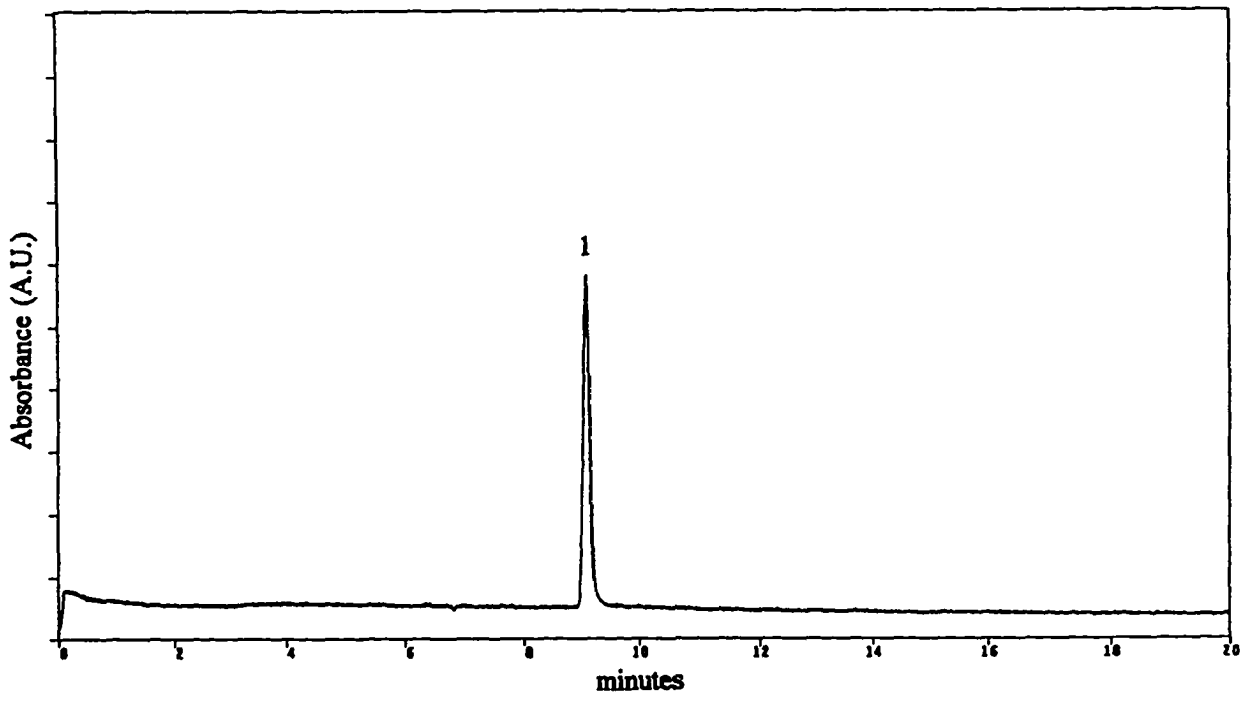

Figure 1B. Electropherogram of 20 μg ml^{-1} of palladium (II) ($PdCl_4^{2-}$). Conditions: fused-silica capillary, 60 cm x 75 μm I.D. (52.25 cm to detector); carrier solution, 4 mM H^+ - 25 mM Cl^-; applied voltage, -10 kV; UV detection at 214 nm; sampling time, 30 s. Peak: (1) $PdCl_4^{2-}$.

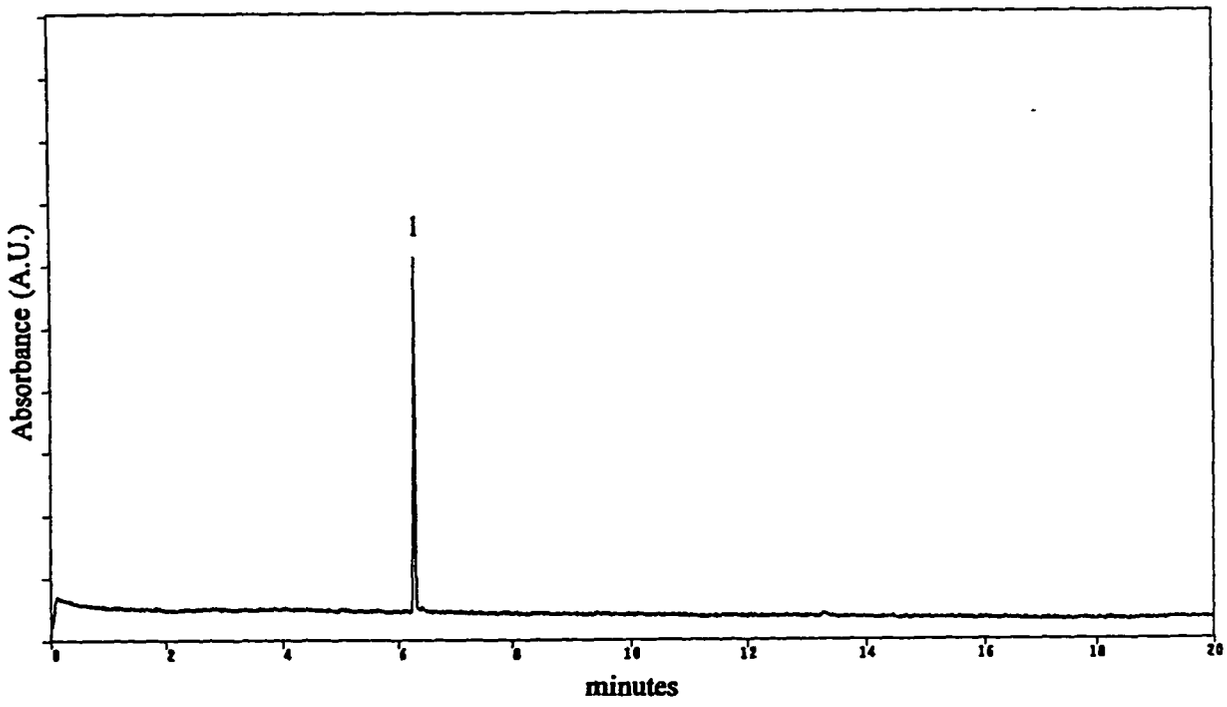

Figure 1C. Electropherogram of 20 μg ml^{-1} of platinum (II) ($PtCl_4^{2-}$). Conditions: fused-silica capillary, 60 cm x 75 μm I.D. (52.75 cm to detector); carrier solution, 4 mM H^+ - 25 mM Cl^-; applied voltage, -10 kV; UV detection at 214 nm; sampling time, 30 s. Peak: (1) $PtCl_4^{2-}$.

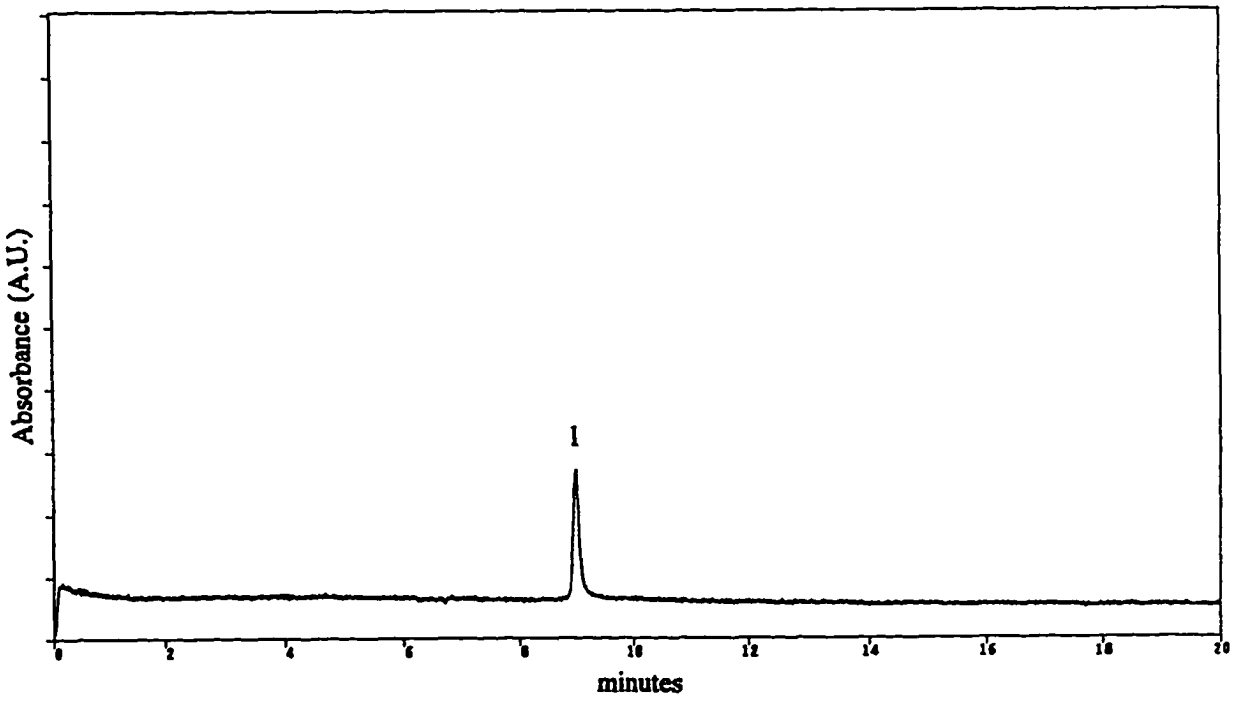

Figure 1D. Electropherogram of 20 μg ml^{-1} of palladium (IV) ($PdCl_6^{2-}$). Conditions: fused-silica capillary, 60 cm x 75 μm I.D. (52.25 cm to detector); carrier solution, 4 mM H^+ - 25 mM Cl^-; applied voltage, -10 kV; UV detection at 214 nm; sampling time, 30 s. Peak: (1) $PdCl_6^{2-}$.

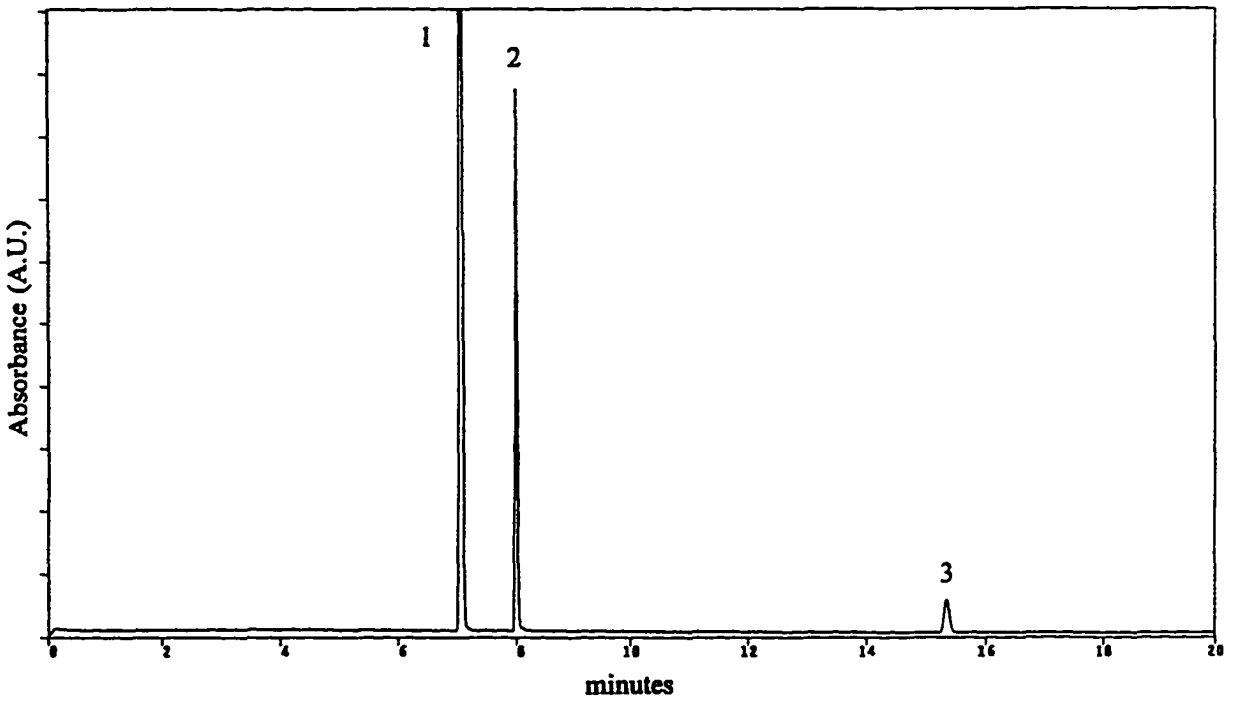

Figure 1E. Electropherogram of 20 μg ml^{-1} of platinum (IV) ($PtCl_6^{2-}$). Conditions: fused-silica capillary, 60 cm x 75 μm I.D. (52.75 cm to detector); carrier solution, 4 mM H^+ - 25 mM Cl^-; applied voltage, -10 kV; UV detection at 214 nm; sampling time, 30 s. Peak: (1) contaminant, (2) $PtCl_6^{2-}$ and (3) $PtCl_5(H_2O)^-$.

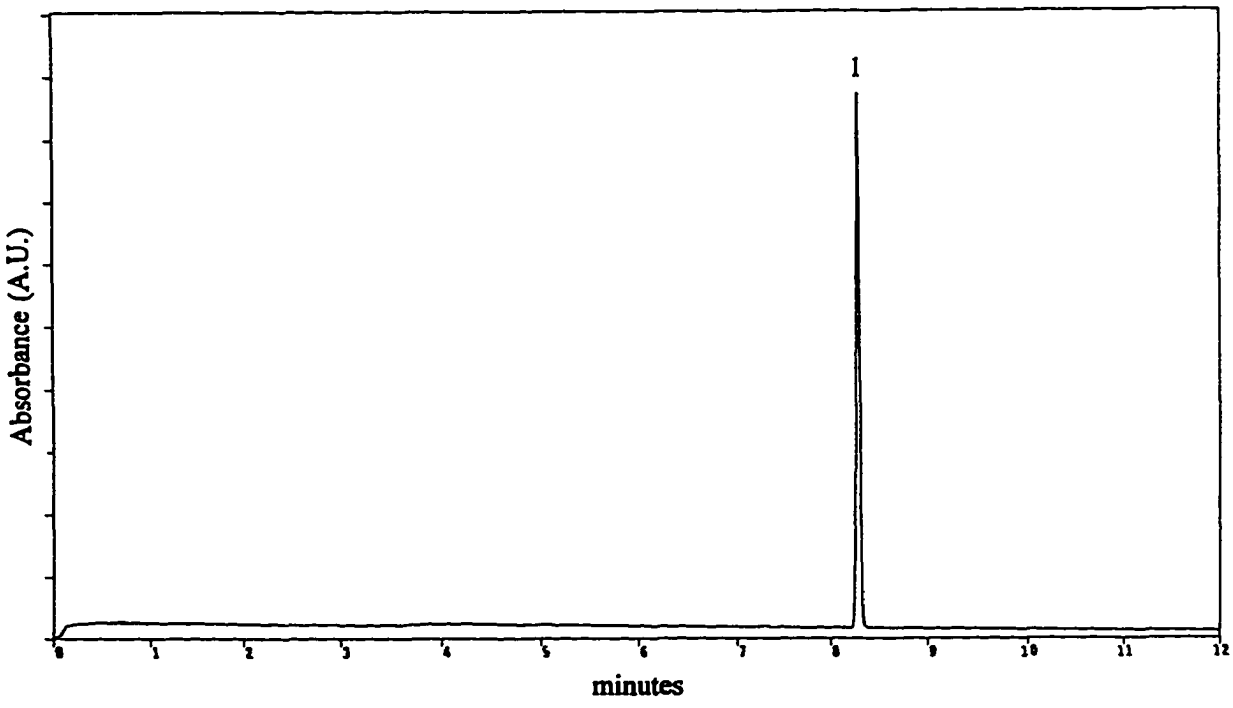

Figure 1F. Electropherogram of 10 μg ml^{-1} of platinum (IV) ($PtCl_6^{2-}$). Conditions: fused-silica capillary, 60 cm x 75 μm I.D. (52.75 cm to detector); carrier solution, 4 mM H^+ - 25 mM Cl^-; applied voltage, -10 kV; UV detection at 254 nm; sampling time, 30 s. Peak: (1) $PtCl_6^{2-}$.

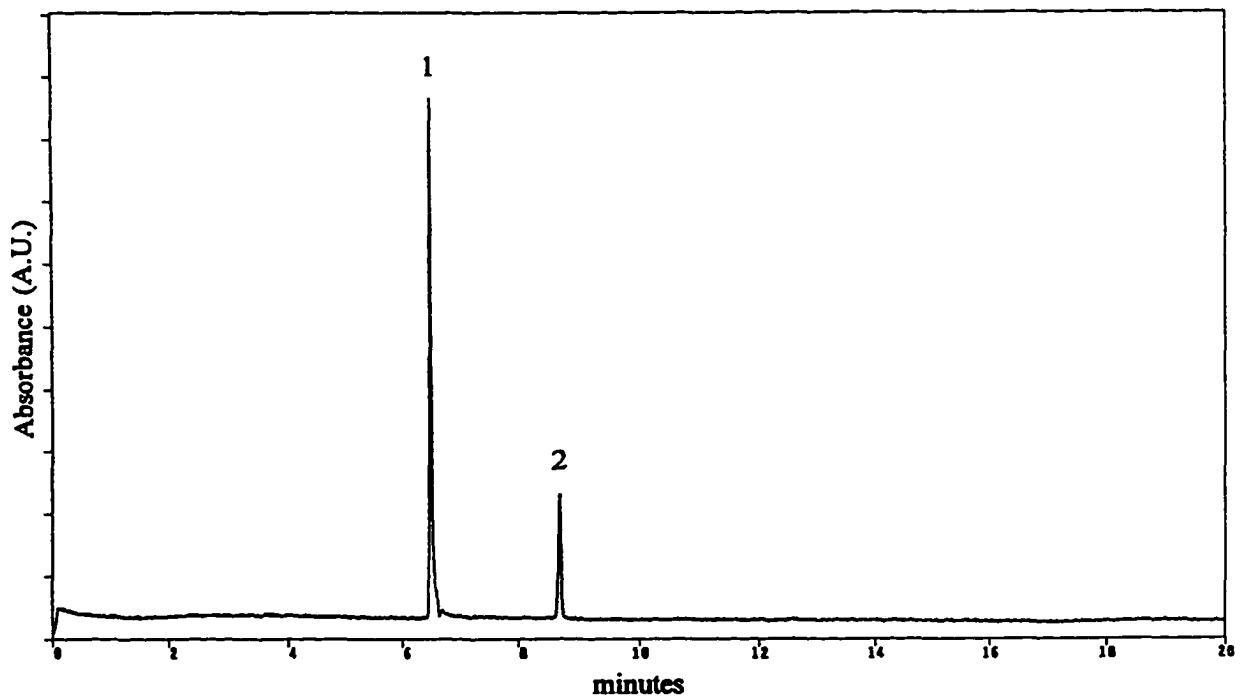

Figure 1G. Electropherogram of 20 μg ml^{-1} of iridium (III) ($IrCl_6^{3-}$). Conditions: fused-silica capillary, 60 cm x 75 μm I.D. (52.75 cm to detector); carrier solution, 4 mM H^+ - 25 mM Cl^-; applied voltage, -10 kV; UV detection at 214 nm; sampling time, 30 s. Peaks: (1) $IrCl_6^{3-}$ and (2) $IrCl_5(H_2O)^{2-}$.

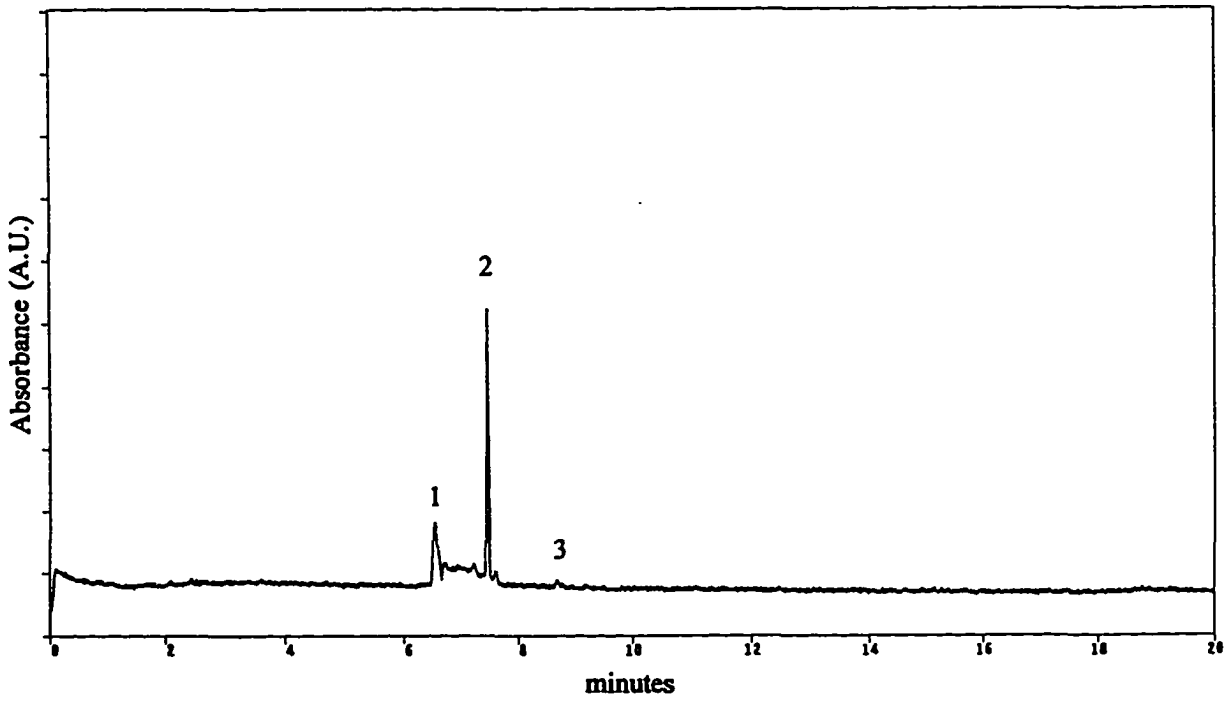

Figure 1H. Electropherogram of 20 μg ml^{-1} of iridium (IV) ($IrCl_6^{2-}$). Conditions: fused-silica capillary, 60 cm x 75 μm I.D. (52.75 cm to detector); carrier solution, 4 mM H^+ - 25 mM Cl^-; applied voltage, -10 kV; UV detection at 214 nm; sampling time, 30 s. Peaks: (1) $IrCl_6^{3-}$, (2) $IrCl_6^{2-}$ and (3) $IrCl_5(H_2O)^{2-}$.

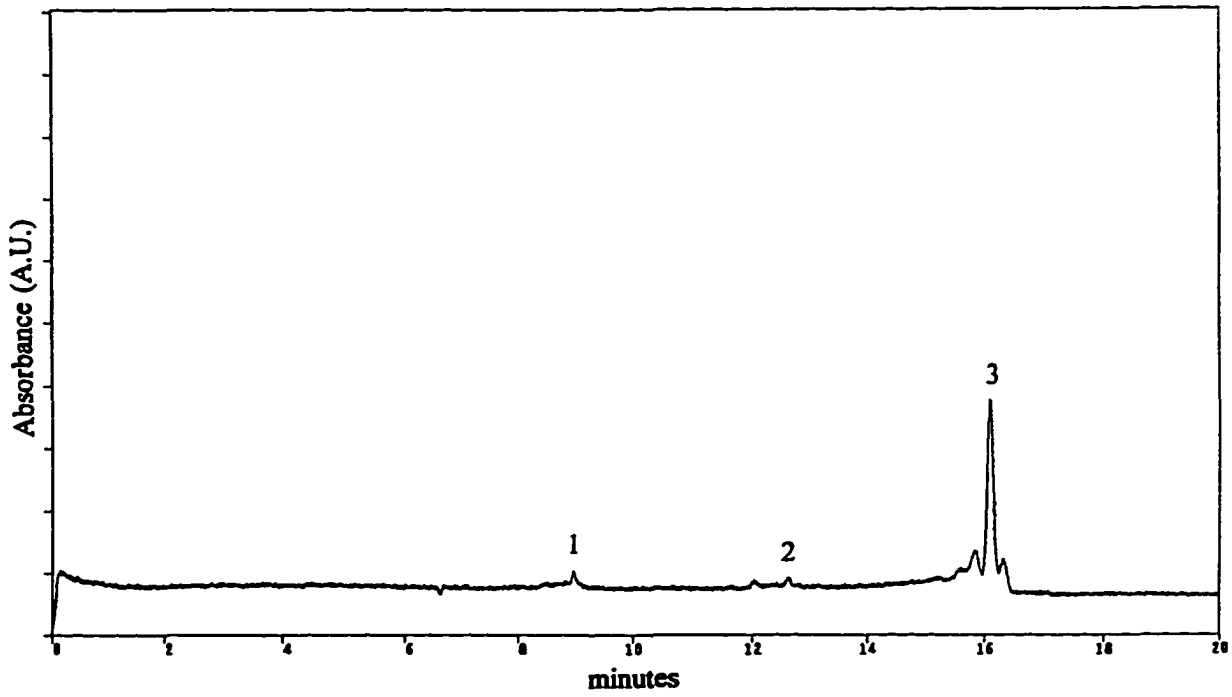

Figure 1I. Electropherogram of 20 μg ml^{-1} of ruthenium (III) ($RuCl_6^{3-}$). Conditions: fused-silica capillary, 60 cm x 75 μm I.D. (52.25 cm to detector); carrier solution, 4 mM H^+ - 25 mM Cl^-; applied voltage, -10 kV; UV detection at 214 nm; sampling time, 30 s. Peaks: (1) $RuCl_5(H_2O)^{2-}$, (2) $RuCl_4(H_2O)_2^-$ and (3) $RuCl_3OH(H_2O)_2^-$.

hydrolysis effects are shown dramatically by rhodium (III). The electropherogram in Fig. 2 shows a major peak for $RhCl_5(H_2O)^{2-}$ and only a very small later peak when the stock solution (in 40% HCl) was diluted and run immediately. In Fig. 3, it can be seen that the electropherogram that was run 24 h after dilution was entirely different. The initial peak had all but disappeared while two large, late peaks had formed. The $RhCl_6^{3-}$ had obviously undergone extensive hydrolysis. Similar behavior was observed for osmium (IV). After 48 h, the initial $OsCl_6^{2-}$ peak (7.4 min) was decreased in size and a second peak at 11.2 min had appeared. The latter peak is believed to be $OsCl_5(H_2O)^-$ (Fig. 3A). This behavior was also observed for Pt (II) (Fig. 3B).

As research on chloro complex anions was being completed, publications by Baraj et al. were noted (9,10). They were able to separate $AuCl_4^-$, $PdCl_4^{2-}$, and $PtCl_6^{2-}$ within 18 min using an electrolyte solution containing 0.1 M HCl and 0.4 M NaCl with a low applied voltage of -7 kV. We tried the same conditions to see whether the increased acidity and higher chloride concentration would slow down the rate of hydrolysis of the complex anions. However, no noticeable improvement was observed. The main differences were a less stable baseline, poorer peak shape, and longer migration times at the higher HCl and NaCl concentrations.

The average migration times for peaks of gold(III) and the PGE are given in Table 1. Reproducibility was quite good, as indicated by the statistical data given in this table. Peaks resulting from partial hydrolysis of the major peaks were assumed to contain H_2O in the coordination sphere in place of one or more of the chloride atoms in the parent peak, but this was not proven.

Samples containing several anionic complexes were separated by CE to confirm the

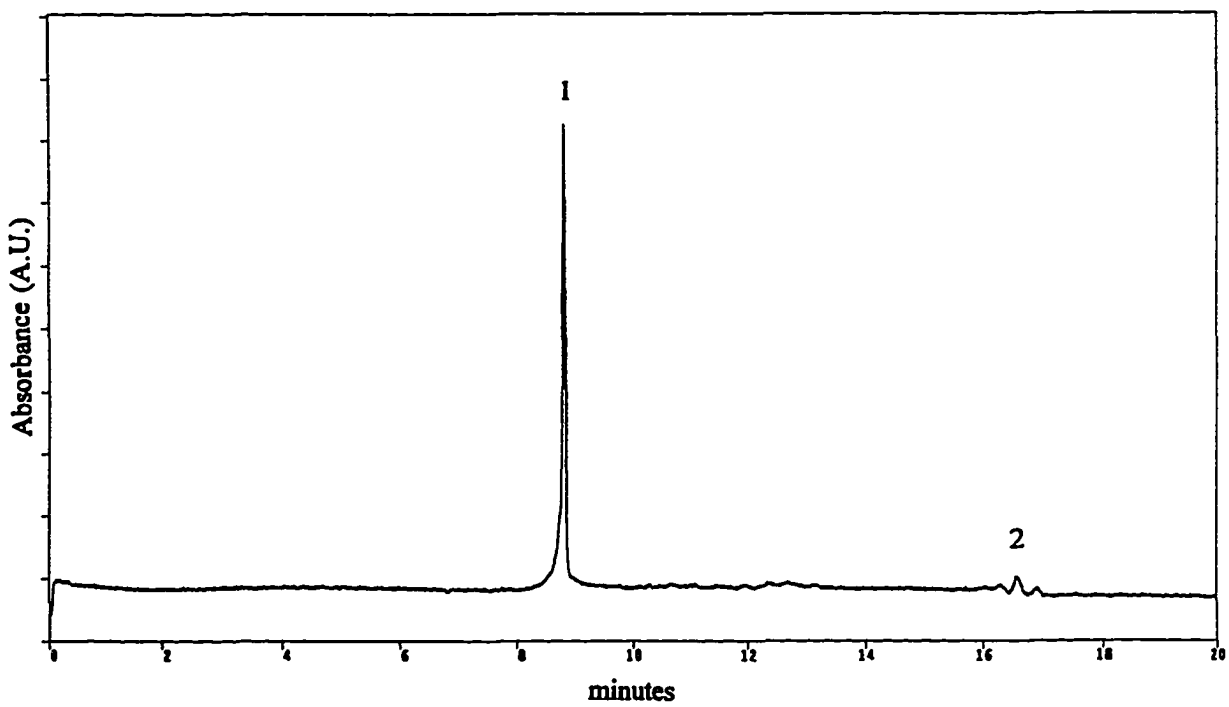

Figure 2. Electropherogram of 10 μg ml^{-1} of rhodium (III) ($RhCl_6^{3-}$). Peaks: (1) $RhCl_5(H_2O)^{2-}$ and (2) $RhCl_4(H_2O)^{2-}$. Conditions as in Fig. 1 except 52.25 cm to detector.

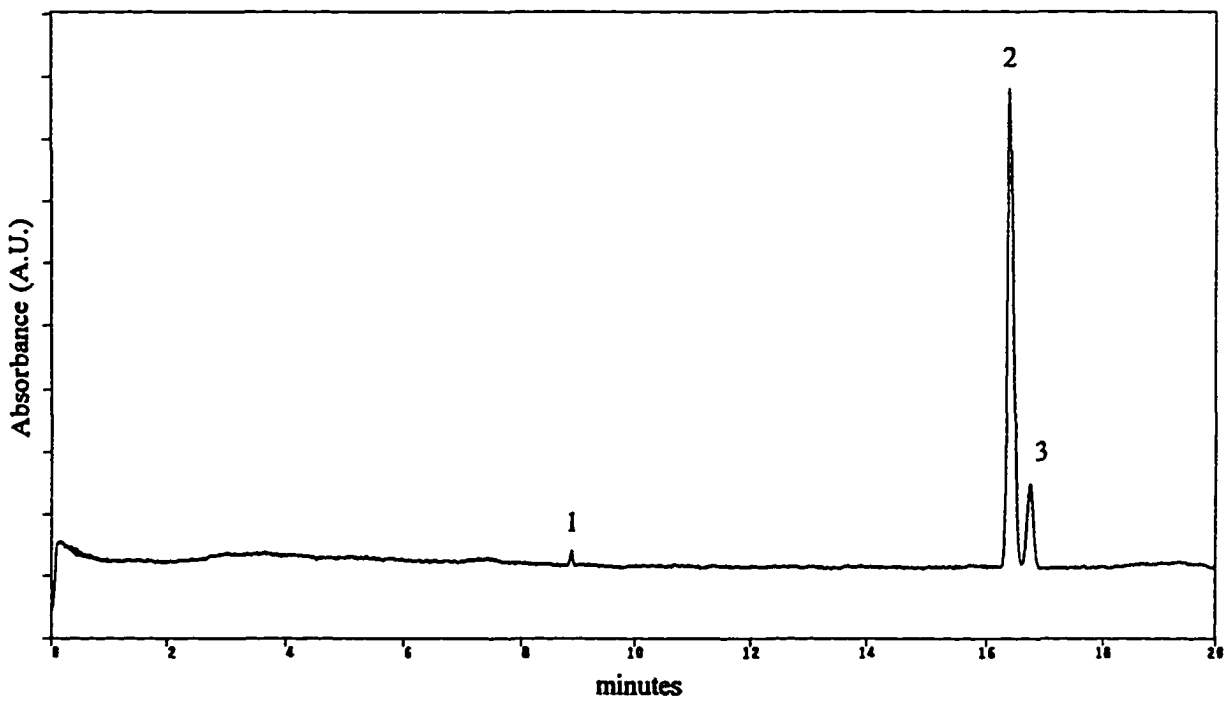

Figure 3. Electropherogram of 10 μg ml^{-1} of rhodium (III) ($RhCl_6^{3-}$) after 24 hours. Peaks: (1) $RhCl_5(H_2O)^{2-}$, (2) $RhCl_4(H_2O)_2^-$ and (3) $RhCl_3OH(H_2O)_2^-$. Conditions as in Fig. 1.

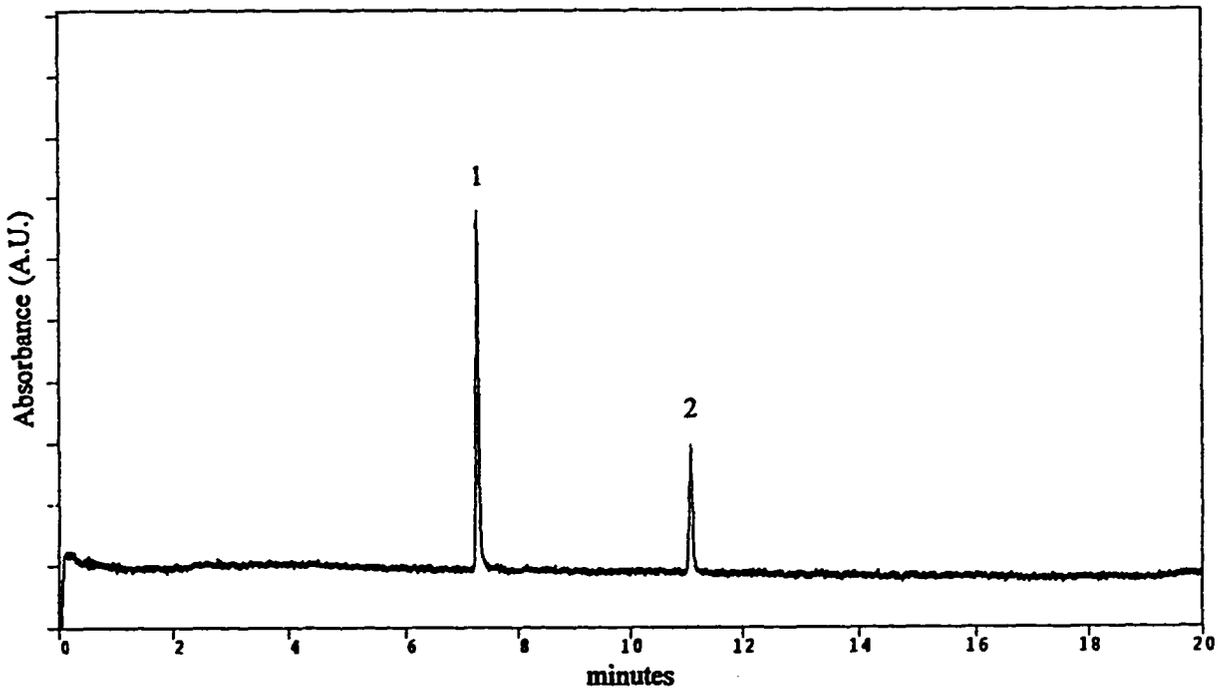

Figure 3A. Electropherogram of 20 μg ml^{-1} of osmium (IV) ($OsCl_6^{2-}$) after 48 hours. Conditions: fused-silica capillary, 60 cm x 75 μm I.D. (52.25 cm to detector); carrier solution, 4 mM H^+ - 25 mM Cl^-; applied voltage, -10 kV; UV detection at 214 nm; sampling time, 30 s. Peaks: (1) $OsCl_6^{2-}$ and (2) $OsCl_5(H_2O)^-$.

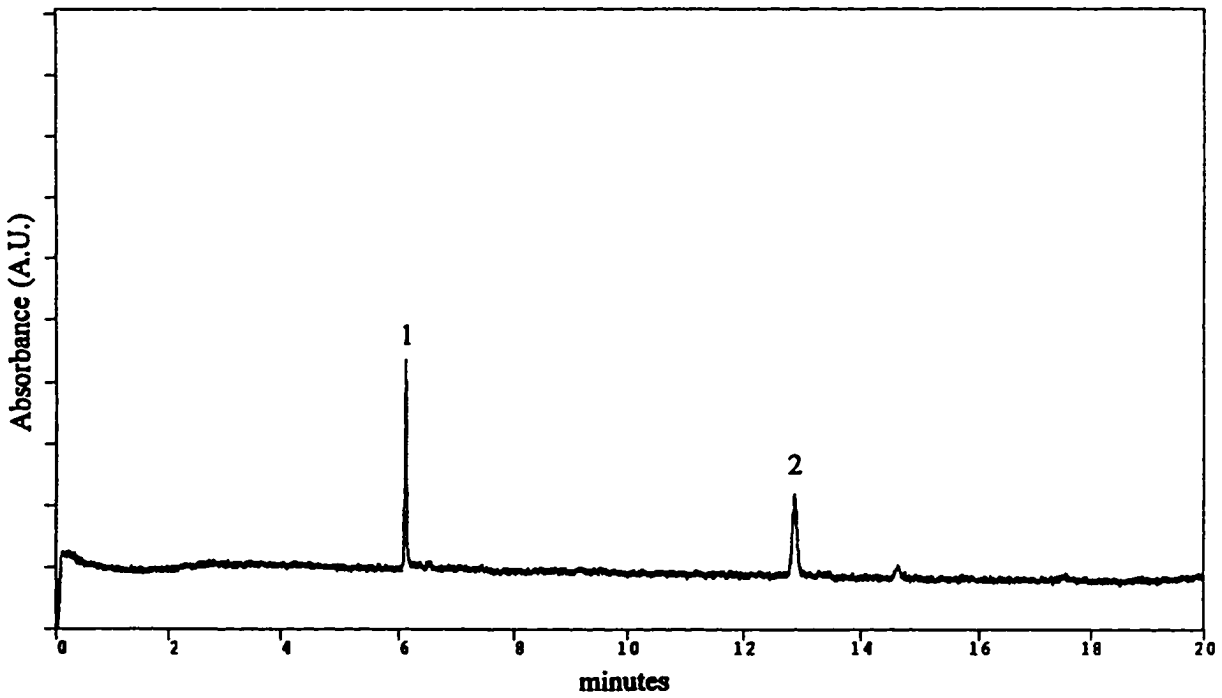

Figure 3B. Electropherogram of 20 μg ml^{-1} of platinum (II) ($PtCl_4^{2-}$) after 48 hours. Conditions: fused-silica capillary, 60 cm x 75 μm I.D. (52.25 cm to detector); carrier solution, 4 mM H^+ - 25 mM Cl^-; applied voltage, -10 kV; UV detection at 214 nm; sampling time, 30 s. Peaks: (1) $PtCl_4^{2-}$ and (2) $PtCl_3(H_2O)^-$.

Table 1. Average migration times (t_m) of the chloro complexes of the noble metals where s.d. is the standard deviation, RSD is relative standard deviation, and n is the number of replications. Conditions as in Fig. 1.

analyte	t_m (min)	s.d.(min)	RSD (%)	n
gold (III)				
$AuCl_4^-$	10.60	0.11	1	7
iridium (III)				
$IrCl_6^{3-}$	6.51	0.03	0.5	3
$IrCl_5(H_2O)^{2-}$	8.78	0.07	0.8	3
$IrCl_4(H_2O)_2^-$	16.49	0.12	0.7	3
iridium (IV)				
$IrCl_6^{3-}$ (Ir III)	6.49	0.04	0.6	3
$IrCl_6^{2-}$	7.47	0.05	0.7	3
$IrCl_5(H_2O)^{2-}$ (Ir III)	8.73	0.08	1	2
$IrCl_5(H_2O)^-$	16.42	0.23	1.4	3
osmium (IV)				
$OsCl_6^{2-}$	7.41	0.05	0.6	8
$OsCl_5(H_2O)^-$	11.19	0.09	0.8	3
palladium (II)				
$PdCl_4^{2-}$	-	0	0	6
$PdCl_3(H_2O)^-$	8.91	0.02	0.2	6

Table 1. (continued)

analyte	t_m (min)	s.d. (min)	RSD (%)	n
palladium (IV)				
$PdCl_6^{2-}$	-	0	0	4
$PdCl_5(H_2O)^-$	9.30	0.08	0.9	4
platinum (II)				
$PtCl_4^{2-}$	6.19	0.03	0.5	8
$PtCl_3(H_2O)^-$	12.98	0.09	0.7	4
platinum (IV)				
contaminant	6.58	0.13	1.9	3
$PtCl_6^{2-}$	7.50	0.13	1.8	4
$PtCl_5(H_2O)^-$	15.00	0.14	0.9	3
rhodium (III)				
$RhCl_6^{3-}$	-	0	0	5
$RhCl_5(H_2O)^{2-}$	8.78	0.07	0.8	5
$RhCl_4(H_2O)_2^-$	16.09	0.06	0.4	3
$RhCl_3OH(H_2O)_2^-$	16.34	0.04	0.2	3
ruthenium (III)				
$RuCl_6^{3-}$	-	0	0	2
$RuCl_5(H_2O)^{2-}$	9.51	0.01	0.1	2
$RuCl_4(H_2O)_2^-$	13.51	0.01	0.1	2
$RuCl_3OH(H_2O)_2^-$	16.32	0.10	0.6	5

predictions that could be made from the data in Table 1. These include: resolution of Pt (II) - (IV) mixtures (Fig. 4); separation of $IrCl_6^{3-}$, $IrCl_6^{2-}$ and $IrCl_5(H_2O)^{2-}$ (Fig. 4A); separation of $OsCl_6^{2-}$, $PdCl_4^{2-}$, $AuCl_4^-$, and $RuCl_4(H_2O)_2^-$; separation of eight anions (Fig. 5, 5A, 5B, 5C, and 5D).

Oxidation-reduction reactions between anions of the noble metals can occur in solution. For example, the standard electrode potentials for $AuCl_4^-$ - $AuCl_2^-$ ($E°$=0.93 V) and $PtCl_6^{2-}$ - $PtCl_4^{2-}$ ($E°$=0.68 V) suggests that gold (III) will oxidize platinum(II) to platinum (IV).

The products of an oxidation-reduction between $AuCl_4^-$ and $PtCl_4^{2-}$ are shown in Fig. 6. The peaks for platinum (IV) chloro complexes appear in the electropherogram along with the peaks for the unreacted chloro complexes of the gold (III) and platinum (II). The gold (I) chloro complex ($AuCl_2^-$) is probably reduced further to Au°, so a peak is not observed for it.

Quantitative determinations are feasible. Linear calibration plots between 3 and 30 ppm were obtained for several elements that give only one peak: Pt (II), r = 0.9997; Au (III), r = 0.998; Os (IV), r = 0.997. However, for plots of peak height vs. concentration, the chloride concentration of samples needs to be kept constant. For $AuCl_4^-$ the greatest peak height occurred when the chloride concentration in the sample was 8 mM (Fig. 7). This is due to electrostacking where the analyte zone becomes concentrated into a thin band within the capillary. The optimum concentration of 8 mM corresponds to a three to one ratio between the chloride concentrations of the carrier electrolyte and the sample.

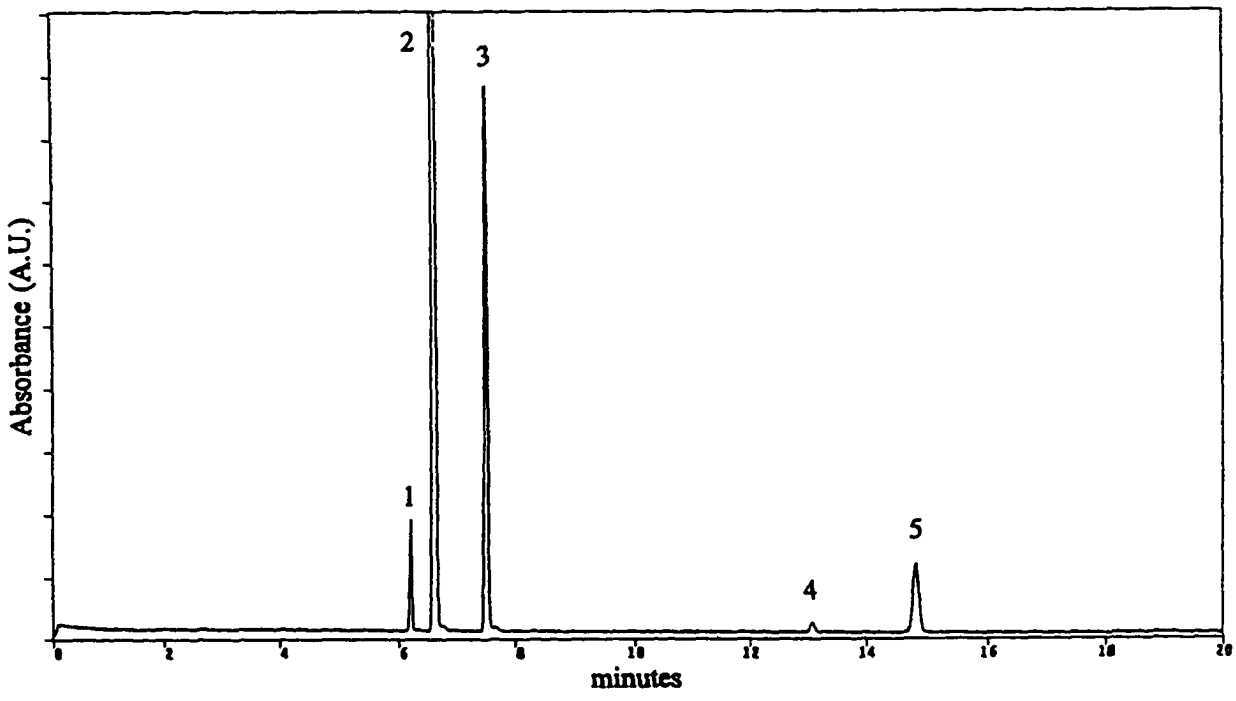

Figure 4. Electropherogram of the chloro complexes of Pt (II) and (IV) at 20 μg ml^{-1} each. Peaks: (1) $PtCl_4^{2-}$, (2) contaminant, (3) $PtCl_6^{2-}$, (4) $PtCl_3(H_2O)^-$ and (5) $PtCl_5(H_2O)^-$. Conditions as in Fig. 1.

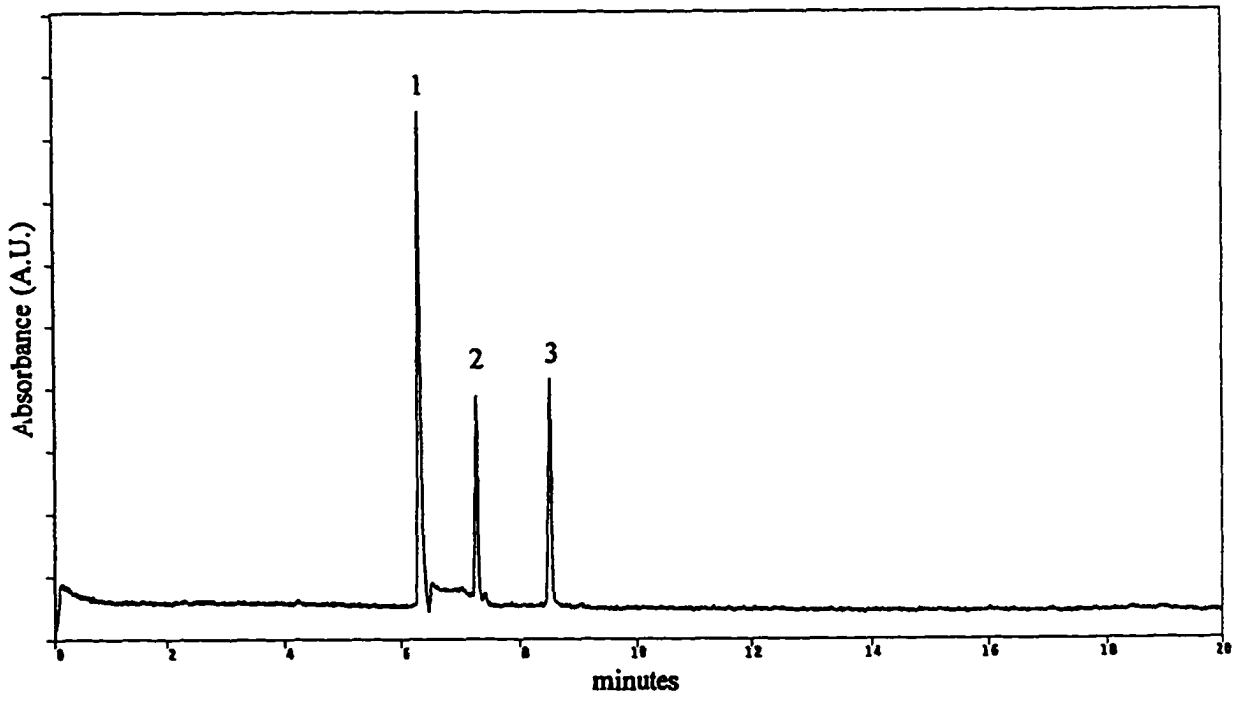

Figure 4A. Electropherogram of the chloro complexes of Ir (III) and (IV) at 20 μg ml^{-1} each. Conditions: fused-silica capillary, 60 cm x 75 μm I.D. (52.75 cm to detector); carrier solution, 4 mM H^+ - 25 mM Cl^-; applied voltage, -10 kV; UV detection at 214 nm; sampling time, 30 s. Peaks: (1) Ir (III) [$IrCl_6^{3-}$], (2) Ir (IV) [$IrCl_6^{2-}$] and (3) Ir (III) [$IrCl_5(H_2O)^{2-}$].

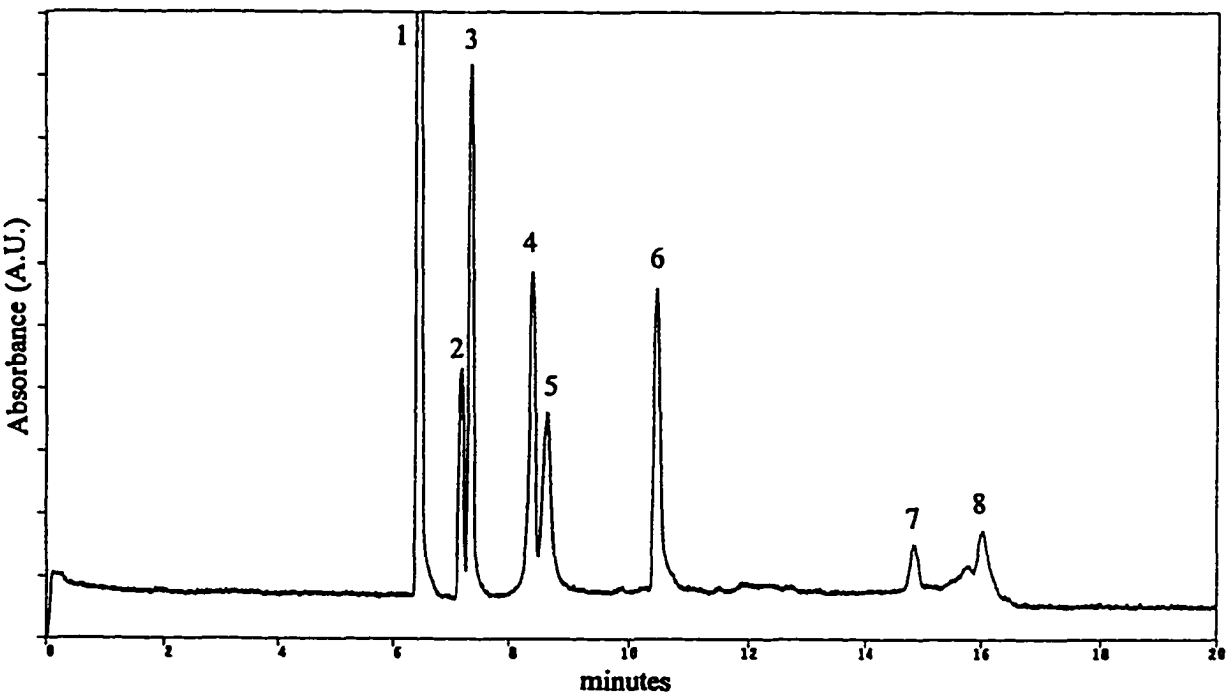

Figure 5. Electropherogram showing the separation of the chloro complexes of osmium (IV), platinum (IV), rhodium (III), palladium (II), gold (III), and ruthenium (III) at 10 μg ml^{-1} each. Peaks: (1) contaminant, (2) Os (IV) [$OsCl_6^{2-}$], (3) Pt (IV) [$PtCl_6^{2-}$], (4) Rh (III) [$RhCl_6^{3-}$], (5) Pd (II) [$PdCl_4^{2-}$], (6) Au (III) [$AuCl_4^-$], (7) Pt (IV) [$PtCl_5(H_2O)^-$], and (8) Ru (III) [$RuCl_3OH(H_2O)_2^-$]. Conditions as in Fig. 2.

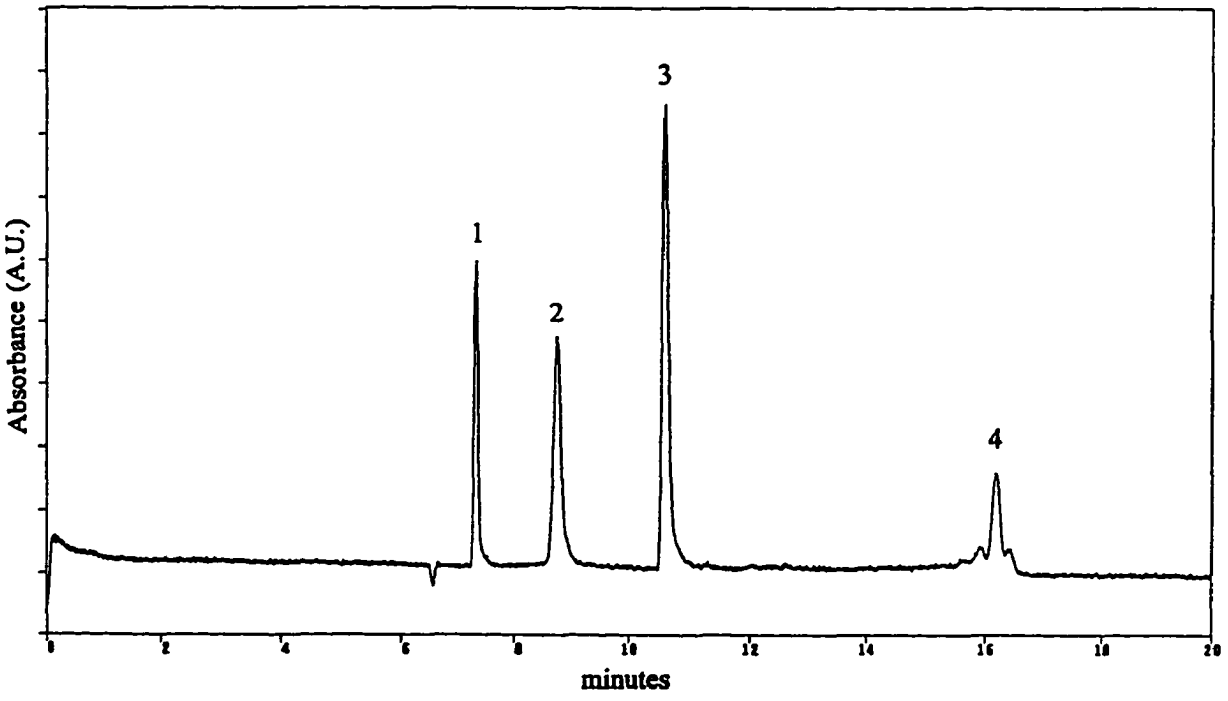

Figure 5A. Electropherogram showing the separation of the chloro complexes of osmium (IV), palladium (II), gold (III) and ruthenium (III) at 10 μg ml^{-1} each. Conditions: fused-silica capillary, 60 cm x 75 μm I.D. (52.25 cm to detector); carrier solution, 4 mM H^+ - 25 mM Cl^-; applied voltage, -10 kV; UV detection at 214 nm; sampling time, 30 s. Peaks: (1) Os (IV) [$OsCl_6^{2-}$], (2) Pd (II) [$PdCl_4^{2-}$], (3) Au (III) [$AuCl_4^-$] and (4) Ru (III) [$RuCl_4(H_2O)_2^-$].

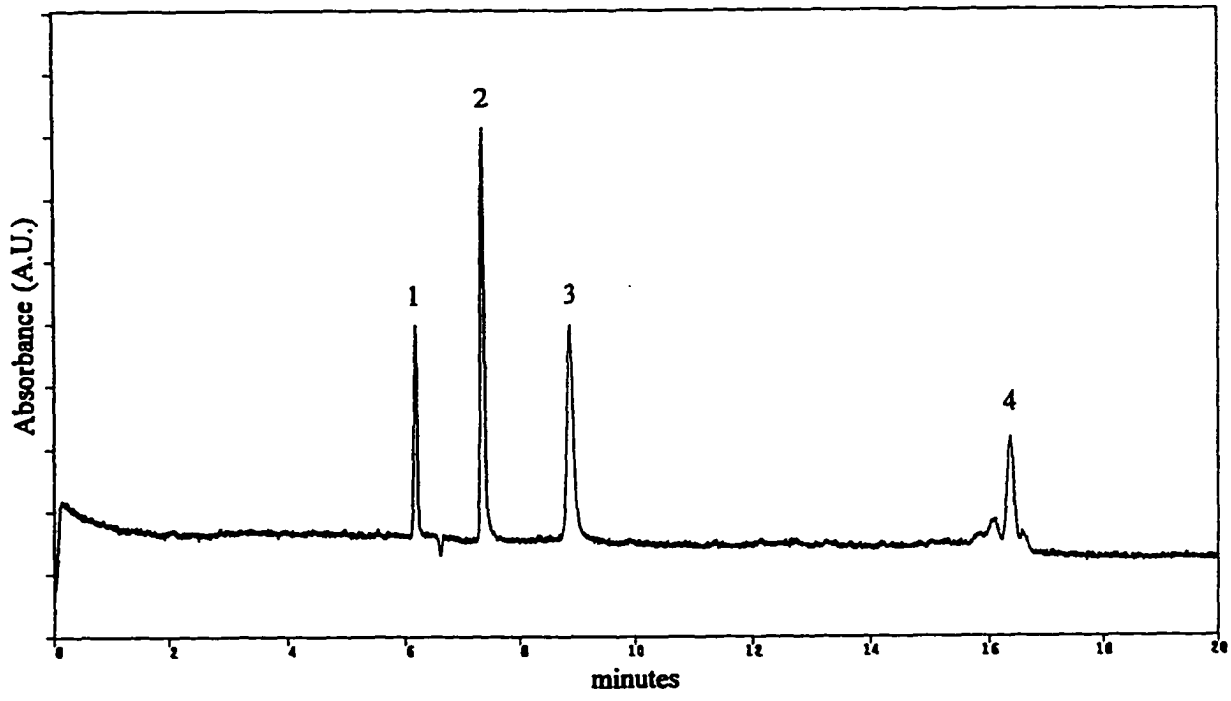

Figure 5B. Electropherogram showing the separation of the chloro complexes of platinum (II), osmium (IV), palladium (II) and ruthenium (III) at 10 μg ml^{-1} each. Conditions: fused-silica capillary, 60 cm x 75 μm I.D. (52.25 cm to detector); carrier solution, 4 mM H^+ - 25 mM Cl^-; applied voltage, -10 kV; UV detection at 214 nm; sampling time, 30 s. Peaks: (1) Pt (II) [$PtCl_4^{2-}$], (2) Os (IV) [$OsCl_6^{2-}$], (3) Pd (II) [$PdCl_4^{2-}$] and (4) Ru (III) [$RuCl_4(H_2O)_2^-$].

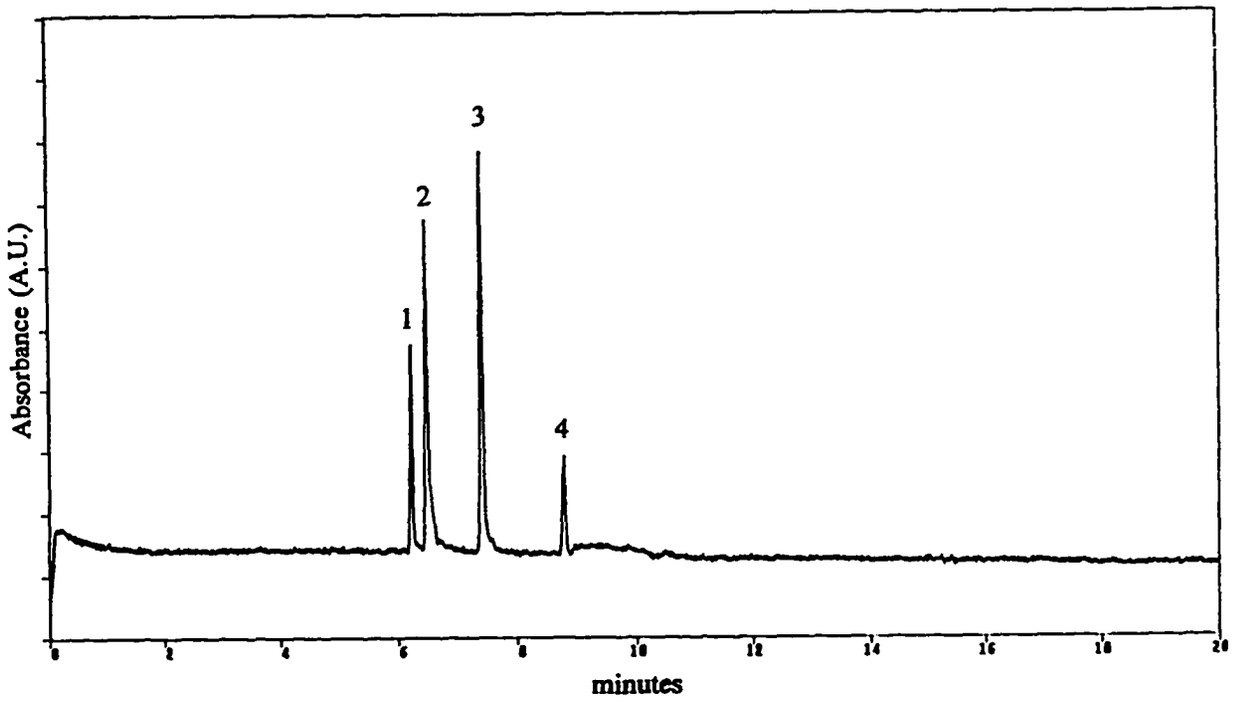

Figure 5C. Electropherogram showing the separation of the chloro complexes of platinum (II), osmium (IV), and iridium (III) at 10 μg ml^{-1} each. Conditions: fused-silica capillary, 60 cm x 75 μm I.D. (52.25 cm to detector); carrier solution, 4 mM H^+ - 25 mM Cl^-; applied voltage, -10 kV; UV detection at 214 nm; sampling time, 30 s. Peaks: (1) Pt (II) [$PtCl_4^{2-}$], (2) Ir (III) [$IrCl_6^{3-}$], (3) Os (IV) [$OsCl_6^{2-}$] and (4) Ir (III) [$IrCl_5(H_2O)^{2-}$].

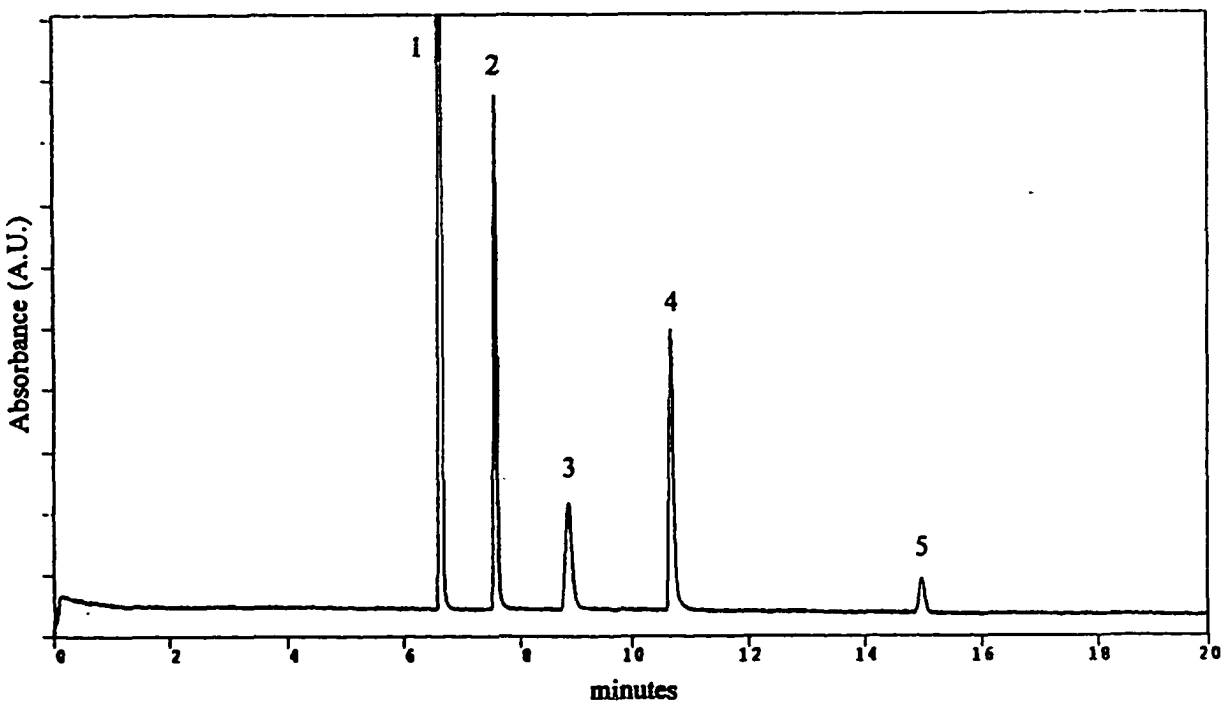

Figure 5D. Electropherogram showing the separation of the chloro complexes of platinum (IV), palladium (II), and gold (III) at 10 μg ml^{-1} each. Conditions: fused-silica capillary, 60 cm x 75 μm I.D. (52.25 cm to detector); carrier solution, 4 mM H^+ - 25 mM Cl^-; applied voltage, -10 kV; UV detection at 214 nm; sampling time, 30 s. Peaks: (1) contaminant, (2) Pt (IV) [$PtCl_6^{2-}$], (3) Pd (II) [$PdCl_4^{2-}$], (4) Au (III) [$AuCl_4^-$] and (5) Pt (IV) [$PtCl_5(H_2O)^-$].

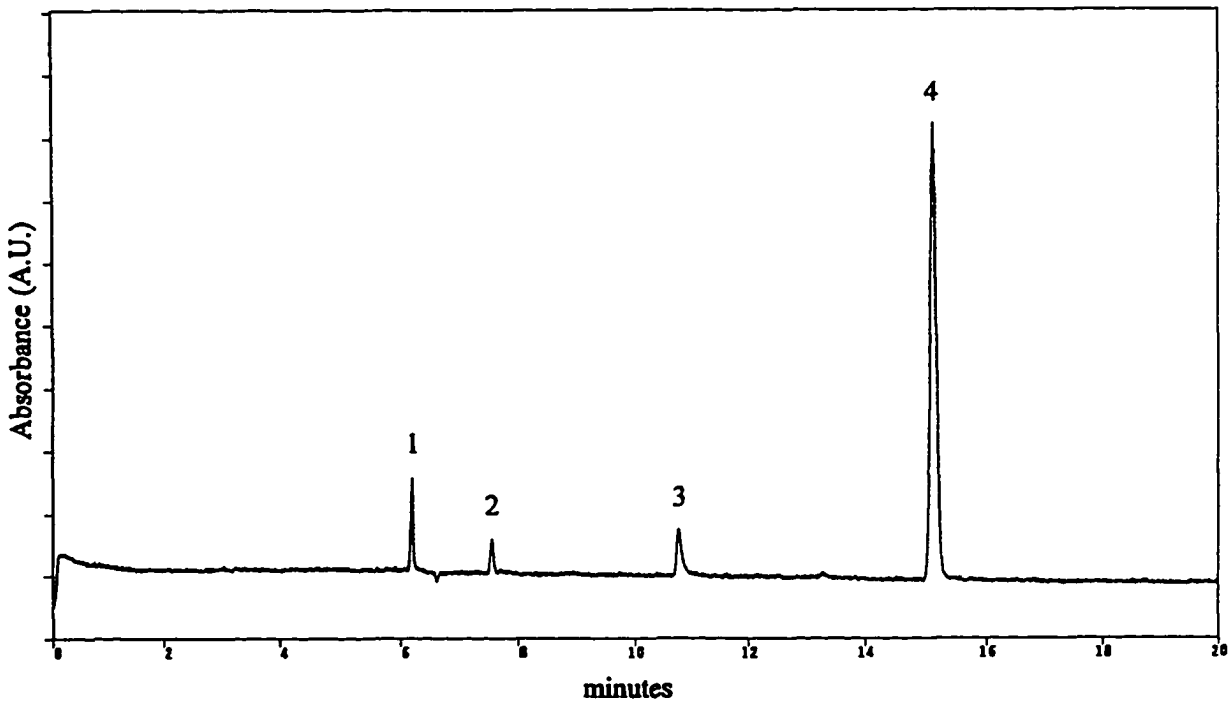

Figure 6. Electropherogram showing the redox reaction between 20 μg ml^{-1} of $PtCl_4^{2-}$ and 10 μg ml^{-1} of $AuCl_4^-$. Peaks: (1) $PtCl_4^{2-}$, (2) $PtCl_6^{2-}$, (3) $AuCl_4^-$ and (4) $PtCl_5(H_2O)^-$. Conditions as in Fig. 2.

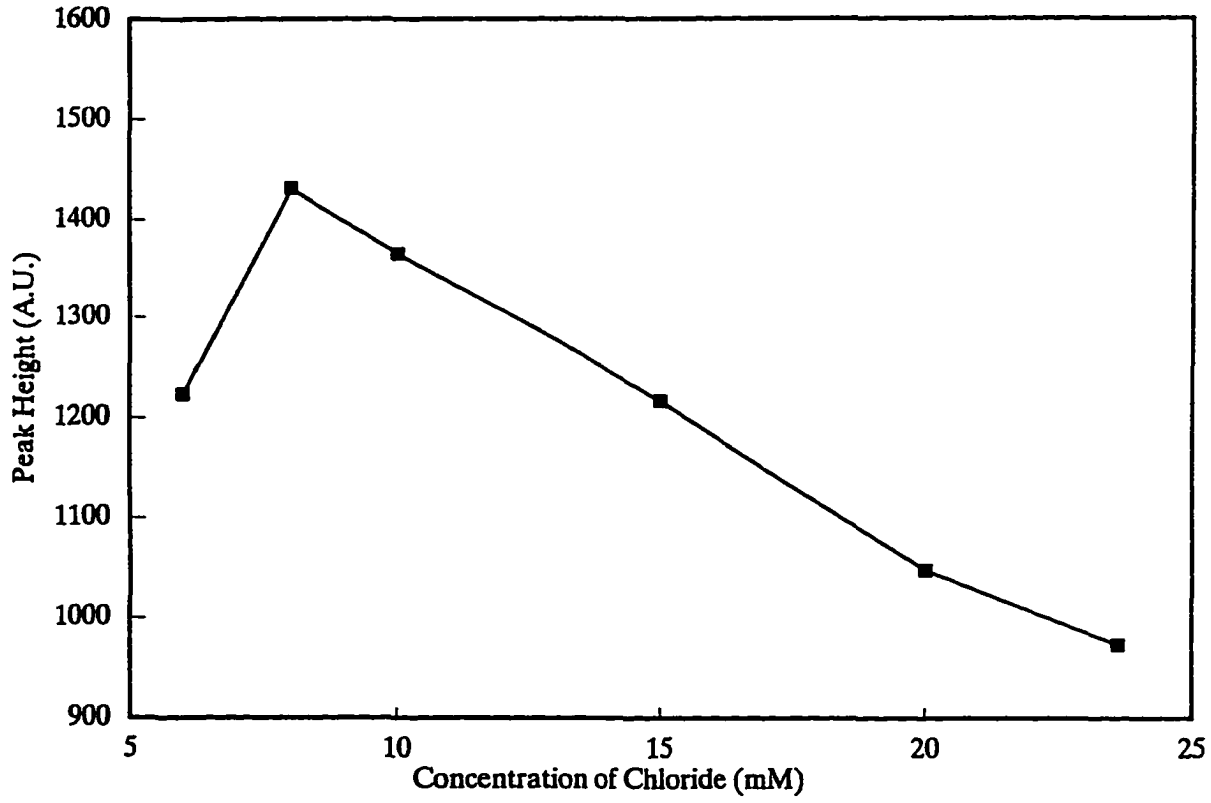

Figure 7. Effect of chloride concentration in the sample dilution of the gold (III) chloro complex on the peak height. Conditions as in Fig. 1.

3.2. Separation of other anions

Other inorganic anions can also be separated by CE at pH 2.4 in a hydrochloric acid solution. Fig. 8 shows a good separation of MnO_4^-, ReO_4^-, VO_3^-, a complex chromium (III) trioxalate anion, and a chromium (VI) anion. CE is attractive for the separation of strongly oxidizing ions such as permanganate and vanadate because the ions are not in contact with any organic matter that might reduce the anions. A chloro complex of mercury (II), probably $HgCl_4^{2-}$, could also be separated (t_m = 14.0 min), although the peak was rather broad (Fig. 8A).

The effect of pH on the CE behavior of chromium (VI) and molybdenum (VI) anions was studied. A symmetrical peak was obtained for chromium (VI) between pH 2.0 and 4.4. At pH 5.1, the peak started to broaden and tail, up to pH 6.7. Between pH 7.2 and 8.5, a sharp symmetrical peak was obtained. The acid dissociation constants for H_2CrO_4 have been given as $k_1 = 1 \cdot 10^{0.2}$ and $k_2 = 1 \cdot 10^{-6.5}$ [11]. Thus, the peak observed between pH 2.0 and 4.4 is most likely $HCrO_4^-$ or the dimer $Cr_2O_7^{2-}$. The peak observed between pH 7.2 and 8.5 would be CrO_4^{2-}.

Acid dissociation constants for H_2MoO_4 have been given as $k_1 = 1 \cdot 10^{-4.0}$ and $k_2 = 1 \cdot 10^{-4.24}$ [11]. No peak was detected for molybdenum (VI) until pH 3.8 and a sharp symmetrical peak was not obtained until pH 6.6 (Fig. 8B). This was probably MoO_4^{2-}.

Sharp peaks were obtained for both ferrocyanide ($Fe(CN)_6^{4-}$, t_m = 8.3 min) and ferricyanide ($Fe(CN)_6^{3-}$, t_m = 6.5 min) (Fig. 8C). From the formulas above, ferrocyanide with a negative four charge would be expected to migrate faster than ferricyanide with a negative three charge. However, the acid dissociation constants need to be considered: for $H_2Fe(CN)_6^{2-}$ $k_1 = 1 \cdot 10^{-1.9}$ and $k_2 = 1 \cdot 10^{-3.7}$ [11]. At pH 2.4, the average charge was

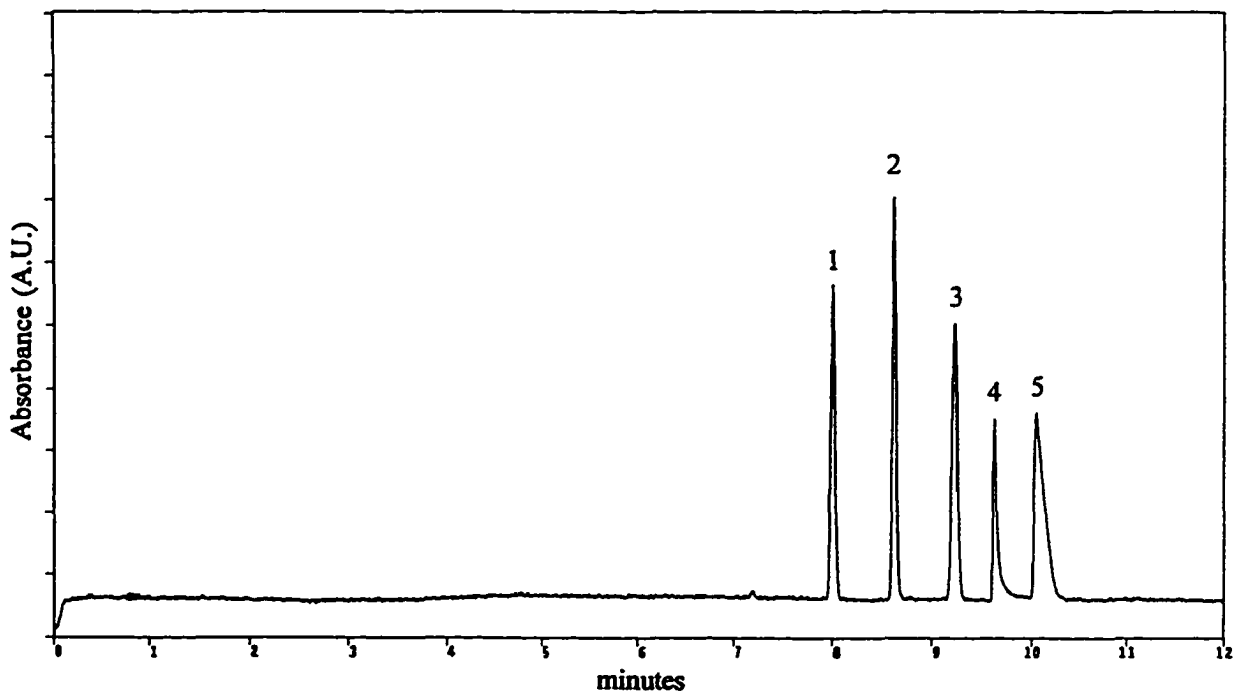

Figure 8. Electropherogram showing the separation of the anions permanganate (35 μg ml^{-1}), chromium oxalate (10 μg ml^{-1}), perrhenate (20 μg ml^{-1}), vanadate (20 μg ml^{-1}), and chromate (20 μg ml^{-1}). Peaks: (1) MnO_4^-, (2) $CrOx_3^{3-}$, (3) ReO_4^-, (4) VO_3^- and (5) $Cr_2O_7^{2-}$. Conditions as in Fig. 2.

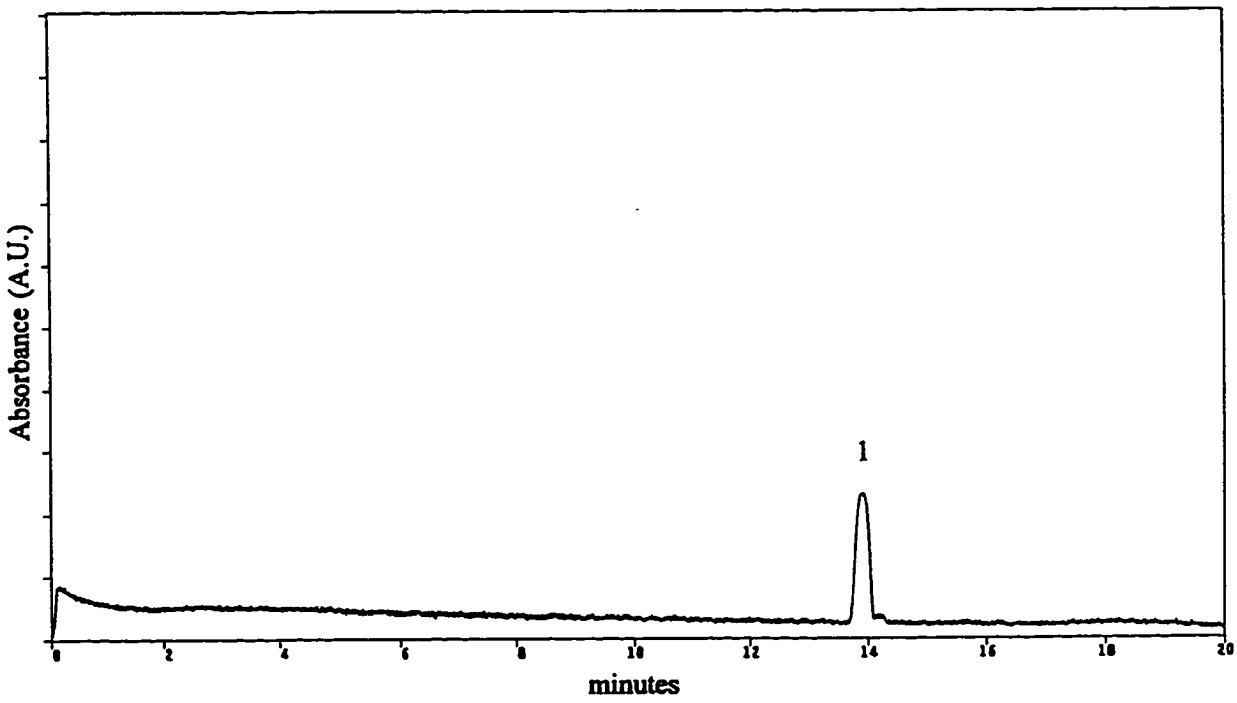

Figure 8A. Electropherogram of 20 μg ml^{-1} of $HgCl_4^{2-}$. Conditions: fused-silica capillary, 60 cm x 75 μm I.D. (52.75 cm to detector); carrier solution, 4 mM H^+ - 25 mM Cl^-; applied voltage, -10 kV; UV detection at 214 nm; sampling time, 30 s. Peak: (1) $HgCl_4^{2-}$.

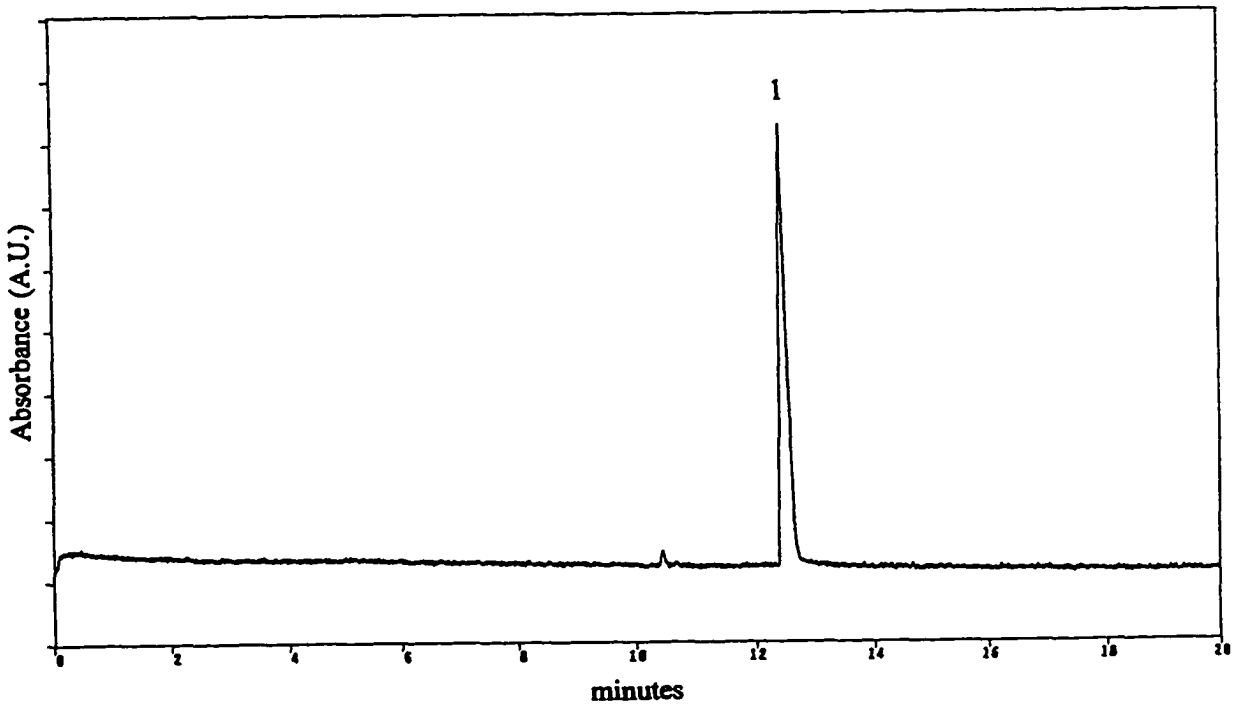

Figure 8B. Electropherogram of 20 μg ml^{-1} of molybdate at pH 6.6. Conditions: fused-silica capillary, 60 cm x 75 μm I.D. (52.75 cm to detector); carrier solution, 0.25 μM H^+, 25 mM Cl^-; applied voltage, -10 kV; UV detection at 214 nm; sampling time, 30 s. Peak: (1) MoO_4^{2-}.

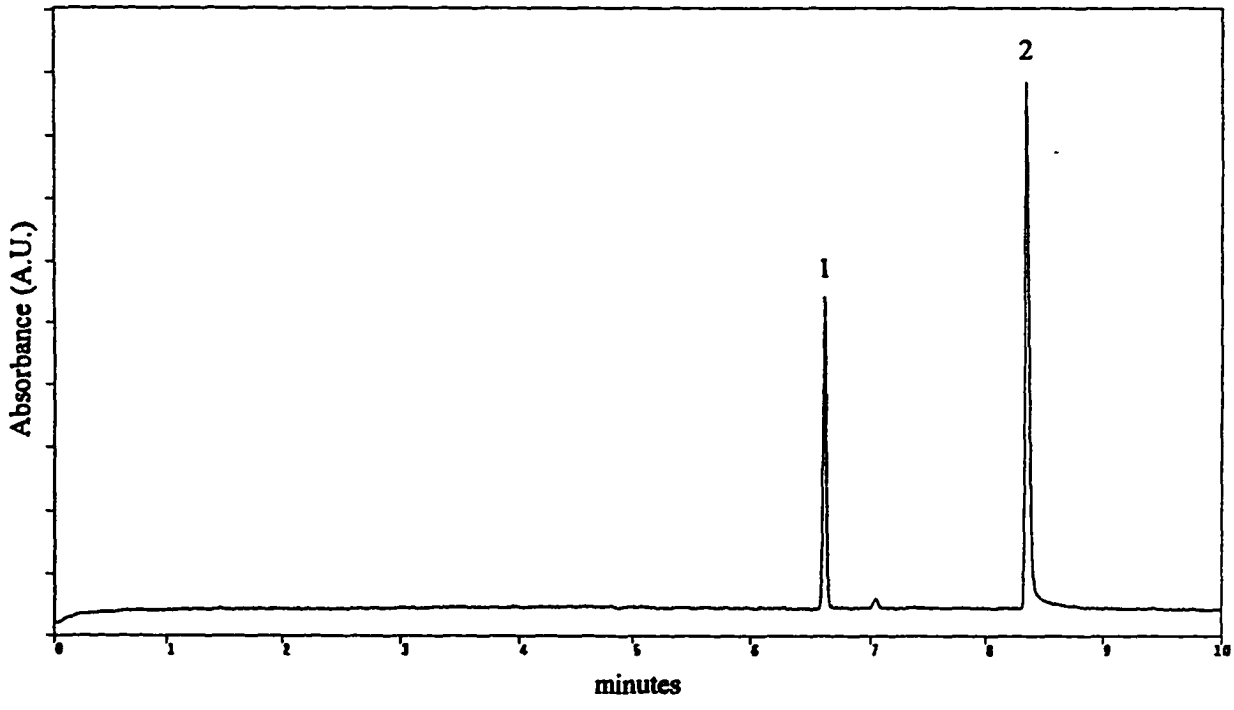

Figure 8C. Electropherogram showing the separation of the cyanide complexes of iron (II) and (III) at 10 μg ml^{-1} each. Conditions: fused-silica capillary, 60 cm x 75 μm I.D. (52.75 cm to detector); carrier solution, 4 mM H^+ - 25 mM Cl^-; applied voltage, -10 kV; UV detection at 214 nm; sampling time, 30 s. Peaks: (1) Fe (III) $[Fe(CN)_6^{3-}]$ and (2) Fe (II) $[HFe(CN)_6^{3-}]$.

calculated to be a negative 2.8 which is less than a negative 3.0, for ferricyanide for which no acid dissociation constants were listed.

Sharp peaks were obtained for several additional inorganic anions in HCl solution at pH 2.4: I^-, Br^-, NO_3^-, SCN^-, IO_4^-, and IO_3^-. Migration times for the inorganic anions studied (other than the noble metals) are given in Table 2. The migration times were very reproducible, with a relative standard deviation of 0.6%.

The use of electrolytes containing perchloric acid instead of hydrochloric acid was investigated briefly. A separation of five anions in perchloric acid at pH 2.4 is shown in Fig. 9. The migration times were similar to those obtained in hydrochloric acid at the same pH. Electropherograms for the same ions (see Fig. 9) were also run in more acidic solutions of perchloric acid. Good separations were obtained in perchloric acid at pH 2.0 and 1.8, but an attempted separation at pH 1.6 gave a very erratic baseline with no good peaks for the anionic analytes.

The effect of pH was studied over a broad range for several anions. Observed mobilities are plotted as a function of pH in Fig. 10. The rapid drop in mobility just above pH 5 is due to an increased electroosmotic mobility as the capillary's silanol groups become more ionized. The electroosmotic mobility, which was measured by reversing the direction of applied voltage, jumped from 0.13 ($cm^2V^{-1}s^{-1}$) at pH 5.0 to 0.40 at pH 5.2 and then increased gradually to 0.46 at pH 8.0. The electroosmotic mobility at pH 4.0 was 0.08 and was too low to be measured at even more acidic pH values. Electrophoretic mobilities remained almost constant between pH 4 and 8. These data show that anions can be separated by CE between pH 1.8 and 5.0.

Table 2. Average migration times (t_m) of other metal anions where s.d. is the standard deviation, RSD is relative standard deviation, and n is the number of replications. Conditions as in Fig. 2 except for molybdate at pH 6.6.

analyte	t_m (min)	s.d. (min)	RSD (%)	n
$Cr_2O_7^{2-}$	10.06	0.03	0.3	3
$CrOx_3^{3-}$	8.62	0.04	0.5	3
$HgCl_4^{2-}$	13.95	0.06	0.4	2
MnO_4^-	8.06	0.08	1	2
ReO_4^-	9.23	0.03	0.3	3
VO_3^-	9.61	0.02	0.2	3
MoO_4^{2-}	12.44	0.00	0	1
$Fe(CN)_6^{3-}$	6.53	0.09	1.4	3
$HFe(CN)_6^{3-}$	8.33	0.03	0.3	3
I^-	5.68	0.01	0.20	3
NO_3^-	6.26	0.01	0.12	6
SCN^-	6.61	0.01	0.12	6
IO_4^-	8.61	0.01	0.18	3
IO_3^-	10.95	0.04	0.36	6
Br^-	5.63	0.01	0.10	3

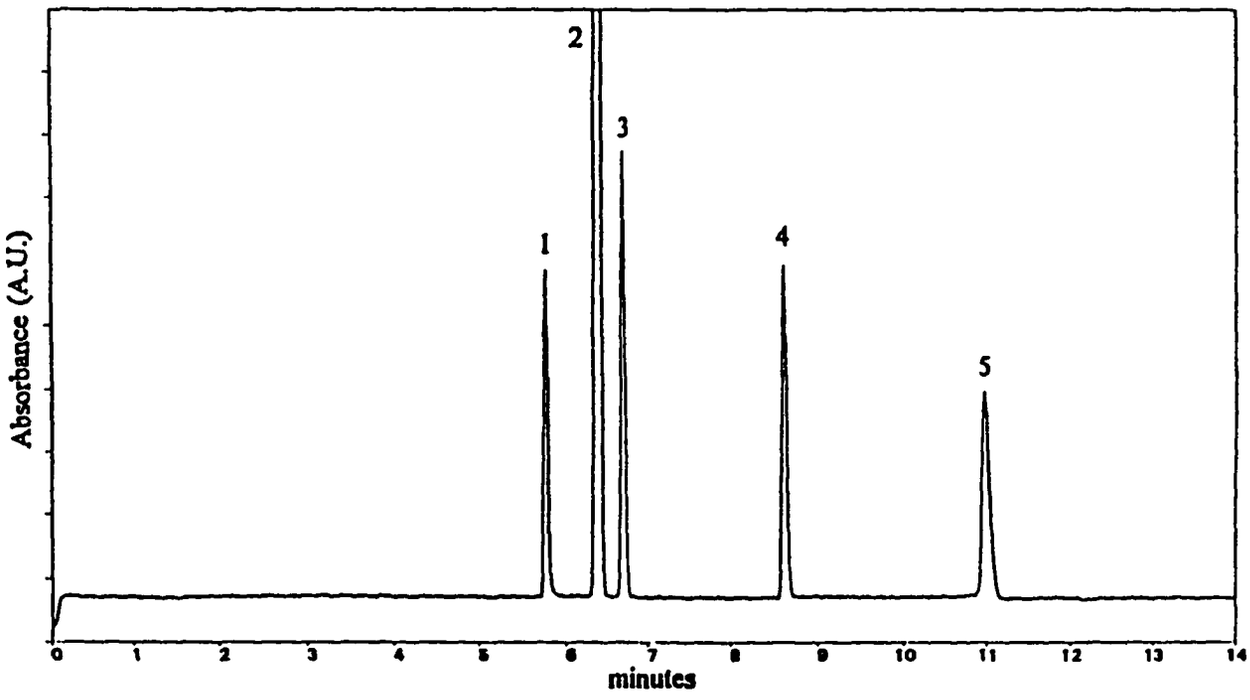

Figure 9. Separation of inorganic anions in 25 mM perchloric acid (pH 2.4). Other conditions as in Figure 2. Peaks: (1) I^-, (2) NO_3^-, (3) SCN^-, (4) IO_4^-, and (5) IO_3^-.

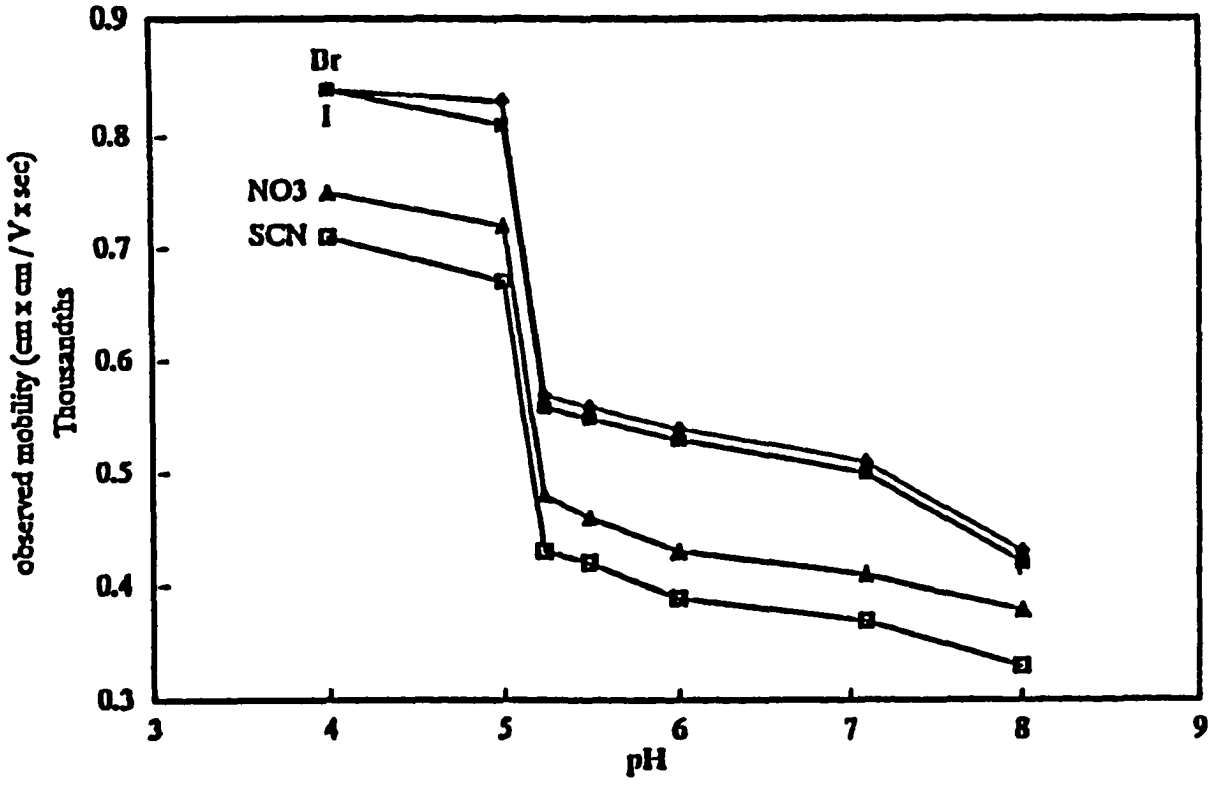

Figure 10. Effect of pH on observed mobility. Acetate-acetic acid, ammonium acetate, or ammonium acetate-sodium acetate buffers were used. Other conditions as in Fig. 2.

4. Conclusions

Anionic chloro complexes of the noble metals, as well as a number of other inorganic anions, can be separated efficiently in very acidic solutions (pH 2.4) by capillary electrophoresis. Although the currents were higher than normally encountered in CE, sharp peaks and stable baselines were obtained by operating at a relatively low applied voltage (-10 kV). The method used was the utmost in simplicity for anions amenable to direct photometric detection. At the acidic pH values used, no buffer was needed other than HCl or $HClO_4$. No flow modifier was required because electroosmotic flow was minimal in the acidic electrolytes that were used. This avoids the possibility of anion precipitation by positively-charged flow modifiers and also avoids the surface buildup that sometimes occurs with such modifiers.

Acknowledgements

We wish to thank Waters Chromatography Division of Millipore for their gift of the Waters Quanta 4000 CE instrument and associated chemicals and supplies.

Ames Laboratory is operated for the U.S. Department of Energy under Contract No. W-7405-Eng-82. This work was supported by the Director of Energy Research, Office of Basic Energy Sciences.

References

1. W. R. Jones and P. Jandik, *Am. Lab.*, 22 (1990) 51.
2. X. Huang, T. J. Pang, M. J. Gordon and R. N. Zare, *Anal. Chem.*, 59 (1987) 2747.

3. J. Romano, P. Jandik, W. R. Jones and P. E. Jackson, *J. Chromatagr.*, 546 (1991) 411.

4. P. Jandik and W. R. Jones, *J. Chromatagr.*, 546 (1991) 431.

5. W. R. Jones and P. Jandik, *J. Chromatagr.*, 546 (1991) 445.

6. B. J. Wildman, P. E. Jackson, W. R. Jones and P. G. Alden, *J. Chromatagr.*, 546 (1991) 459.

7. M. Aguilar, X. Huang and R. N. Zare, *J. Chromatogr.*, 480 (1989) 427.

8. W. Buchberger, O. P. Semenova and A. R. Timerbaev, *J. High Resolut. Chromatogr.*, 16 (1993) 153.

9. B. Baraj, A. Sastre, A. Merkoci and M. Martínez, *J. Chromatogr. A*, 718 (1995) 227.

10. B. Baraj, A. Sastre, M. Martínez and K. Spahiu, *Anal. Chim. Acta*, 319 (1996) 191.

11. A. E. Martell and R. M. Smith, *Critical Stability Constants, Volume 6: Second Supplement*, Plenum Press, New York, 1989, pp. 432-433.

CHAPTER 3. SEPARATION OF NATIVE AMINO ACIDS AT LOW PH BY CAPILLARY ELECTROPHORESIS

A paper submitted to the Journal of High Resolution Chromatography

Michelle J. Thornton[1,2], Christian W. Klampfl[3] and James S. Fritz[1,4]

Abstract

Amino acids are cations at low pH and can be readily separated by capillary electrophoresis provided that an alkanesulfonic acid is added to the electrolyte carrier. Formation of a positive net charge on the bare fused-silica surface at low pH was confirmed by measurement of an anodic electroosmotic flow. The addition of ethanesulfonic acid or octanesulfonic acid to the electrolyte carrier causes a reversal of the EOF. A mechanism is proposed in which the alkanesulfonate adsorbs to the positively-charged capillary wall through electrostatic attraction. Adsorption of a second molecule of alkanesulfonate by hydrophobic attraction to the carbon chain forms a negatively-charged coating on the capillary wall. The alkanesulfonate also imparts selectivity to the system by participation in ion-pairing interactions with the native amino acids to improve resolution. The CE separation of a mixture of the twenty common amino acids at pH 2.8 with direct absorbance detection at 185 nm resulted in 17 amino

---

[1]Graduate student and Professor, respectively, Department of Chemistry and Ames Laboratory, Iowa State University, Ames, IA 50011, USA.

[2]Primary researcher and author

[3]Department of Analytical Chemistry, Johannes Kepler University Linz, Altenbergerstrasse 69, A-4040 Linz, Austria.

[4]Author for correspondence

acid peaks in 20 minutes with a 30 kV applied voltage. The effect of several variables was studied including electrolyte carriers containing different alkanesulfonic acids, the influence of pH, applied voltage, and concentration of electrolyte carrier.

I. Introduction

Most studies involving the separation and detection of amino acids have been done under neutral or alkaline conditions. Amino acids separated by capillary electrophoresis (CE) are usually detected by fluorescence or laser-induced fluorescence through derivatization with fluorescent probes [1,2]. Detection of underivatized amino acids has also been achieved by indirect fluorescence [3,4], indirect UV absorbance [5-9], amperometric [10], and refractive index gradient [11].

Little has been published on the direct UV detection of underivatized amino acids separated by CE at an acidic pH. Bergman et al. [12] reported the use of direct UV detection at 214 nm in the CE separation of six amino acids with 50 mM phosphate at pH 2.5 as the electrolyte carrier. McCormick [13] reported the use of low pH aqueous buffers in CE separations of peptides and proteins in modified silica capillaries. He separated six dipeptides, differing by one amino acid, using a 150 mM H_3PO_4 buffer at pH 1.5.

In the present research, the use of alkanesulfonic acids as the buffer and an ion-pairing reagent under acidic conditions was investigated. The alkanesulfonic acids studied were octanesulfonic, butanesulfonic, ethanesulfonic, and methanesulfonic. The length of the hydrocarbon chain of the alkanesulfonic acid, the concentration of the alkanesulfonic acid, and the pH influence on the separation of the amino acids were

investigated. The alkanesulfonic acids were shown to affect the direction and magnitude of the electroosmotic flow (EOF).

2. Experimental

2.1 Apparatus

CE experiments were performed with a Waters Quanta 4000 capillary electrophoresis system (Waters Corporation, Milford, MA, USA). The polyimide-coated, fused-silica capillaries (Polymicro Technology, Phoenix, AZ, USA) were 50 μm I.D. and 60 cm in length. The distance from the point of injection to the window of on-column detection was 52.4 cm. Direct UV detection was employed at 185 nm. A voltage range of +10 to +30 kV was applied for the separations depending upon the pH of the electrolyte carrier. The time of hydrodynamic injection was 10 seconds. Electropherograms were collected and plotted by the data acquisition system Chrom Perfect Direct (Justice Innovations, Mountain View, CA, USA).

2.2 Procedure

New capillaries were conditioned by rinsing with 0.1 M NaOH for one hour followed by a one hour rinse with deionized (DI) water. Between different electrolyte carriers, the capillary was rinsed with acetonitrile for five minutes, 0.1 M NaOH for ten minutes, DI water for 10 minutes, and the electrolyte carrier for 30 minutes. The capillary was also purged with the electrolyte carrier for five minutes before each run.

2.3 Reagents

All standards and electrolytes were prepared with analytical-reagent grade chemicals and 18 MΩ deionized water obtained from a Barnstead Nanopure II system (Sybron Barnstead, Boston, MA, USA). The twenty common amino acids and the sodium salts of methanesulfonic, ethanesulfonic, butanesulfonic, and octanesulfonic acids, and the polyethylene oxide (MW 8 000) were obtained from Aldrich (Milwaukee, WI, USA). The alkanesulfonic acids were prepared as 0.6 M stock solutions. They were diluted to 25, 50, 75, or 100 mM for the electrolyte carrier. The pH was adjusted, as required, by adding aliquots of 0.1 M $HClO_4$ or H_3PO_4. Stock 5 to 10 mM solutions of amino acids were prepared in deionized water. Aliquots of each were mixed to obtain a mixture of twenty amino acids, each with a final concentration of 0.3 to 0.6 mM and 0.04 mM for the aromatic amino acids. The stock solution of PEO and acidified 0.2% PEO solution were prepared as described by Preisler and Yeung [14].

2.4 Electroosmotic mobility determination

Acetophenone and dimethyl sulfoxide (DMSO) were used as the neutral markers for the electroosmotic mobility determinations. The mobilities for the electrolyte carriers were determined by the accelerated measurement method described by Sandoval and Chen [15]. The neutral marker was injected in the HD mode for 2 to 10 seconds. For the aqueous buffers, the CE voltage of +20 or -20 kV was applied for 20 minutes. A voltage of +10 or -10 kV was applied for the most acidic electrolyte carriers. For the alkanesulfonate buffers, a voltage of +15 kV was applied for 30 or 60 minutes.

3. Results and Discussion

3.1 Conditions for amino acid separation

Experiments were first performed to check on the feasibility of a CE separation of underivatized amino acids and to establish the general conditions for a separation. Then each major variable was examined to determine its effect on the CE behavior and to optimize the conditions for the separation.

Initial attempts to separate the amino acid cations at low pH were disappointing. At pH 2.0, the protonated amino acid peaks were short, broad and badly tailed. Resolution was poor. However, it was found that addition of a fairly low concentration of octanesulfonic acid to the electrolyte carrier greatly improved both peak shape and resolution. Experiments with butane-, ethane-, and methanesulfonic acids showed that ethanesulfonic acid gave the best separations.

Our first successful experiments were carried out mostly at pH 3.2 with octanesulfonic acid or at pH 2.3 with 50 mM ethanesulfonic acid added to the electrolyte carrier. Figure 1 shows the electropherogram of twenty amino acids in 50 mM ethanesulfonate at pH 2.3. Eighteen amino acid peaks are identified. The migration order for the twenty amino acids is as follows and will be labelled this way throughout the text and figures: (1) lysine (Lys), (2) arginine (Arg), (3) histidine (His), (4) glycine (Gly), (5) alanine (Ala), (6) valine (Val), (7) serine (Ser), (8) isoleucine (Ile), (9) leucine (Leu), (10) threonine (Thr), (11) asparagine (Asn), (12) methionine (Met), (13) glutamine (Gln), (14) tryptophan (Trp), (15) glutamic acid (Glu), (16) phenylalanine (Phe), (17) proline (Pro), (18) tyrosine (Tyr), (19) cysteine (Cys), and (20) aspartic acid (Asp). Some of the amino acids co-migrated including Asn and Thr, Met and Gln, and

Figure 1. Electropherogram of twenty common amino acids. Electrolyte, 50 mM ethanesulfonate, pH 2.3; applied voltage, 20 kV; injection time, 10 s. Peaks: 1 = Lys; 2 = Arg; 3 = His; 4 = Gly; 5 = Ala; 6 = Val; 7 = Ser; 8 = Ile; 9 = Leu; 10 = Thr; 11 = Asn; 12 = Met; 13 = Gln; 14 = Trp; 15 = Glu; 16 = Phe; 17 = Pro; 18 = Tyr; 19 = Cys; 20 = Asp.

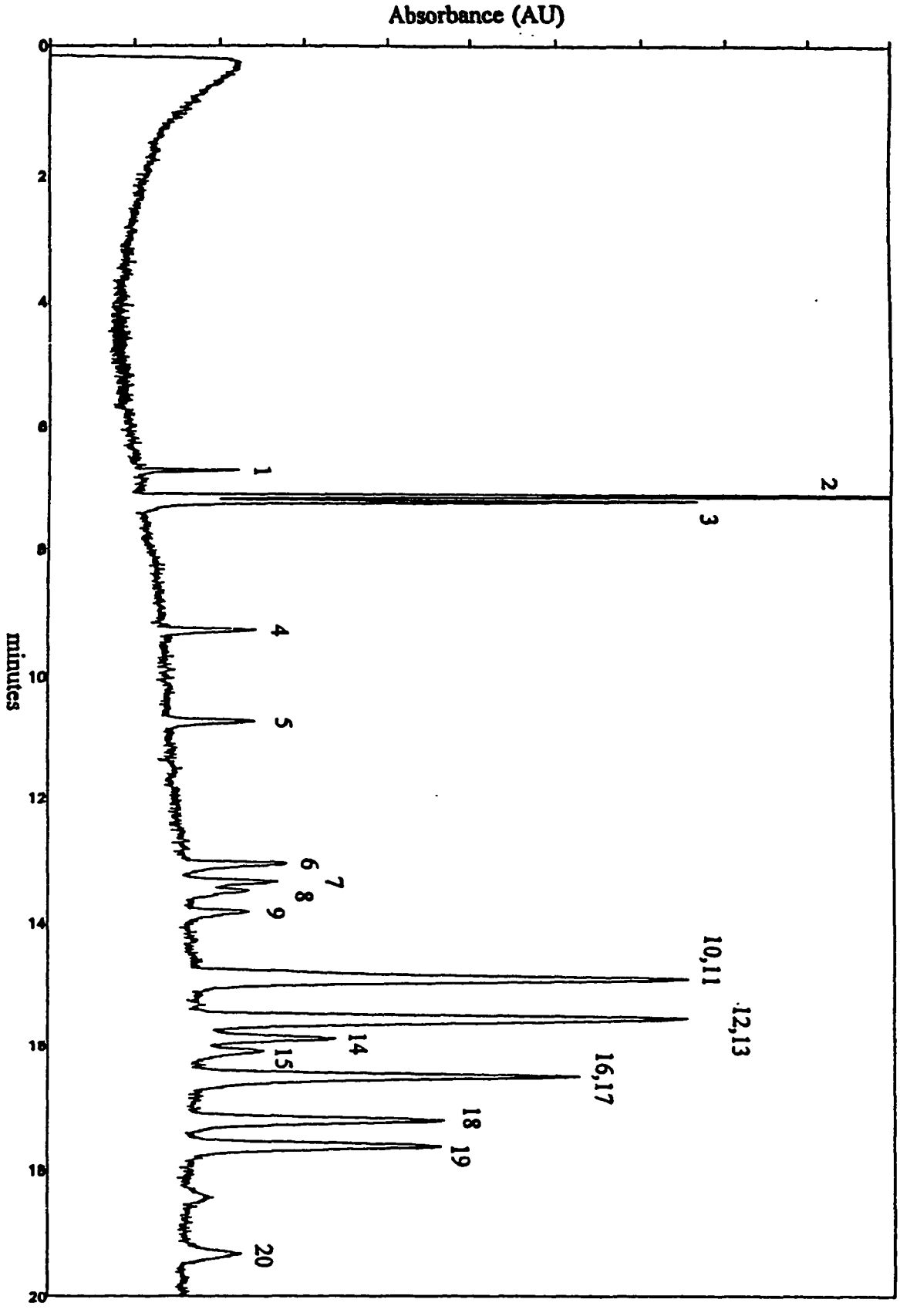
Absorbance (AU)
minutes
0
2
4
6
8
10
12
14
16
18
20
1
2
3
4
5
6
7
8
9
10,11
12,13
14
15
16,17
18
19
20

Phe and Pro.

3.2 Effect of alkanesulfonic acid

Addition of octane-, butane-, ethane-, and methanesulfonic acids to the running electrolyte was investigated to determine their effect on CE behavior. In the absence of any alkanesulfonic acid, no cathodic electroosmotic flow (EOF) was observed at pH 2.8 and lower. Addition of 50 mM concentrations of an alkanesulfonic acid induced a cathodic EOF. A negatively charged surface apparently was created by adsorption of some RSO_3^- onto the capillary surface. This coating could occur by a dynamic equilibrium between the alkanesulfonic acid in solution and on the capillary surface. Figure 2 shows that the EOF increases with longer chain length of the R group.

The effect of octanesulfonic acid concentration on the observed mobilities of several amino acids was determined at pH 2.4. The results in Figure 3 show a decrease in the mobilities up to 30 mM octanesulfonate with a leveling or slight increase thereafter. This behavior might be explained by an ion-pairing mechanism in solution between the amino acid cation (C^+) and the octanesulfonate anion (A^-).

$$C^+ + A^- \rightleftharpoons C^+A^-$$

This equilibrium would reduce the concentration of free C^+ and thus reduce the average positive charge on the amino acids, thereby slowing their migration. Little, if any, ion-pairing was evident when ethanesulfonate was used in place of octanesulfonate.

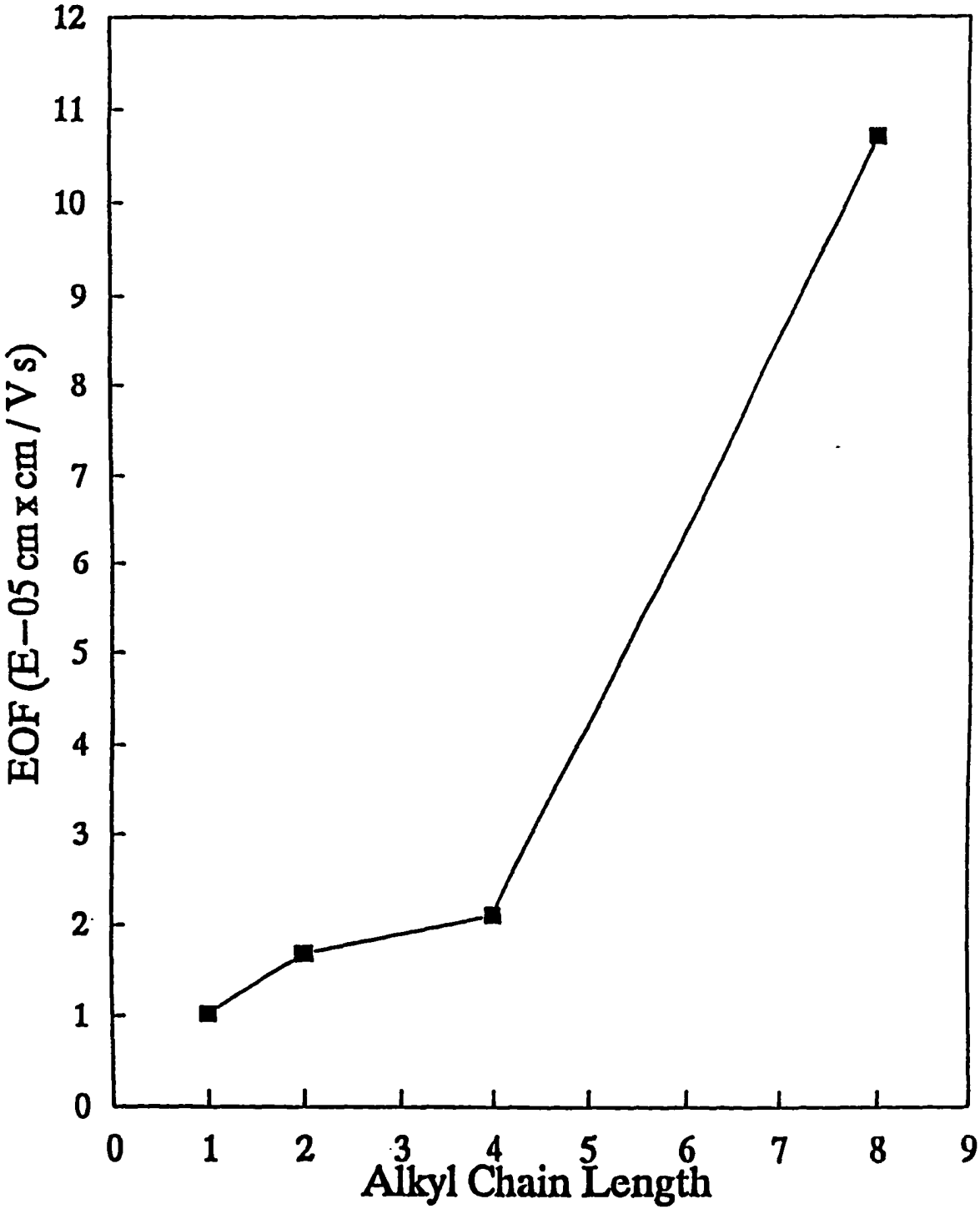

Figure 2. Effect of the alkyl chain length on the electroosmotic flow at pH 2.8.

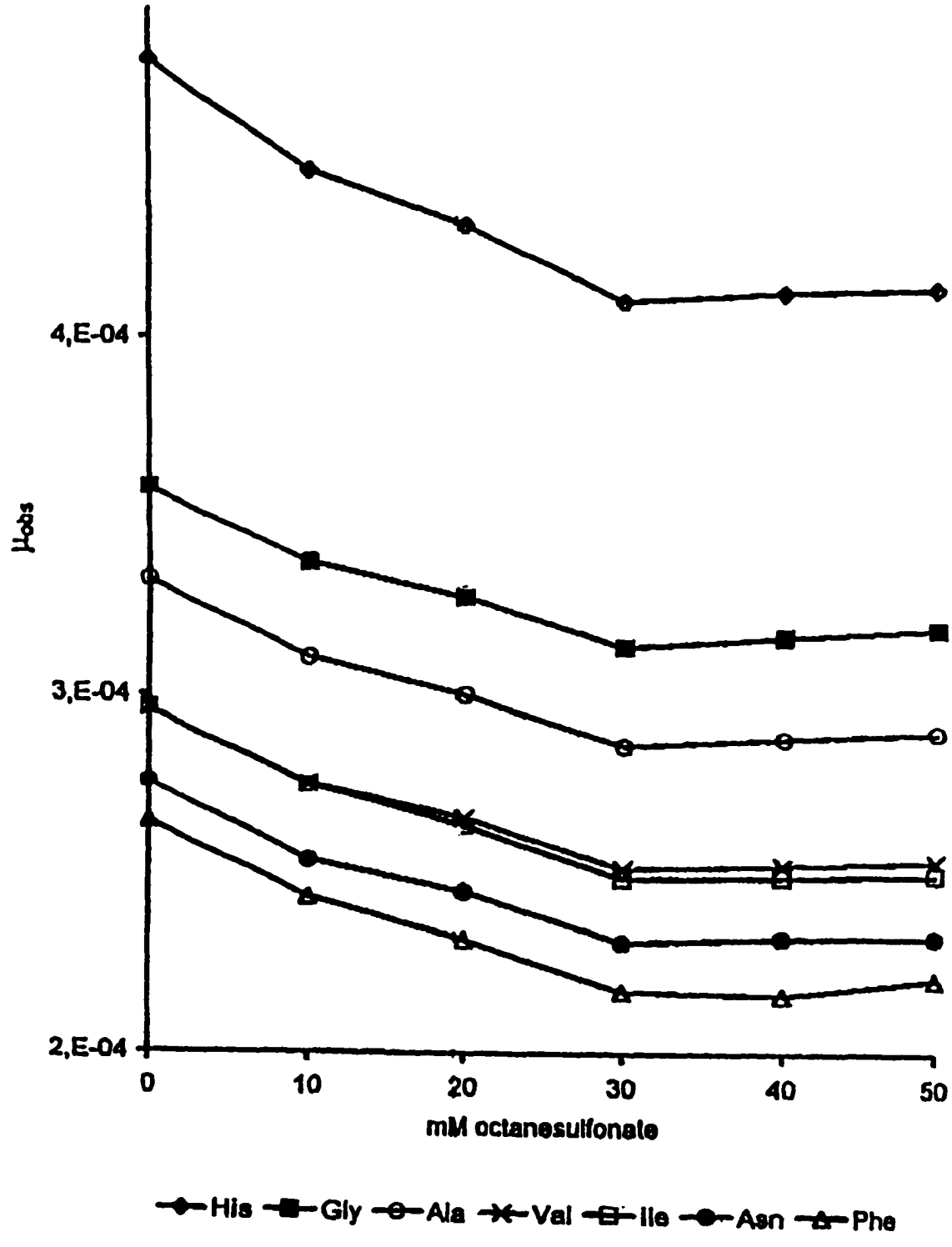

Figure 3. Effect of the octanesulfonate concentration on the apparent mobility of selected amino acids at pH 2.4.

3.3 Effect of pH

The EOF was measured as a function of pH in aqueous perchloric acid solutions containing, where appropriate, 20 mM of acetate buffer. Two different markers gave similar results and the measurements were made in triplicate. As might be expected, the top curve in Figure 4 shows no cathodic EOF up to about pH 2.7 and then only a small EOF up to about pH 3.5 where the EOF begins a rapid increase as the pH is increased further and the ionization of capillary silanol groups becomes more pronounced. It seemed likely that a positively-charged silica surface would be created at the more acidic pH values due to adsorption of H^+. To test for this, the direction of applied potential was reversed and an anodic EOF was indeed observed, as indicated by the lower curve in Figure 4. Both anodic and cathodic electroosmotic flows were found to coexist in the pH range 2.7 to 3.5.

The effect of 50 mM ethanesulfonic acid on EOF was also studied as a function of pH. The results in Figure 5 show that the presence of ethanesulfonate causes a cathodic EOF as low as pH 2.0. It is interesting that the EOF at somewhat higher pH values is lower when ethanesulfonate is present.

Although electroosmotic flow will of course affect the overall migration of amino acid cations, it is actually small compared to the electrophoretic migration. Electrophoretic effects thus become the dominant factor in CE of amino acids in acidic solutions. The effects of pH on the apparent mobilities are plotted for the first five amino acids in 50 mM ethanesulfonate in Figure 6. Lys, His, and Arg each carry a maximum charge of a positive two under acidic conditions, resulting in faster mobilities than Gly and Ala, which can have a maximum net charge of a positive one. The other

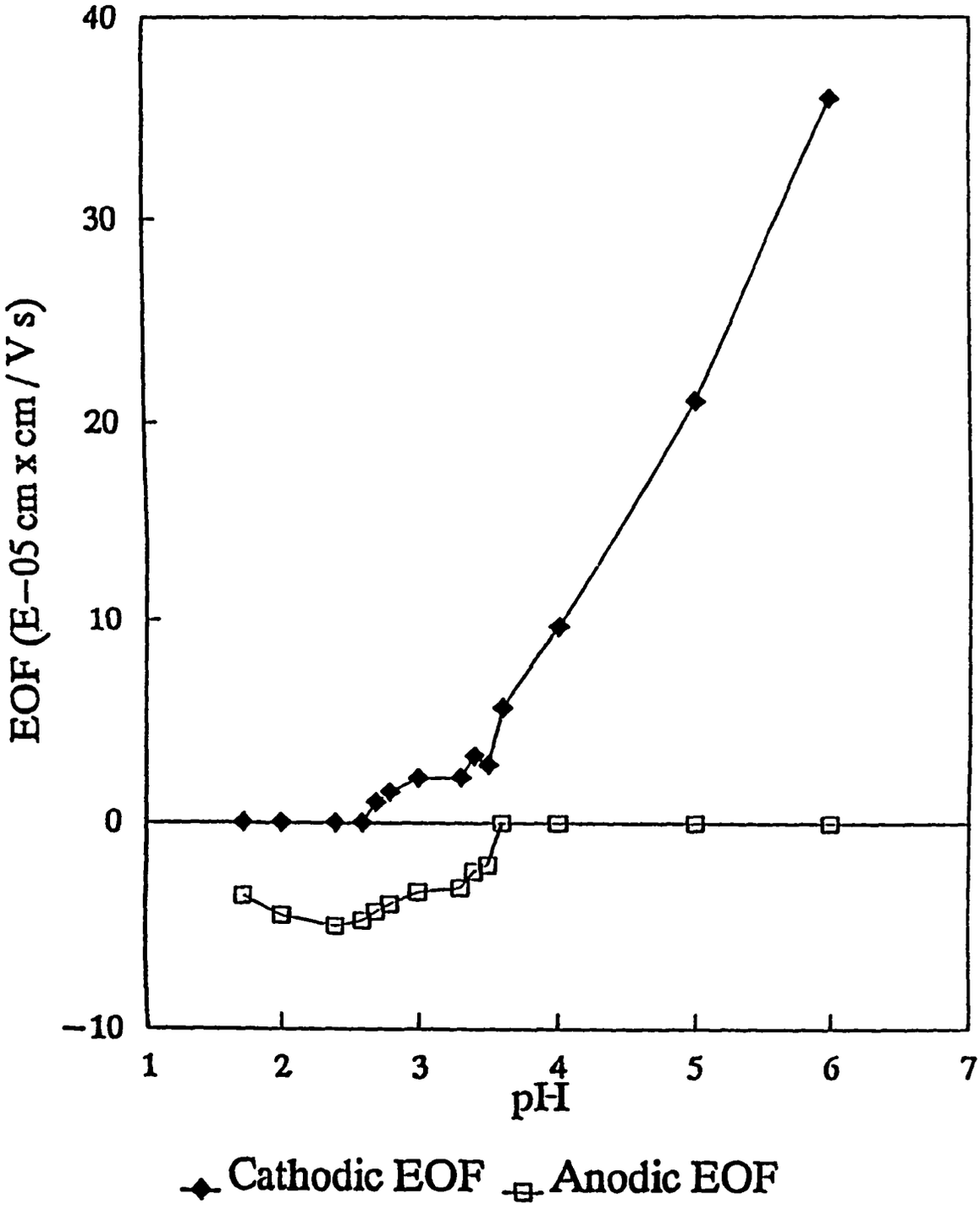

Figure 4. Effect of pH on the direction and magnitude of the EOF in 20 mM acetate buffer.

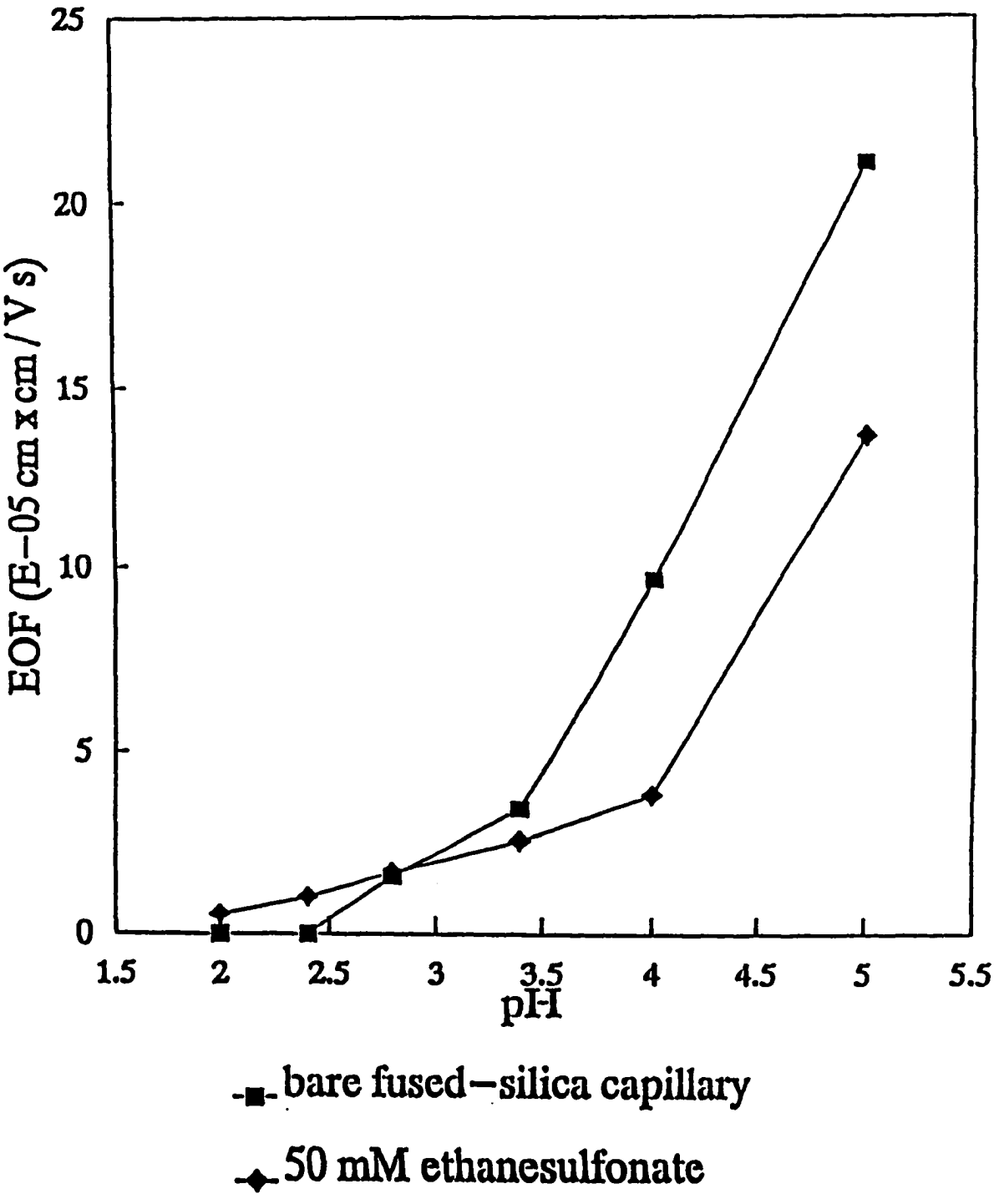

Figure 5. Effect of pH on the electroosmotic flows of an aqueous 20 mM acetate buffer and a 50 mM ethanesulfonate buffer with injection at the anode.

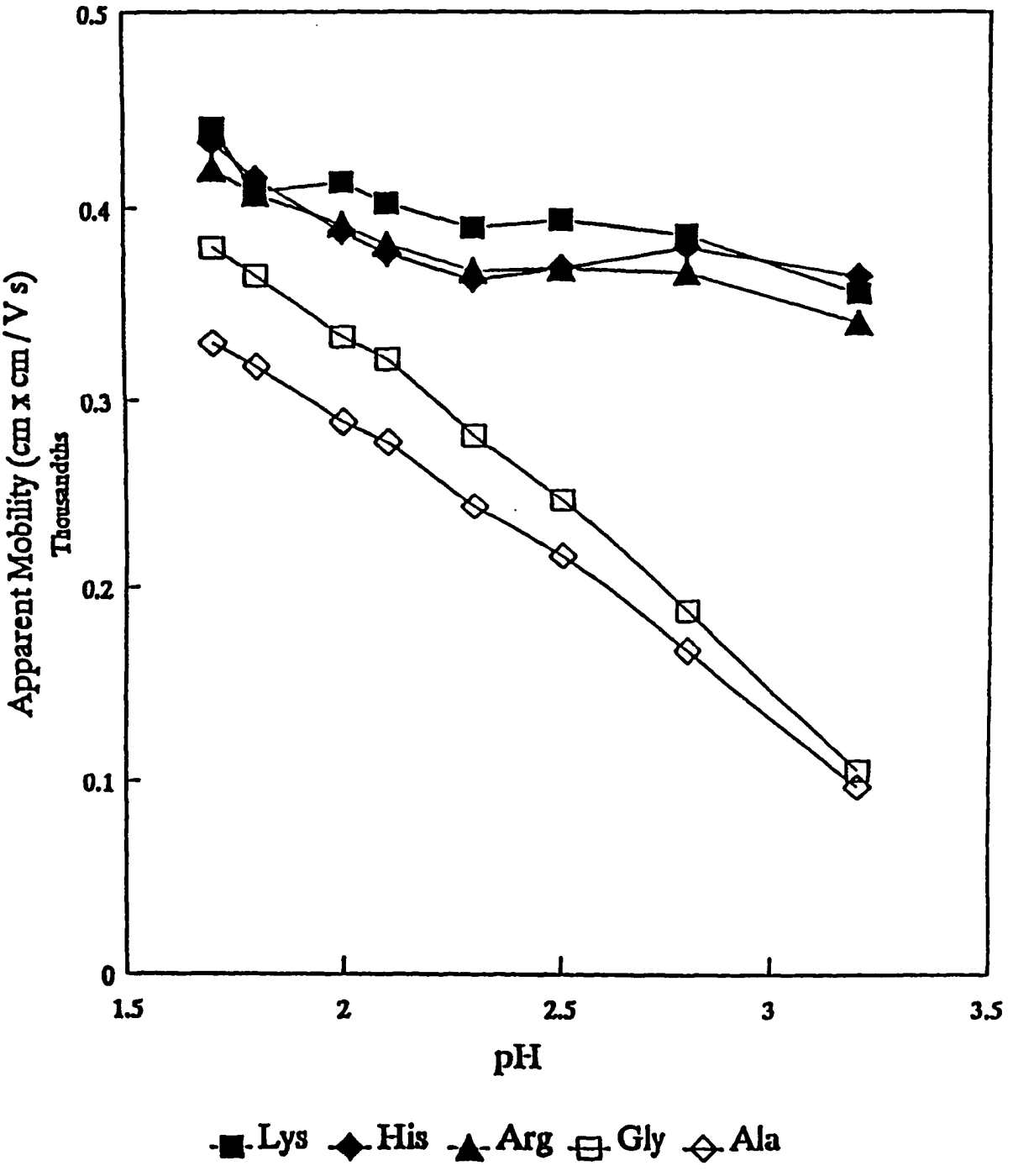

Figure 6. Effect of pH on the apparent mobilities of Lys, His, Arg, Gly, and Ala in 50 mM ethanesulfonate.

amino acids which can have a maximum charge of a positive one exhibit the same general trend as Gly and Ala, but they have small but important individual differences in their change with pH. In several cases, it is these small differences that either improve the separation of certain amino acid pairs or else make the separation more difficult.

Figure 1 showed a separation of amino acids carried out in 50 mM ethanesulfonic acid at pH 2.3. Figure 7 shows the effect of increasing the pH to 2.8 on the separation of the amino acid mixture. With the increased pH, a higher voltage of 30 kV could be applied which resulted in sharper peaks with better resolution of the amino acid mixture. In the separation at pH 2.8, 17 amino acid peaks could be identified. Ile co-migrated with Val. Thr was resolved from Asn. Met co-migrated with Asn but was resolved from Gln. The change in pH also affected the migration order of the amino acids. Ser migrated after Leu. Trp migrated before Thr, Asn, Met, and Gln. Glu and Pro migrated after Phe and Tyr.

A separation of 20 amino acids plus ornithine in the presence of 35 mM octanesulfonic acid at pH 2.4 is shown in Figure 8. In this case, the fused silica capillary was 50 μm i.d. and 100 cm in length. In some cases, the resolution of amino acid pairs is better than in Figure 7 with ethanesulfonic acid and in other cases it is not quite as good. Comparison of Figures 7 and 8 also shows a few differences in elution order.

Figure 7. Electropherogram of twenty common amino acids. Conditions as in Fig. 1 except pH 2.8; applied voltage, 30 kV.

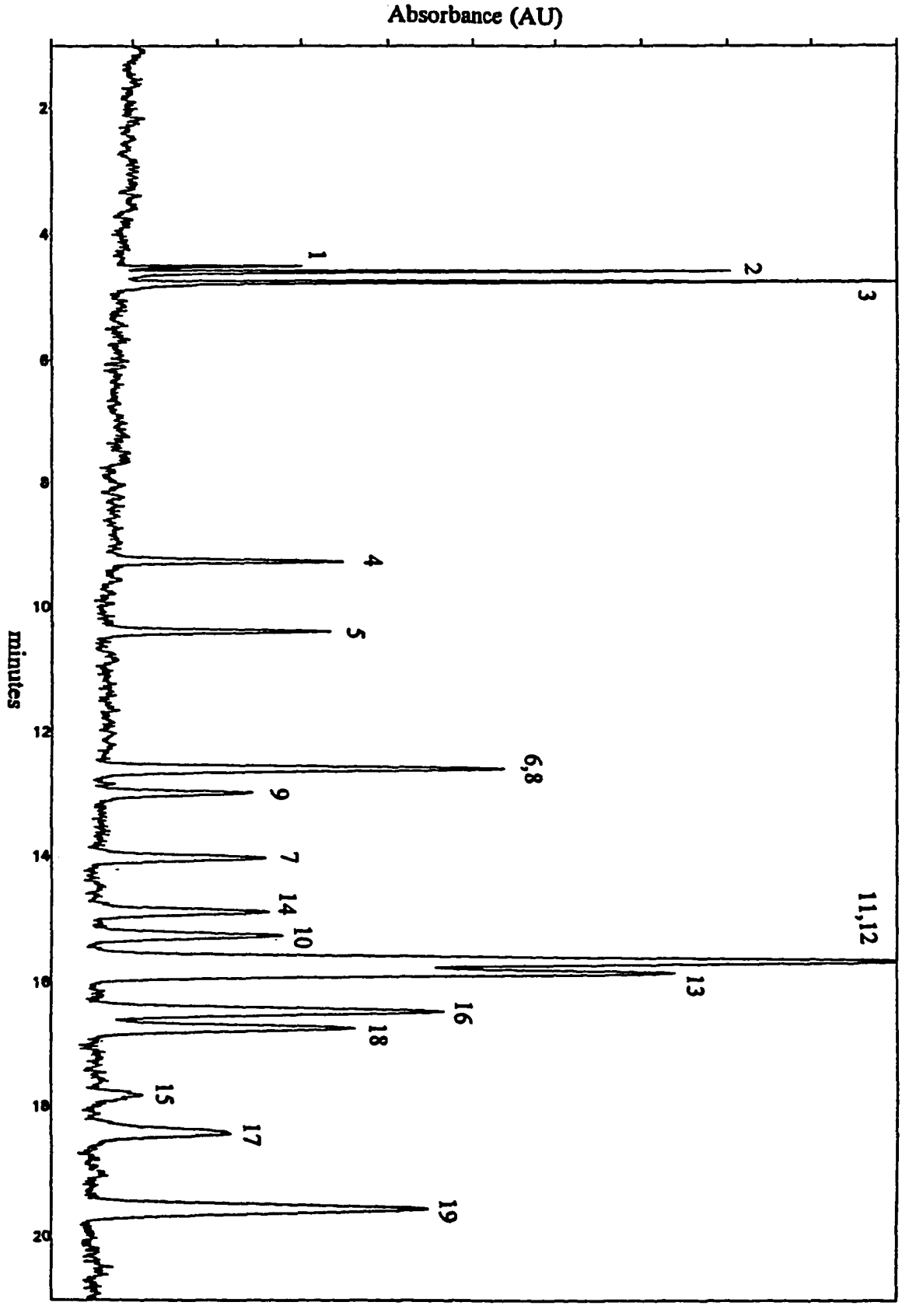
Absorbance (AU)
minutes
2
4
6
8
10
12
14
16
18
20
1
2
3
4
5
6,8
9
7
14
10
11,12
13
16
18
15
17
19

Figure 8. Separation of amino acids on a 100 cm x 50 μm i.d. fused silica capillary. Electrolyte, 35 mM octanesulfonate, 10 mM sodium dihydrogen phosphate, pH 2.4; applied voltage, 30 kV.

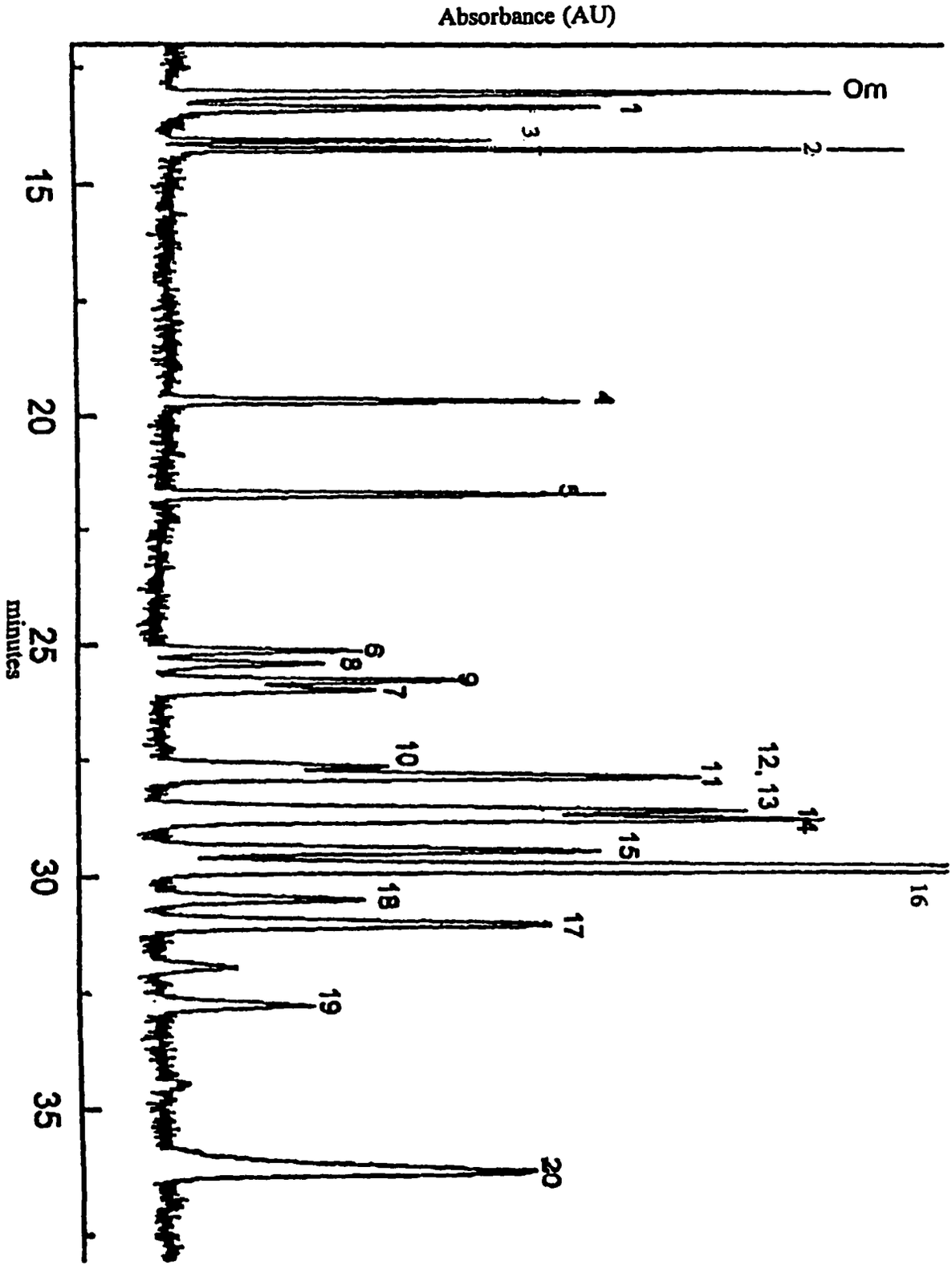
Absorbance (AU)
Om
1
3
2
4
5
6
8
7
9
10
11
12, 13
14
15
16
18
17
19
20
15
20
25
30
35
minutes

3.4 Coated capillaries

Further experiments were performed to clarify the mechanism by which ethanesulfonic acid was able to improve markedly the peak sharpness and resolution. It was found that ethanesulfonic acid was actually being adsorbed onto the capillary wall. A solution of 50 mM ethanesulfonate at pH 2.8 was flushed through the capillary for 30 minutes. The capillary was then rinsed for 30 minutes with an aqueous electrolyte carrier of $HClO_4$ adjusted to pH 2.8 to remove any excess ethanesulfonate. An electrophoretic separation of the amino acid mixture was carried out and sharp peaks with good resolution of 14 amino acid peaks was achieved. After rinsing the capillary with 0.1 M NaOH, the same separation was tried using the aqueous electrolyte carrier of $HClO_4$. The results were very different, the peaks being short and broad with poor resolution.

The effects of the capillary surface on the separation of amino acids was investigated further by coating the capillary with polyethylene oxide (PEO) [14]. Figure 9 shows the electropherogram of the amino acid mixture obtained with only an aqueous electrolyte carrier of $HClO_4$ adjusted to pH 2.8 in the PEO coated capillary. The 14 peaks have a larger peak height than those obtained in a bare fused-silica capillary. Figure 10 shows an electropherogram of the same amino acid mixture but with 50 mM ethanesulfonate at pH 2.8 as the electrolyte carrier in the PEO coated capillary. Some improvement in peak sharpness and resolution was obtained by adding ethanesulfonate.

Figure 9. Electropherogram of twenty common amino acids using a PEO coated capillary with an aqueous $HClO_4$ electrolyte carrier at pH 2.8. Other conditions as in Fig. 1.

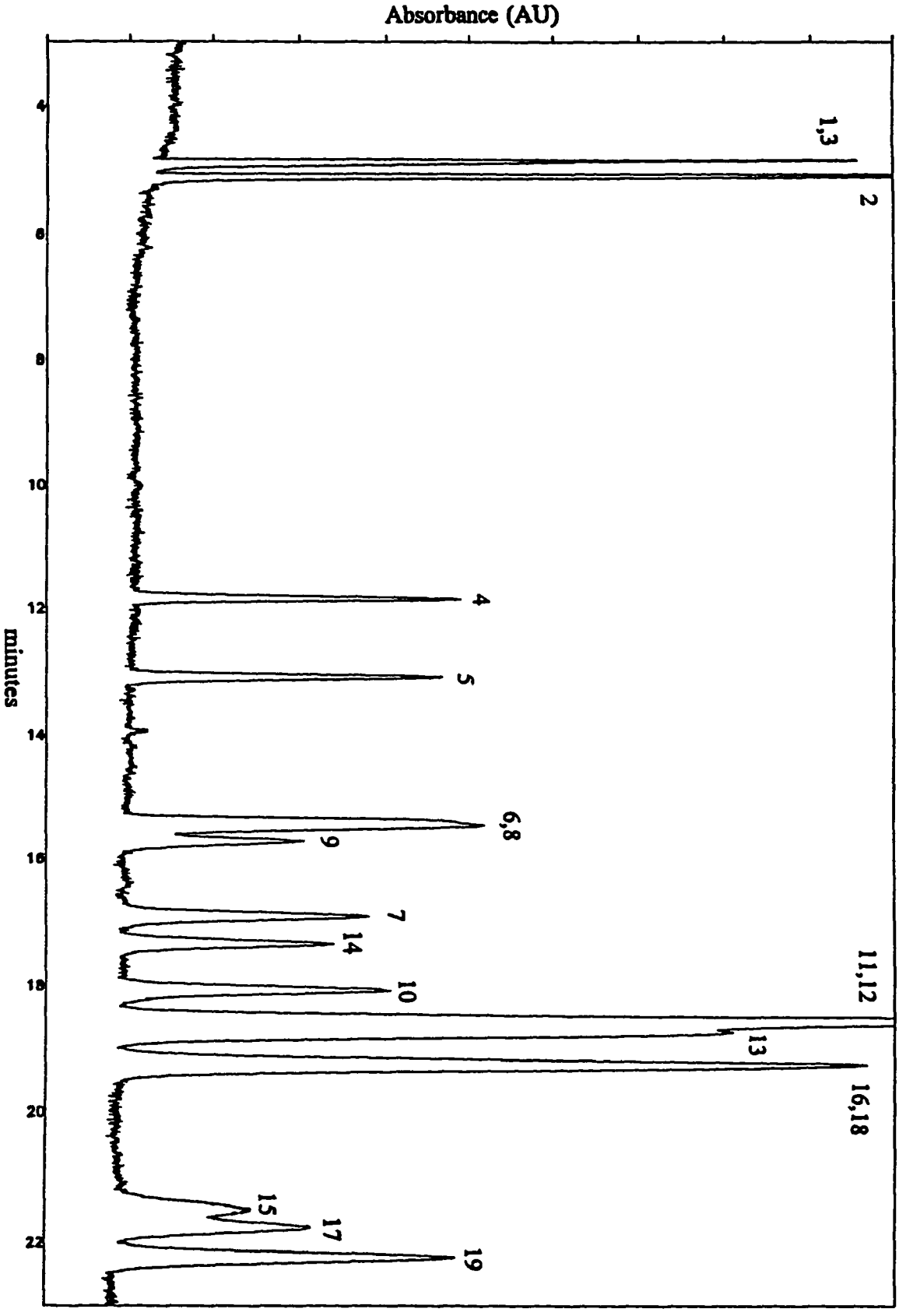
Absorbance (AU)
minutes
4
6
8
10
12
14
16
18
20
22
1,3
2
4
5
6,8
9
7
14
10
11,12
13
16,18
15
17
19

Figure 10. Electropherogram of twenty common amino acids using a PEO coated capillary with a 50 mM ethanesulfonate electrolyte carrier at pH 2.8. Other conditions as in Fig. 1.

Absorbance (AU)
minutes
4
6
8
10
12
14
16
18
20
22
24
1
3
2
4
5
6,8
9
7
14
10
11,12
13
16
18
15,17
19

3.5 Effect of cyclodextrins

In a recently published paper, Lee et al. [9] showed that the migration behavior of some amino acids in basic solution can be influenced by the addition of cyclodextrins (CDs) to the carrier electrolyte. In particular, the presence of α-CD in the running buffer led to selectivity changes that increased the number of amino acids that could be separated within one single electropherogram. Our preliminary investigations showed that inclusion complexes between amino acids and α-CD molecules also form at acidic pH values, leading to an increase in migration times that correspond to the stability constants of the soluble CD complexes. Electropherograms were obtained for a set of 10 amino acids using 10 mM phosphate carrier electrolytes, pH 2.0 to 3.4, with 2 to 20 mM α-CD added. Compared to separations under similar conditions but with alkanesulfonates instead of α-CD, the EOF as well as peak shape was not affected greatly by the α-CD. Nevertheless, addition of α-CD changed the migration behavior of some of the analytes to a certain extent. Phe, Met, Trp and Leu form inclusion complexes with the α-CD leading to increased migration times for these analytes. This behavior was found to be independent from the pH of the running buffer within the pH range under investigation. But, it must be stated, that compared to the improvements obtained by the addition of alkanesulfonates to the carrier electrolytes, the use of the α-CD did not lead to an appreciably better separation.

4. Conclusions

Amino acids can be separated in their native form as protonated cations under acidic conditions with direct UV detection. No derivatization is needed. The success of such

a separation depends on obtaining a satisfactory surface on the fused silica capillary. This can be accomplished quickly and reproducibly simply by including a low concentration of either ethanesulfonic acid or octanesulfonic acid in the running electrolyte. Studies showed that the capillary surface is coated dynamically by the alkanesulfonate.

The practical separation of amino acids is highly dependent on pH. The migration order of some amino acids may change with only a few tenths change in pH. The most satisfactory separations were obtained at pH 2.3, 2.4 or 2.8.

Acknowledgements

We wish to thank Waters Corporation for their gift of the Waters Quanta 4000 CE instrument and associated chemicals and supplies.

This work was performed in the Ames Laboratory at Iowa State University, Ames, Iowa, USA and in the Institüt für Chemie at Johannes Kepler University, Linz, Austria. Ames Laboratory is operated for the U.S. Department of Energy under Contract No. W-7405-Eng-82. This work was supported in part by the Director of Energy Research, Office of Basic Energy Sciences.

References

1. J. Liu, Y.-Z. Hsieh, D. Wiesler and M. Novotny, *Anal. Chem.*, 63 (1991) 408.
2. M. Albin, R. Weinberger, E. Sapp and S. Moring, *Anal. Chem.*, 63 (1991) 417.
3. W. G. Kuhr and E. S. Yeung, *Anal. Chem.*, 60 (1988) 1832.
4. E. S. Yeung and W. G. Kuhr, *Anal. Chem.*, 63 (1991) 275A.

5. F. Foret, S. Fanali, L. Ossicini and P. Boček, *J. Chromatogr.*, 470 (1989) 299.

6. G. J. M. Bruin, A. C. van Asten, X. Xu and H. Poppe, *J. Chromatogr.*, 608 (1992) 97.

7. Y. Ma, R. Zhang and C. L. Cooper, *J. Chromatogr.*, 608 (1992) 93.

8. Y.-H. Lee and T.-I. Lin, *J. Chromatogr. A.*, 680 (1994) 287.

9. Y.-H. Lee and T.-I. Lin, *J. Chromatogr. A.*, 716 (1995) 335.

10. T. M. Olefirowicz and A. G. Ewing, *J. Chromatogr.*, 499 (1990) 713.

11. J. Pawliszyn, *Anal. Chem.*, 60 (1988) 2796.

12. T. Bergman, B. Agerberth and H. Jörnvall, *FEBS Letters*, 283 (1991) 100.

13. R. M. McCormick, *Anal. Chem.*, 60 (1988) 2322.

14. J. Preisler and E. S. Yeung, *Anal. Chem.*, 68 (1996) 2885.

15. J. E. Sandoval and S.-M. Chen, *Anal. Chem.*, 68 (1996) 2771.

CHAPTER 4. SEPARATION OF METAL CATIONS IN ACIDIC SOLUTION BY CAPILLARY ELECTROPHORESIS WITH DIRECT AND INDIRECT UV DETECTION

A paper to be submitted to the Journal of Chromatography A

Michelle J. Thornton[1,2] and James S. Fritz[1,3]

Abstract

Methods for the detection of metal cations under acidic conditions, near pH 2, in capillary electrophoresis (CE) were investigated. Conditions for direct UV detection of UV absorbing metal cations such as Cr^{3+}, Cu^{2+}, Fe^{3+}, UO_2^{2+}, VO^{2+}, and VO_2^{+} were established with aqueous HCl or $HClO_4$ as the electrolyte carrier. The speciation of vanadium (IV) and vanadium (V) at pH 2.3 by CE was achieved with direct detection at 185 nm. With the strong absorbance at 185 nm, no complexation was needed to detect the metal cations. An indirect UV detection scheme for acidic conditions was also investigated. Several background carrier electrolytes (BCEs) were studied including 4-methylbenzylamine, nicotinamide, pyridazine, guanidine, 3-picoline, and chromium (III) to determine their effectiveness under very acidic conditions. The effect of ionic surfactants and the nonionic surfactant, Triton X-100, on the peak heights and N values was also studied.

---

[1]Graduate student and Professor, respectively, Department of Chemistry and Ames Laboratory, Iowa State University, Ames, IA 50011, USA.

[2]Primary researcher and author

[3]Author for correspondence

1. Introduction

The first separation of metal cations by capillary electrophoresis (CE) was reported by Hjerten [1] in 1967 when he described the separation of bismuth and copper. Since 1967, the number of papers discussing CE separations of inorganic cations [2-28] has remained relatively low compared to the publications on inorganic and organic anions.

CE separations are the result of differences in the electrophoretic mobilities of ions in an electrolyte carrier under the influence of an electrical field. If the electrophoretic mobilities of the ions are similar, a weak complexing reagent can be added to the electrolyte carrier to increase the differences in the mobilities [7,15-20]. An auxiliary complexing reagent such as a crown ether may also be added for selective complexation based on physical size [17].

Direct UV absorption has mainly been used for the determination of UV-absorbing anions. Indirect UV absorption is the preferred approach when a universal detection mode is required. A UV absorbing reagent is added to the electrolyte carrier, and the analyte ions are monitored as a decrease in the background absorbance. Aromatic bases are usually used to detect cations. The electrolyte ion should have both a sufficiently large absorptivity at the selected wavelength and an ionic mobility similar to that of the analytes being detected [12,14].

With indirect UV detection, many background carrier electrolytes (BCEs) are chosen based on their pk_as, so they also work as buffers in the desired working range. However, if it is working as a buffer, only half of the BCE is in the cationic form. The neutral fraction does not contribute to the detection, but it does affect the linearity range.

The role of pH in the separation and its optimization has been investigated

[14,15,18], but the optimum pH is dependent upon the visualization and weak complexing reagents being used. The most common pH range studied in the separation of metal cations is pH 3 to pH 5. Barger et al. [27] worked at pH 2.8 due to the unique solubility of aluminum compounds.

In this work, we investigated a more acidic pH range. Several BCEs were studied including 4-methylbenzylamine, nicotinamide, pyridazine, guanidine, 3-picoline, and chromium (III) to determine their effectiveness under very acidic conditions. Guanidine with a pk_a of 13.54 should offer advantages for indirect detection.

2. Experimental

2.1 Apparatus

CE experiments were performed with a Waters Quanta 4000 capillary electrophoresis system (Waters Corporation, Milford, MA, USA). The polyimide coated, fused silica capillaries (Polymicro Technology, Phoenix, AZ, USA) were 50 μm I.D. and 60 cm in length. The distance from the point of injection to the window of on-column detection was 52.4 cm. Direct UV detection was employed at 185 and 214 nm. Indirect UV detection was employed at 185 nm. A voltage of +10 kV was applied for the separations. The time of hydrodynamic injection was 10 s unless otherwise indicated. Electropherograms were collected and plotted by the data acquisition system Chrom Perfect Direct (Justice Innovations, Mountain View, CA, USA).

2.2 Procedure

New capillaries were conditioned by rinsing with 0.1 M NaOH for one hour followed by a one hour rinse with deionized (DI) water. At the start of each day, the capillary was rinsed with the electrolyte carrier for 30 minutes. The capillary was also purged with the electrolyte carrier for 5 minutes before each run.

2.3 Reagents

All standards and electrolytes were prepared with analytical reagent grade chemicals and 18 MΩ deionized (DI) water obtained from a Barnstead Nanopure II system (Sybron Barnstead, Boston, MA, USA). The electrolyte carrier used for direct detection was prepared by diluting 0.1 M $HClO_4$ or HCl (Fisher Scientific, Fairlawn, NJ, USA) with DI water until the appropriate pH of 2.1 to 2.4 and a total volume of 50 mL.

The stock solutions of 4-methylbenzylamine, 3-picoline, pyridazine, guanidine nitrate, chromium (III) nitrate (Aldrich, Milwaukee, WI, USA) and nicotinamide (Sigma, St. Louis, MO, USA) were prepared at a concentration of 0.2 M in DI water and adjusted to pH 2.1 with concentrated $HClO_4$ or concentrated ultrapure HNO_3 (J.T. Baker Inc., Phillipsburg, NJ, USA). The electrolyte carrier used for indirect detection was prepared by diluting the 0.2 M stock solution of the visualization reagent with DI water to the appropriate concentration in a total volume of 40 mL. An aliquot, *ca* 8 μL, of concentrated ultrapure HNO_3 was used to adjust the pH to 2.3. Methanesulfonic acid, octanesulfonic, cetyltrimethylammonium chloride, and Triton X-100 were obtained from Aldrich (Milwaukee, WI, USA).

Stock solutions of 1000 ppm VO^{2+} and VO_2^+ were prepared by dissolving

$VOSO_4 \cdot 3H_2O$ and NH_4VO_3 (Aldrich, Milwaukee, WI, USA), respectively in DI water and adjusting the pH to 1.5 with concentrated $HClO_4$. Some metals were ICP standard solutions in 1, 2, or 10 wt. % HNO_3 (PlasmaChem Corp., Farmingdale, NJ, USA) and atomic absorption standard solutions in 1 wt. % HCl (Aldrich, Milwaukee, WI, USA). They were diluted with DI water prior to analysis.

3. Results and discussion

3.1 Direct detection

Some metal cations have a reasonably large absorptivity in the UV spectral range to be detected directly. In a previous paper [29], we found that by working at a sufficiently acidic pH an additional buffer did not need to be added. The absence of the additional buffer led to an increase in the detection sensitivity and also assured conditions where only free, uncomplexed ions would be present. When a buffer like β-alanine or glycine was used, the baseline noise was rather high. The use of a very acidic pH also avoided complications from hydrolysis of the metal ions.

Figures 1 and 2 show electropherograms of 20 ppm Cu (II) and Cr (III), respectively. An electrolyte carrier of aqueous $HClO_4$ was used with direct UV detection at 185 nm. Detection sensitivities were good with S/N ratios of 21 and 35, respectively.

Due to the equilibrium between iron (III) and chloride, an aqueous HCl electrolyte carrier was used for the direct detection of $FeCl_3$. The electropherogram for Fe (III) is shown in Figure 3. The broad peak for Fe (III) is caused by the slow equilibrium

Figure 1. Electropherogram of 20 μg ml^{-1} copper (II). Conditions: fused silica capillary, 60 cm x 50 μm I.D. (52.4 cm to detector); electrolyte carrier, aqueous $HClO_4$ at pH 2.3; applied voltage, +10 kV; UV detection at 185 nm; sampling time, 10 s. Peak: (1) Cu^{2+}.

Absorbance (A.U.)
1
minutes
0
1
2
3
4
5
6
7
8
9
10
11
12
13
14

Figure 2. Electropherogram of 20 μg ml^{-1} chromium (III). Peak: (1) Cr^{3+}. Conditions as in Fig. 1.

Absorbance (A.U.)
minutes
0
1
2
3
4
5
6
7
8
9
10
11
12
13
14

Figure 3. Electropherogram of 33 μg ml^{-1} iron (III). Conditions: fused silica capillary, 60 cm x 50 μm I.D. (52.4 cm to detector); electrolyte carrier, aqueous HCl at pH 2.4; applied voltage, +10 kV; UV detection at 214 nm; sampling time, 30 s. Peak: (1) Fe^{3+}.

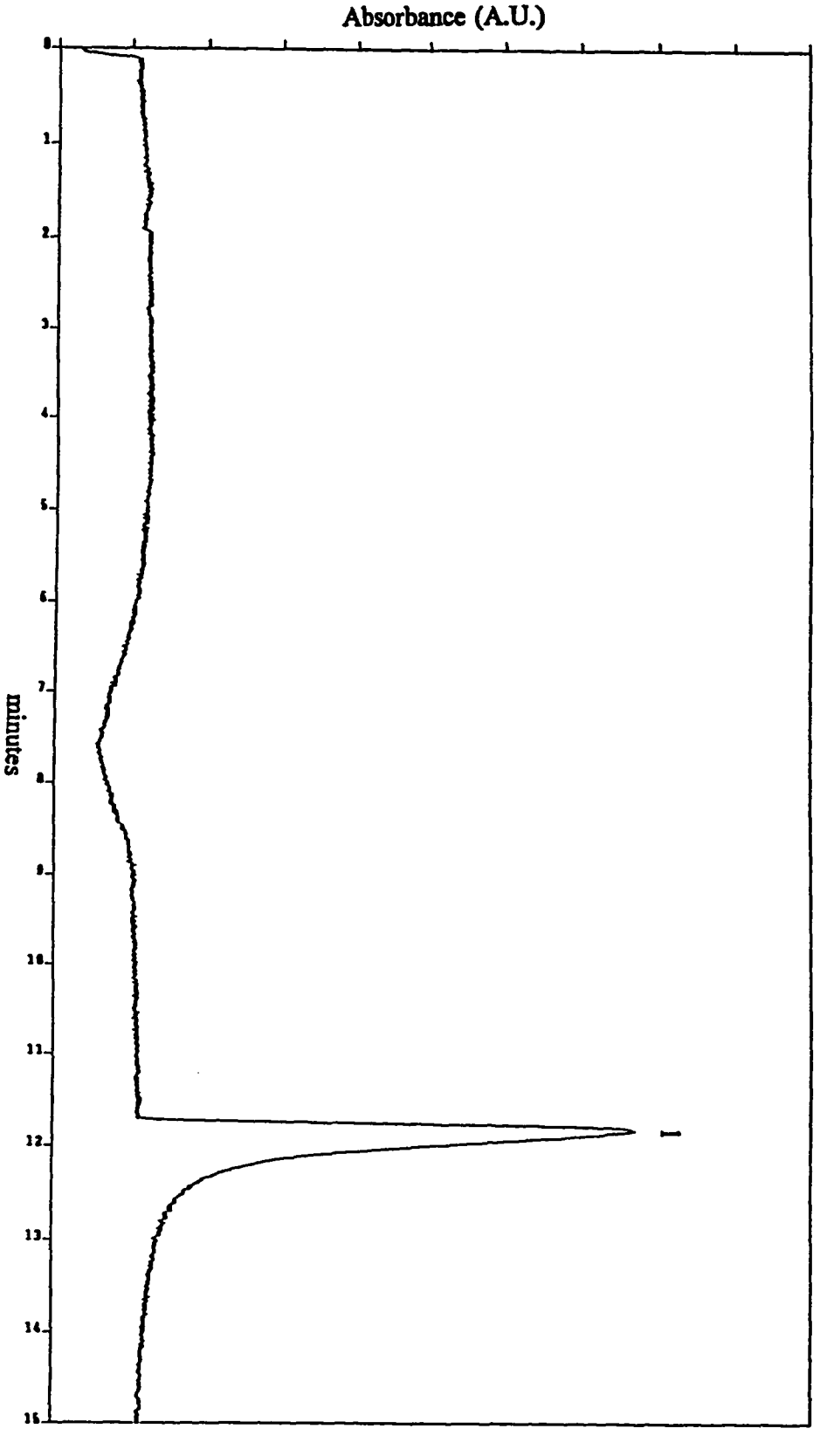
Absorbance (A.U.)
minutes
0
1
2
3
4
5
6
7
8
9
10
11
12
13
14
15

kinetics between the iron and chloride ions. Uranium (VI) was also detected directly at 214 nm. The electropherogram of UO_2^{2+} is shown in Figure 4.

The speciation of vanadium (IV) and vanadium (V) ions with direct UV detection was achieved. The vanadium (IV) and vanadium (V) oxidation states are present in the cationic species of vanadyl, VO^{2+}, and vanadate, VO_2^+, respectively. The electropherogram of the simultaneous determination of vanadium (IV) and vanadium (V) is shown in Figure 5. An aqueous $HClO_4$ electrolyte carrier adjusted to pH 2.3 was used with direct UV detection at 185 nm. The migration times for V (IV) and V (V) were quite reproducible with 0.10 % and 0.16 % relative standard deviations, respectively based on nine determinations.

Linear calibration plots of vanadium (IV) and vanadium (V) were achieved. The calibration plots of the peak areas versus the concentrations of V (IV) and V (V) are shown in Figures 6 and 7, respectively. The calibration data are shown in Table 1. A linear range was possible for V (IV) between 5 and 100 ppm with a correlation coefficient of 0.9993. A linear range was only possible between 20 and 100 ppm for V (V) with a correlation coefficient of 0.9976. The nonlinearity in the lower concentration range may be due to the equilibrium between the vanadate cation and vanadate anion in very dilute solutions where the acidity is too low

($VO_2^+ + H_2O \rightleftharpoons VO_3^- + 2\ H^+$).

The relative and absolute detection limits for vanadium (IV) and vanadium (V) were determined. The data are shown in Table 2. The relative detection limits for V (IV) and V (V) are 5 ppm and 10 ppm, respectively at a S/N ratio of three using an injection time of 10 seconds. By increasing the injection time to 75 seconds, absolute detection

Figure 4. Electropherogram of 33 μg ml^{-1} UO_2^{2+}. Conditions: fused silica capillary, 60 cm x 50 μm I.D. (52.4 cm to detector); electrolyte carrier, aqueous HCl at pH 2.1; applied voltage, +10 kV; UV detection at 214 nm; sampling time, 30 s. Peak: (1) UO_2^{2+}.

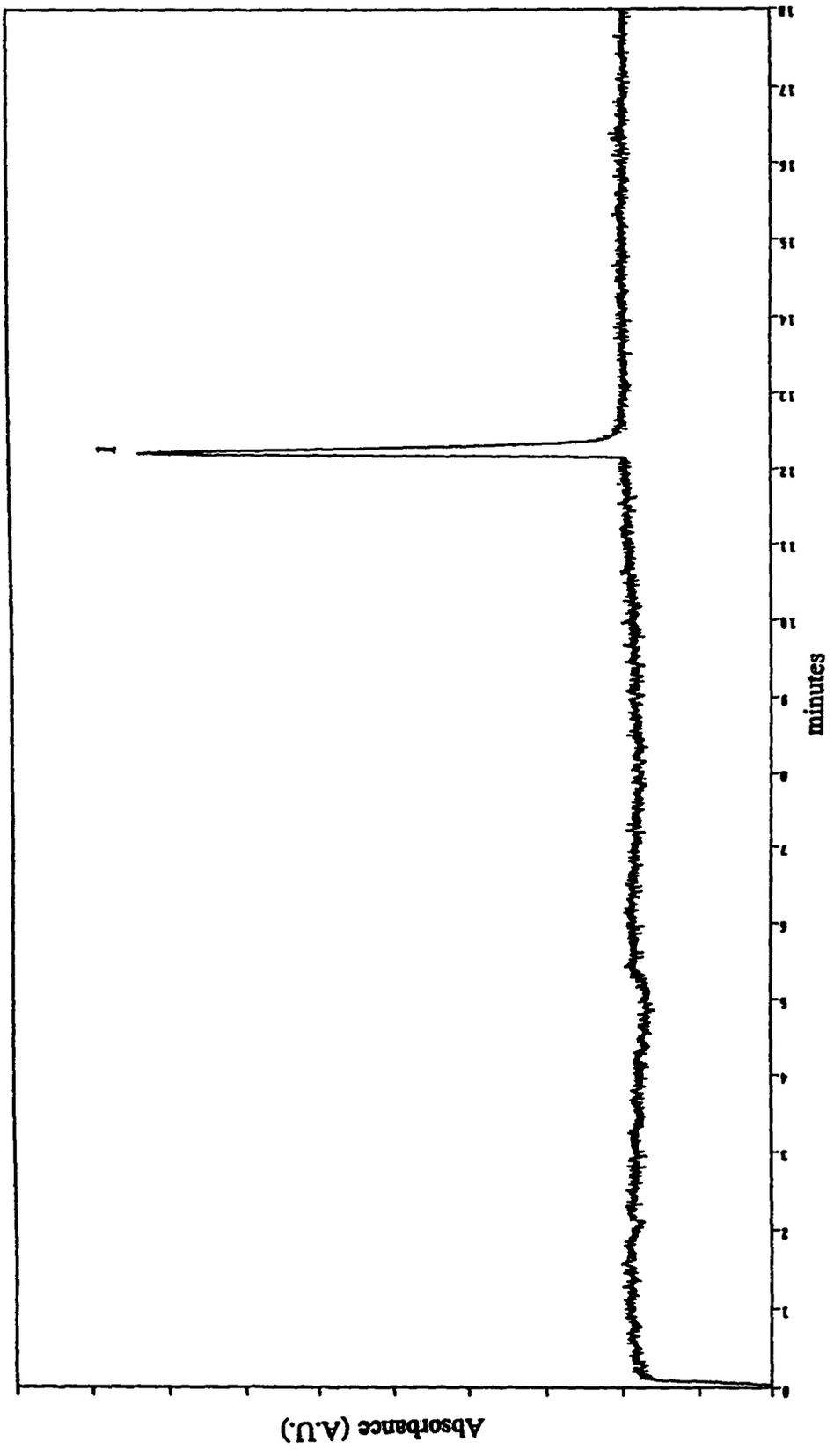
Absorbance (A.U.)
minutes
1

Figure 5. Electropherogram showing the separation of vanadium (IV) and vanadium (V) at 20 μg ml^{-1} each. Conditions: fused silica capillary, 60 cm x 50 μm I.D. (52.4 cm to detector); electrolyte carrier, aqueous $HClO_4$ at pH 2.3; applied voltage, +10 kV; UV detection at 185 nm; sampling time, 10 s. Peaks: (1) VO^{2+} and (2) VO_2^+.

Absorbance (A.U.)
0
2
4
6
8
10
12
14
16
18
20
22
24
26
28
30
minutes
1
2

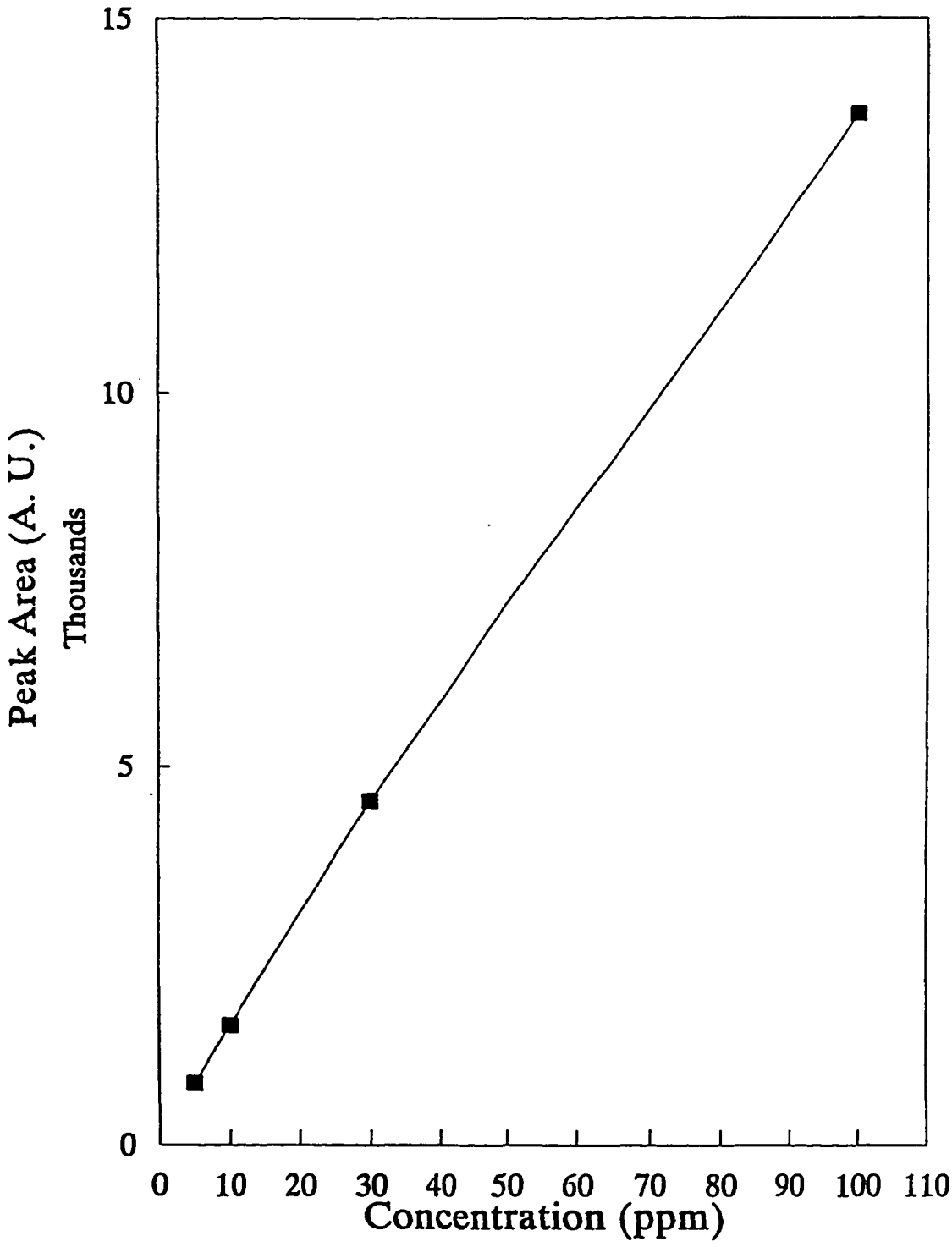

Figure 6. Calibration plot of vanadium (IV).

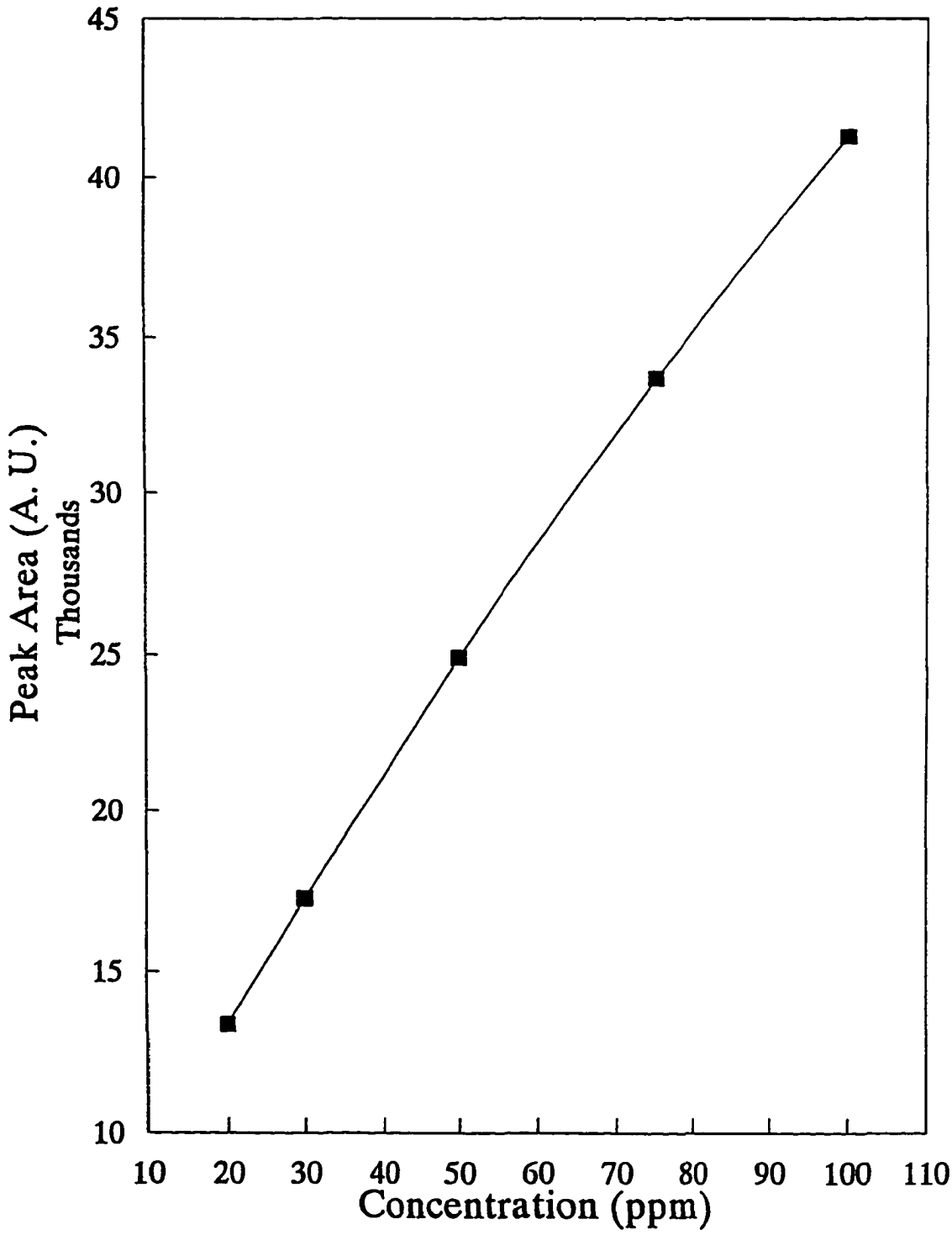

Figure 7. Calibration plot of vanadium (V).

Table 1. Calibration data for vanadium (IV) and vanadium (V).

Species	Linear range (ppm)	Correlation Coefficient	Equation
V (IV)	5 - 100	.9993	y = 135.3x + 258.6
V (V)	20 - 100	.9976	y = 350.9x + 6807.7

Table 2. Limits of detection (LOD) for vanadium (IV) and vanadium (V).

Species	Concentration LOD[a] (ppm)	Absolute LOD (pg)
V (IV)	5	20[b]
V (V)	10	102[c]

S/N = 3

[a]10 second injection time

[b]75 second injection time of 1 ppm solution

[c]75 second injection time of 5 ppm solution

limits of 20 pg and 102 pg were measured for 1 ppm V (IV) and 5 ppm V (V), respectively.

3.2 Indirect detection

The absorbance of many other metal ions is not great enough to be detected directly by UV absorption. An indirect UV detection scheme offers the ability to detect these metal ions with higher sensitivity and the advantage of multi-element detection at one wavelength.

Several backgroumd carrier electrolytes (BCEs) were investigated for their sensitivity and baseline stability near pH 2. In the pH range of 1.7 to 2.1, no metal ion peaks were detected using 4-methylbenzylamine, nicotinamide, 3-picoline, or pyridazine. Concentration ranges between 1 mM to 10 mM were studied for the BCEs. Detection at wavelengths of 214 nm and 254 nm was also investigated.

Metal ion peaks for Cu^{2+} and Sr^{2+} were detected at 185 nm by using 5 mM chromium (III) as the BCE at pH 2.1. However, the detection sensitivity was rather poor. Metal ions peaks were also detected at 185 nm when using guanidine as the BCE at pH 2.1. Initial results showed sharp peaks for metal ions and good detection sensitivity. Figures 8 to 11 show electropherograms for Mn^{2+}, Ni^{2+}, UO_2^{2+}, and Y^{3+}, respectively using 11 mM guanidine as the BCE at pH 2.3. The initial negative peak in each electropherogram is the H^+ cation. Figure 12 shows a separation of the metal ions, Ag^+ and Al^{3+}. Table 3 lists some of the metal cations that are able to detected indirectly with guanidine as the BCE. Guanidine was also found to have a similar mobility to that of the metal ions.

Figure 8. Electropherogram of 20 μg ml^{-1} of Mn^{2+}. Electrolyte, 11 mM guanidine, adjusted to pH 2.3 with nitric acid. Other conditions as in Fig. 1. Peak: (1) Mn^{2+}.

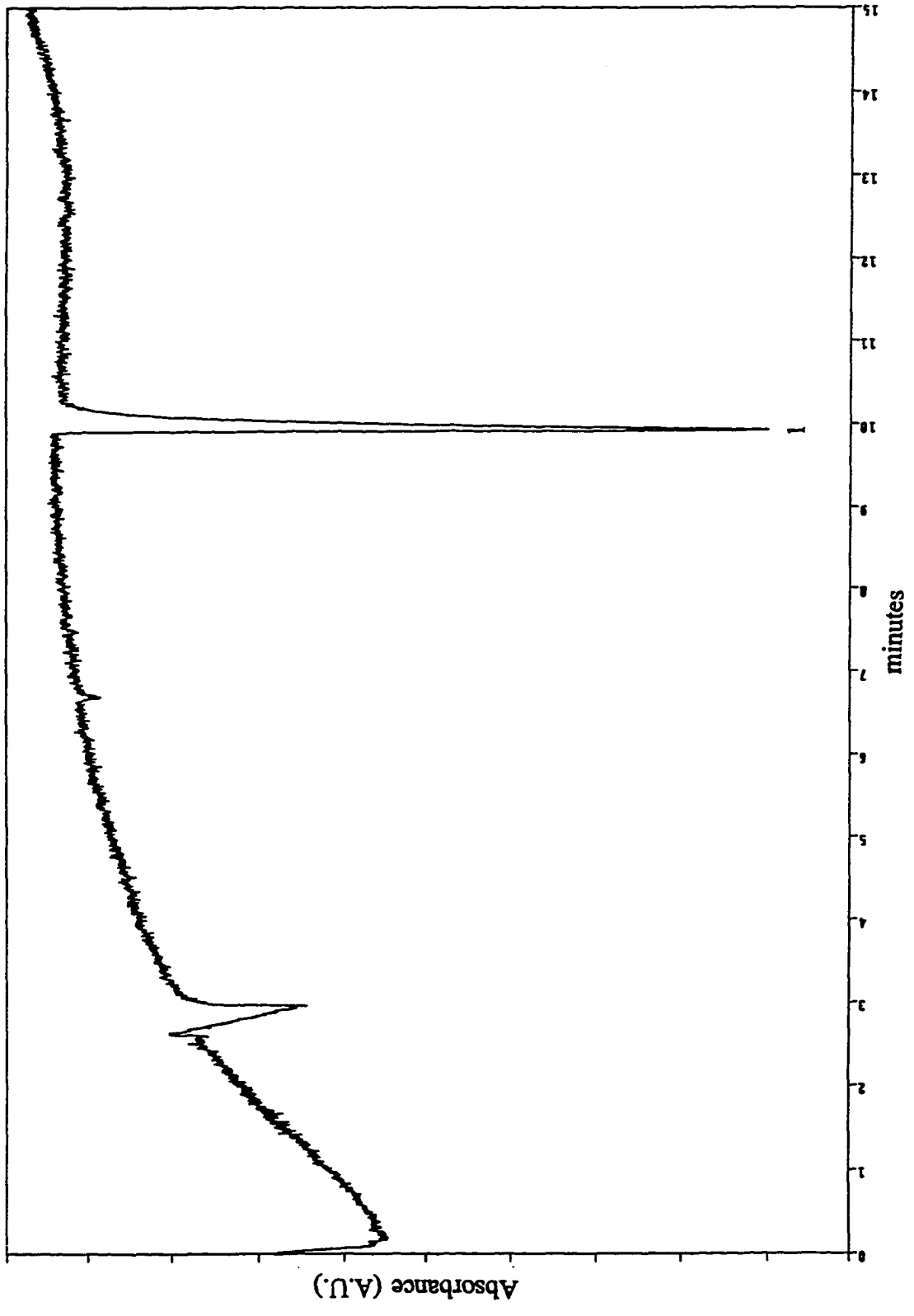
Absorbance (A.U.)
minutes
1

Figure 9. Electropherogram of 20 μg ml^{-1} of Ni^{2+}. Electrolyte, 11 mM guanidine, adjusted to pH 2.3 with nitric acid. Other conditions as in Fig. 1. Peak: (1) Ni^{2+}.

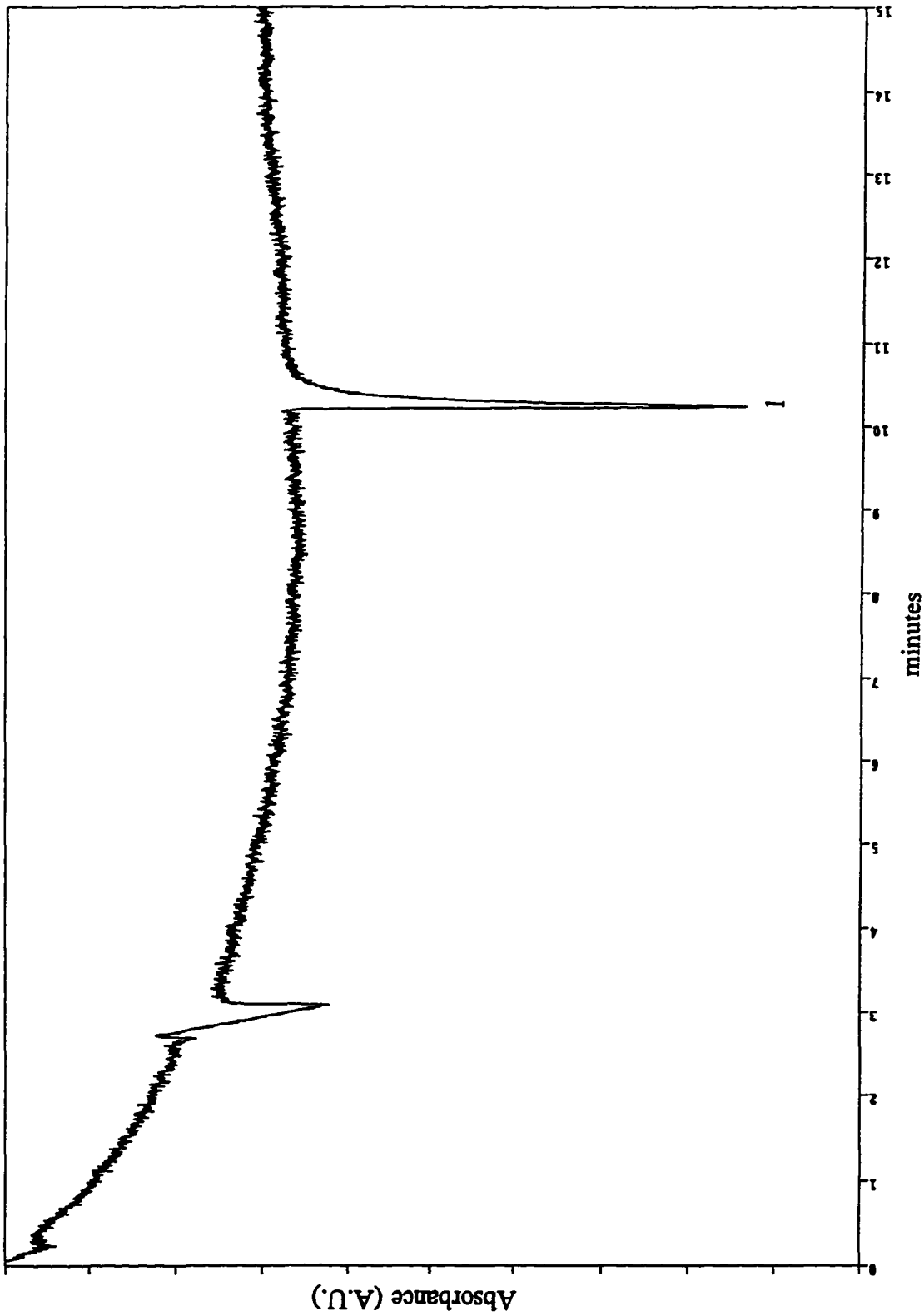
Absorbance (A.U.)
minutes
0
1
2
3
4
5
6
7
8
9
10
11
12
13
14
15

Figure 10. Electropherogram of 20 μg ml^{-1} of UO_2^{2+}. Electrolyte, 11 mM guanidine, adjusted to pH 2.3 with nitric acid. Other conditions as in Fig. 1. Peak: (1) UO_2^{2+}.

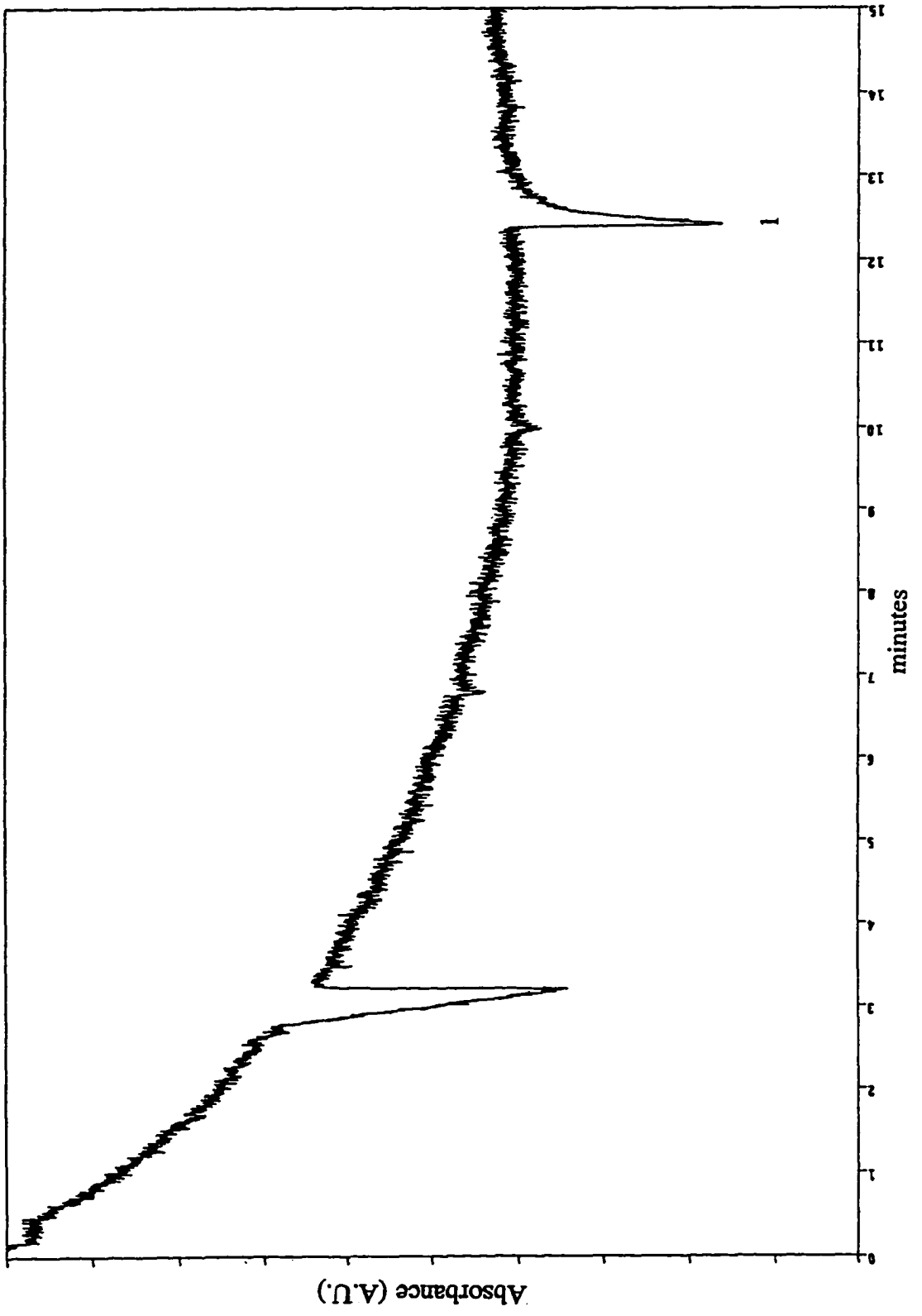
Absorbance (A.U.)
minutes
0
1
2
3
4
5
6
7
8
9
10
11
12
13
14
15

Figure 11. Electropherogram of 33 μg ml^{-1} of Y^{3+}. Electrolyte, 11 mM guanidine, adjusted to pH 2.3 with nitric acid. Other conditions as in Fig. 1. Peak: (1) Y^{3+}.

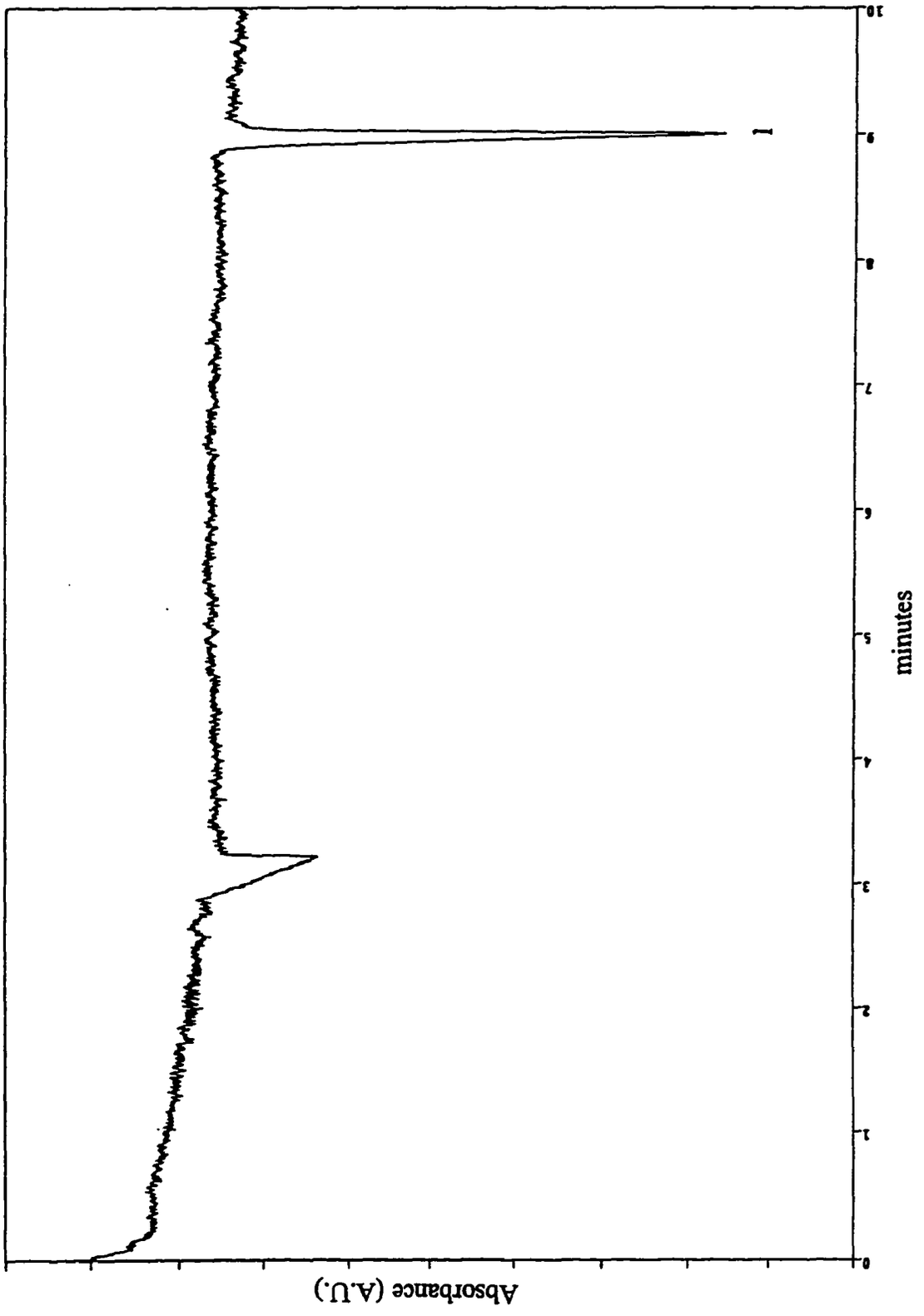
Absorbance (A.U.)
minutes
0
1
2
3
4
5
6
7
8
9
10

Figure 12. Electropherogram of Ag^{+} and Al^{3+} at 20 μg ml^{-1} each. Electrolyte, 11 mM guanidine, adjusted to pH 2.3 with nitric acid. Other conditions as in Fig. 1. Peaks: (1) Ag^{+} and (2) Al^{3+}.

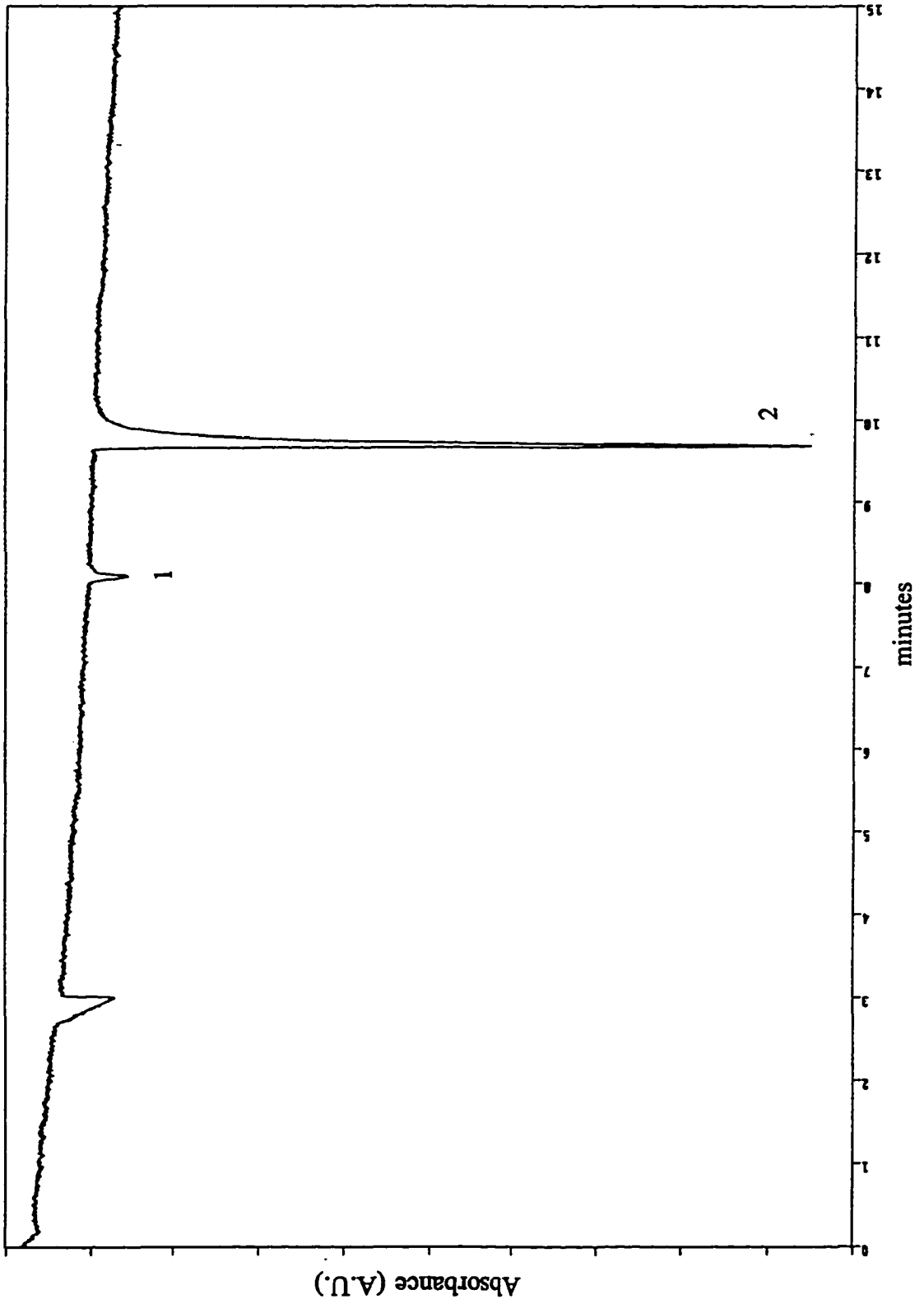
Absorbance (A.U.)
minutes
0
1
2
3
4
5
6
7
8
9
10
11
12
13
14
15
1
2

Table 3. Migration times of metal cations detected indirectly. Electrolyte, 11 mM guanidine, adjusted to pH 2.3 with nitric acid; other conditions as in Fig. 1.

Cation	t_m (min)	Cation	t_m (min)
Ag^+	8.14	Y^{3+}	9.01
Al^{3+}	9.68	Zn^{2+}	10.07
Ca^{2+}	9.25		
Ce^{3+}	8.62		
Cd^{2+}	10.22		
Co^{2+}	10.24		
Cr^{3+}	9.65		
Cu^{2+}	9.76		
Fe^{2+}	9.94		
Fe^{3+}	11.00		
K^+	7.00		
Li^+	12.47		
Mg^{2+}	10.00		
Mn^{2+}	9.93		
Na^+	9.80		
Ni^{2+}	10.24		
Pb^{2+}	8.28		
Rb^+	6.50		
Sc^{3+}	9.61		
Sr^{2+}	9.25		
UO_2^{2+}	12.26		
VO^{2+}	11.43		
VO_2^+	19.59		

3.3 Inner diameter of capillary

In principle, smaller inner diameter (i.d.) capillaries have higher heat dissipation and higher column efficiencies. Fused silica capillaries with 50 μm i.d. and 75 μm i.d. were compared for the peak heights obtained with an injection of $1 \cdot 10^{-4}$ M Ce^{3+}. They were also compared for their numbers of theoretical plates (N), signal to noise (S/N) values, and observed currents. The results are shown in Table 4. The capillaries had similar S/N ratios, and the 75 μm capillary had a larger N. As expected, the peak height was larger for the 75 μm i.d. capillary, but the baseline noise also increased due to the higher current. With smaller i.d. capillaries, it is possible to work with higher concentrations of the UV visualization reagent, which should extend the upper part of the linear working range. Therefore, 50 μm i.d. capillaries were used for the remainder of the studies.

3.4 Effect of guanidine concentration

The effect of the guanidine concentration on peak heights and N values was studied. The guanidine concentration was varied between 2 and 11 mM. The peak heights and N values for injections of $1 \cdot 10^{-4}$ M cerium (III) and $3.8 \cdot 10^{-4}$ M chromium (III) are shown in Table 5. The results show that the peak heights for both metal ions were greatest when using a concentration of 5 mM guanidine. However, the column efficiency, as indicated by the N values, increased as the concentration of guanidine increased. The baseline absorbance was also found to be more stable as the concentration of guanidine increased. With the lower concentrations of guanidine, the absorbance of the baseline increased steeply after a certain length of time. This may be

Table 4. Peak height, theoretical plate number (N) and S/N ratio of Ce (III) and observed current for different capillaries. Conditions: Electrolyte, 11 mM guanidine, pH 2.3 adjusted with HNO_3; applied voltage, 10 kV; injection time, 10 s; Ce^{3+} concentration, $1 \cdot 10^{-4}$ M.

Capillary size (μm)	Peak height	N	S/N	Current (μA)
50	1459	114346	15	11
75	2327	144317	17	26

Table 5. Effect of the guanidine concentration on the peak heights, theoretical plate numbers (N), and migration times for cerium (III) and chromium (III). Electrolyte, adjusted to pH 2.3 with nitric acid; Ce^{3+} concentration, $1 \cdot 10^{-4}$ M; Cr^{3+} concentration, $3.8 \cdot 10^{-4}$ M.

	Ce^{3+}			Cr^{3+}		
Guanidine (mmol/l)	Peak height	N	t_m (min)	Peak height	N	t_m (min)
2	2093	24255	7.08	6654	31668	9.98
5	2172	75819	8.54	9981	117319	9.75
8	1982	110885	8.63	9203	220245	9.77
11	1566	154363	8.68	6426	279330	9.88

due to the guanidine being reduced, so it becomes neutral in charge. This would cause the overall concentration of guanidine within the detection window to increase steadily because the nonionic guanidine would not be moving at the same rate as the guanidine cations.

3.5 Effect of surfactants

The use of surfactants was investigated as a way to stabilize the absorbance of the baseline for a longer period of time during an electrophoretic separation. The electroosmotic flow (EOF) can be manipulated by adding small amounts of surfactants which can coat the capillary wall [30,31]. Nonionic surfactants reduce the EOF, cationic surfactants can reduce and reverse the EOF, and anionic surfactants can reduce and reverse the EOF depending upon the pH of the BCE. The influence of Triton X-100, cetyltrimethylammonium chloride (CTAC), and alkylsulfonic acids was examined.

Methanesulfonic acid and octanesulfonic acid, at a 10 mM concentration, helped to stabilize the absorbance of the baseline, but the signals for the metal ions were significantly reduced due to ion-pairing. Low concentrations of metal ions could not be detected at all. CTAC, at a concentration of 1 mM, reversed the EOF. A stable baseline was achieved, but no peaks were detected for the alkali and alkaline earth metals. Chen and Cassidy [28] found that Triton X-100, a nonionic surfactant, increased column efficiency in their system. Consequently, the influence of Triton X-100 was investigated with guanidine as the BCE at pH 2.3.

The effect of varying the concentration of Triton X-100, between 0.02 and 0.30 mM, on the peak heights and N values for injections of $1 \cdot 10^{-4}$ M Ce^{3+} and $3.8 \cdot 10^{-4}$ M Cr^{3+} are

shown in Table 6. The effect was examined with both 5 mM and 11 mM guanidine as the BCE. The results in Table 6 show that the peak heights decrease as the concentration of Triton X-100 increases. The peak heights for 5 mM and 11 mM guanidine decreased by 590 absorbance units (A. U.) approximately for Ce^{3+} over the concentration range studied. The peak height for Cr^{3+} decreased by 900 A. U. approximately when 5 mM guanidine was used and by 1240 A. U. when 11 mM guanidine was used over the concentration range studied. An increase in the concentration of Triton X-100 caused an increase in the column efficiency to some extent, in regards to the N values. Addition of 0.10 mM Triton X-100 helped to stabilize the absorbance of the baseline when using 5 mM guanidine as the BCE. Figure 13 shows a separation of K^+, Ce^{3+}, and Cr^{3+} using 5 mM guanidine and 0.14 mM Triton X-100 as the BCE. Stability was also observed in the baseline absorbance for 11 mM guanidine upon addition of 0.02, 0.05, and 0.10 mM Triton X-100.

4. Conclusions

Capillary electrophoresis can be used under more acidic conditions for the detection of metal cations than have previously been pursued. CE can be used to detect UV absorbing metal cations directly near pH 2 with a detection wavelength of 185 nm or 214 nm. Simultaneous speciation of metal cations such as vanadium (IV) and vanadium (V) can easily be done without complexation prior to analysis. Of the UV visualization reagents studied, guanidine was found to perform the best under acidic conditions for the indirect UV detection of metal cations.

Table 6. Effect of the concentration of the surfactant, Triton X-100, on the peak heights, theoretical plate numbers (N), and migration times of cerium (III) and chromium (III). Electrolyte, 5 mM or 11 mM guanidine; adjusted to pH 2.3 with nitric acid; Ce^{3+} concentration, $1 \cdot 10^{-4}$ M; Cr^{3+} concentration, $3.8 \cdot 10^{-4}$ M.

Guanidine (mmol/l)		5			11		
Analyte	TX-100 (mmol/l)	Peak height	N	t_m (min)	Peak height	N	t_m (min)
Ce^{3+}	0	2172	75819	8.54	1566	154363	8.62
	0.02	2265	76306	8.45	1554	157221	8.76
	0.05	2270	74546	8.12	1273	213121	8.63
	0.10	1772	101208	8.42	1324	171448	8.62
	0.20	1322	169663	8.40	1082	219031	8.56
	0.30	1590	91488	8.61	970	265642	8.54
Cr^{3+}	0	9981	117319	9.75	6426	279330	9.90
	0.02	10094	121601	9.63	6850	247293	9.93
	0.05	10266	137057	9.29	6315	222959	9.83
	0.10	8634	169134	9.61	6143	242831	9.84
	0.20	8832	136926	9.59	4804	216206	9.68
	0.30	9075	117560	9.76	5186	292460	9.65

Figure 13. Electropherogram of 17 μg ml^{-1} K^+, 15 μg ml^{-1} Ce^{3+}, and 17 μg ml^{-1} Cr^{3+}. Electrolyte, 11 mM guanidine, 0.14 mM Triton X-100, adjusted to pH 2.3 with nitric acid. Other conditions as in Fig. 1. Peaks: (1) K^+, (2) Ce^{3+}, and (3) Cr^{3+}.

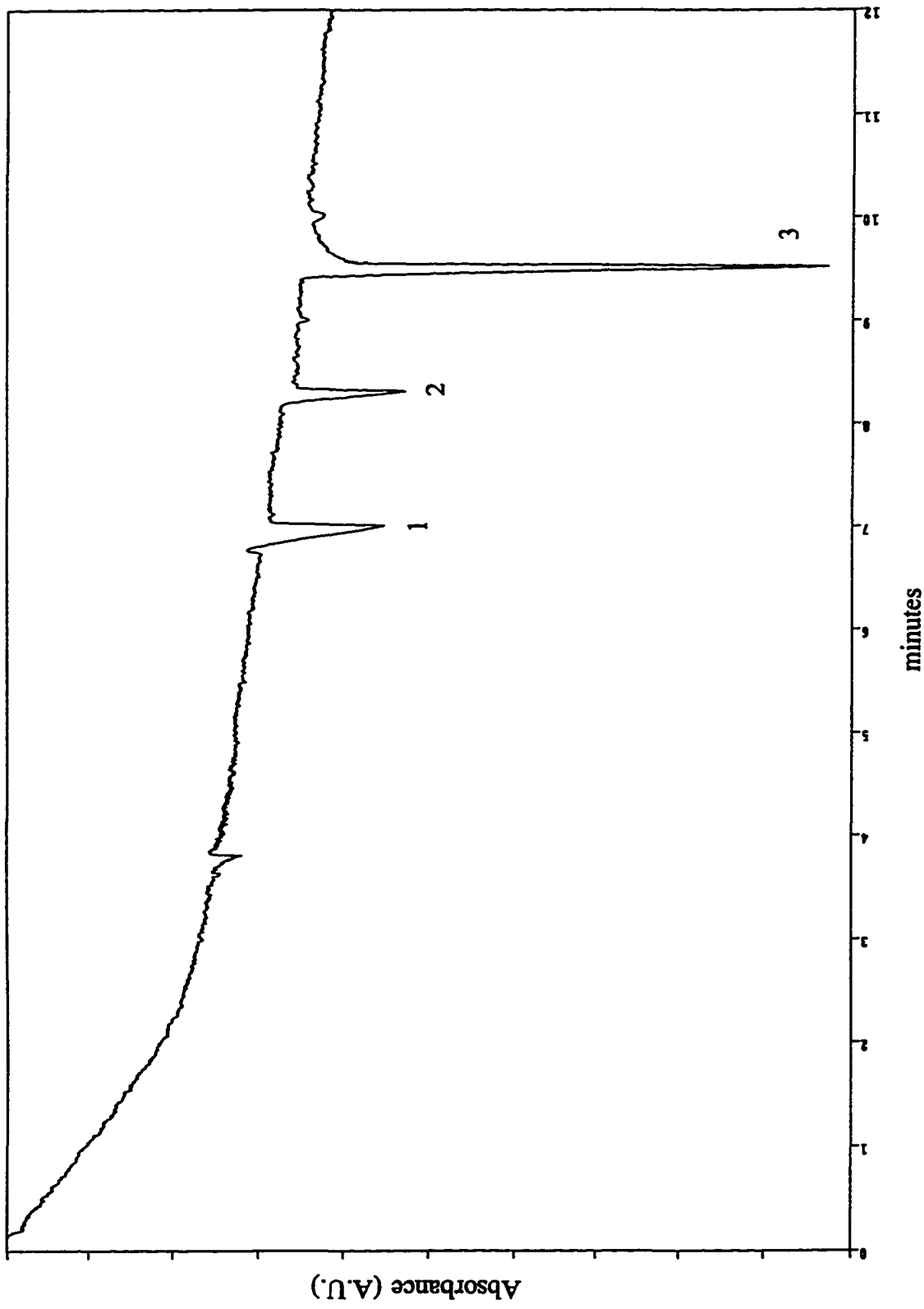
Absorbance (A.U.)
minutes
0
1
2
3
4
5
6
7
8
9
10
11
12
1
2
3

Acknowledgements

We wish to thank Waters Corporation for their gift of the Waters Quanta 4000 CE instrument and associated supplies.

This work was performed in the Ames Laboratory at Iowa State University, Ames, Iowa, USA. Ames Laboratory is operated for the U.S. Department of Energy under Contract No. W-7405-Eng-82. This work was supported in part by the Director of Energy Research, Office of Basic Energy Sciences.

References

1. S. Hjérten, *Chromatogr. Rev.*, 9 (1967) 122.
2. X. Huang, T. J. Pang, M. J. Gordon and R. N. Zare, *Anal. Chem.*, 59 (1987) 2747.
3. A. R. Timerbaev, W. Buchberger, O. P. Semenova and G. K. Bonn, *J. Chromatogr.*, 630 (1993) 379.
4. M. Iki, H. Hoshino and T. Yotsuyanagi, *Chem. Lett.*, (1993) 701.
5. M. Aguilar, X. Huang and R. N. Zare, *J. Chromatogr.*, 480 (1989) 427.
6. W. Buchberger, O. P. Semenova and A. R. Timerbaev, *J. High Resolut. Chromatogr.*, 16 (1993) 153.
7. F. Foret, S. Fanali, A. Nardi and P. Boček, *Electrophoresis*, 11 (1990) 780.
8. D. F. Swaile and M. J. Sepaniak, *Anal. Chem.*, 63 (1991) 179.
9. L. Gross and E. S. Yeung, *Anal. Chem.*, 62 (1990) 427.
10. T. Tsuda, K. Nomura and G. Nakagawa, *J. Chromatogr.*, 264 (1983) 385.
11. J. L. Beckers, Th. P. E. M. Verheggen and F. M. Everaerts, *J. Chromatogr.*, 452 (1988) 591.
12. W. Beck and H. Engelhardt, *Chromatographia*, 33 (1992) 313.

13. W. Beck and H. Engelhardt, *Fresenius' J. Anal. Chem.*, 346 (1993) 618.

14. A. Weston, P. R. Brown, P. Jandik, A. L. Heckenberg and W. R. Jones, *J. Chromatogr.*, 602 (1992) 249.

15. A. Weston, P. R. Brown, P. Jandik, W. R. Jones and A. L. Heckenberg, *J. Chromatogr.*, 593 (1992) 289.

16. Y. Shi and J. S. Fritz, *J. Chromatogr.*, 640 (1993) 473.

17. Y. Shi and J. S. Fritz, *J. Chromatogr. A*, 671 (1994) 429.

18. T.-I. Lin, Y.-H. Lee and Y.-C. Chen, *J. Chromatogr. A*, 654 (1993) 167.

19. Y.-H. Lee and T.-I. Lin, *J. Chromatogr. A*, 675 (1994) 227.

20. C. Vogt and S. Conradi, *Anal. Chim. Acta*, 294 (1994) 145.

21. S. Motomizu, S. Nishimura, Y. Obata and H. Tanaka, *Anal. Sci.*, 7 (1991) 253.

22. S. Motomizu, M. Oshima, S. Matsuda, Y. Obata and H. Tanaka, *Anal. Sci.*, 8 (1992) 619.

23. A. R. Timerbaev, O. P. Semenova, G. K. Bonn and J. S. Fritz, *Anal. Chim. Acta*, 296 (1994) 119.

24. K. Bachmann, J. Boden and I. Haumann, *J. Chromatogr.*, 626 (1992) 259.

25. J. J. Corr and J. F. Anacleto, *Anal. Chem.*, 68 (1996) 2155.

26. Y. Lui, V. Lopez-Avila and J. J. Zhu, *Anal. Chem.*, 67 (1995) 2020.

27. W. R. Barger, R. L. Mowery and J. R. Wyatt, *J. Chromatogr. A*, 680 (1994) 659.

28. M. Chen and R. M. Cassidy, *J. Chromatogr.*, 640 (1993) 425.

29. M. J. Thornton and J. S. Fritz, in press, *J. Chromatogr. A*, (1997).

30. M. Chen and R. M. Cassidy, *J. Chromatogr.*, 602 (1992) 227.

31. M. J. Thornton, C. W. Klampfl and J. S. Fritz, submitted for publication, *J. High Resolut. Chromatogr.*.

CHAPTER 5. GENERAL CONCLUSIONS

The method presented in Chapter 2 was successful. Excellent separations were obtained for the metal chloro complexes as well as for a number of metal-oxygen anions. This is the first time that all of the platinum group elements as their chloro complexes have been separated by CE. Speciation of Ir (III) and (IV) and Pt (II) and (IV) was achieved also.

This method offers significant advantages because metal anions can be analyzed at an acidic pH and detected directly. This is important because the pretreatment of many metals involves the use of mineral acids to dissolve them and keep their solutions stable. Another advantage of this method is the absence of an electroosmotic flow modifier, so there is no possibility of the metals precipitating within the capillary. The advantages of using direct detection are that it offers higher sensitivity and there is no need to match the mobilities of the analytes with that of the visualization reagent. Direct detection, thus offers better peak efficiency in symmetry of shape and sharpness. The method gives excellent results for the separation and detection of the chloro complexes of the noble metal anions and also for metal-oxygen anions. Better separations and baselines with faster analysis times are achieved than have been published previously. Separations of noble metal chloro complexes are better with CE than by HPLC with greater baseline resolution.

Amino acids can be separated in their native form as cations under acidic conditions without being derivatized and can also be detected directly with UV absorbance. The addition of ethanesulfonate, adjusted to an optimum pH, helps to resolve a majority of

the common amino acids from each other. Separation and resolution of the amino acid mixture are achieved through two mechanisms with ethanesulfonate. Selectivity is achieved through ion-pairing interactions between the amino acids and the ethanesulfonate in solution and also through the ethanesulfonate-coating of the capillary wall to prevent adsorption of the amino acids to the bare fused-silica capillary wall.

Capillary electrophoresis can be used under more acidic conditions than have previously been pursued for the detection of metal cations. Chapter 4 presents a method for CE that can be used to detect UV absorbing metal cations directly near pH 2 with a detection wavelength of 185 nm or 214 nm. Simultaneous speciation of metal cations such as vanadium (IV) and vanadium (V) can easily be done without complexation prior to analysis. Of the UV visualization reagents studied, guanidine was found to perform the best under acidic conditions for the indirect UV detection of metal cations.

ACKNOWLEDGEMENTS

I would like to extend my thanks to Dr. Fritz for accepting me into his group and being my major professor. I greatly appreciate the guidance and advice I have received.

I would like to thank all the professors who have served my POS committee. for their patience and support: Dr. Dennis Johnson, Dr. Robert Angelici, Dr. R. S. Houk, Dr. Tim Ellis, Dr. Charles Oulman, and Dr. Patricia Thiel.

I would also like to thank all the past and present Fritz group members including Ron, Wei, Nancy, Phil, John, Luther, Tom, Youchun, Dianna, Xue, and Jie for their help and friendship. It was a pleasure to work with such great people.

I am very grateful for the support I have received from my family and friends. I especially thank my parents, Joe and Denise, for always believing in me and loving me. I want to thank my friends from college, Angie and Cheryl, for their constant support, love, and friendship over the years.

I would also like to thank all the friends that I have made during my time in Ames for adding a dimension of fun to graduate school including Ron & Ann, Charles, Pat, Jay, Steve, Dave, Teresa & Patrick, JeNell & Morgan, Dave, John, Leslie, Nancy, Wei, Karl and Kristi.

I would also like to acknowledge my advisors at the College of St. Catherine, Sr. Mary Thompson and Sr. Betty Shakal, for their encouragement to go into the field of chemistry.

Most importantly, I thank God for all the gifts He has given me to make all of this possible.

I also thank Ames Laboratory and the Department of Education for financial support.

This work was performed at Ames Laboratory under Contract No. W-7405-Eng-82 with the U.S. Department of Energy. The United States government has assigned the DOE Report number IS-T 1819 to this thesis.